Links Between Oceanic Ozone Uptake and Ocean Biology

Katherine Weddell

Doctor of Philosophy

University of York
Chemistry
November 2023

Abstract

Dry deposition is a major sink of tropospheric ozone, with approximately one third of this deposition going to the ocean surface.[1-3] Organic matter at the sea surface, which is primarily produced by marine biota such as phytoplankton, likely plays a key role in oceanic ozone deposition. This study investigates the fatty acid component of organic matter in the sea surface microlayer (SML) and underlying seawater (ULW). A solid phase extraction (SPE) method was used to extract fatty acids from SML, ULW and phytoplankton culture extracts. Overall, 150 SML and ULW samples collected off the southwestern UK coast over 18 months, and during a trans-Atlantic cruise were analysed using this method. Median total, saturated and unsaturated SML concentrations were 29.56, 11.22 and 5.56 µg L^{-1} respectively for the coastal samples and 15.69, 12.76 and 0.73 µg L^{-1} respectively for the open ocean. The measured fatty acids contributed between 0.002% - 8% of the total dissolved organic carbon. The fatty acids observed were predominantly of even carbon numbers, suggesting a phytoplankton source, with their carbon number distributions being comparable to the *Phaeodactylum tricornutum* and *Synechococcus* culture extracts and to intracellular phytoplankton fatty acid distributions reported in the literature. These results highlight the link between marine biota and seawater fatty acids and provide a better understanding of the biological and chemical drivers of marine ozone dry deposition.

Acknowledgments

Author's Declaration

I declare that the work presented in this thesis is my own and that this work has not been previously submitted to this University or any other University. I am the sole author of thesis, however sections of the Abstract and Chapter Three – Analysis of Seawater from the Footprint of the Penlee Point Atmospheric Observatory and CONNECT SO287 and Impacts on Ozone Uptake present the work of a soon to be submitted paper which features amendments and additions made by Lucy Carpenter and Rosie Chance. All the sources for this work are referenced and can be found in the references section of this thesis.

Table of Contents

List of Figures

List of Tables

List of Schematics

List of Equations

Glossary

Autotroph	An organism that produces organic matter without consuming other living organisms
Axenic	A culture containing only one species
CPI	Carbon preference index
CTD	Instrument used in oceanography to measure conductivity, temperature and depth
DOC	Dissolved organic carbon
DOM	Dissolved organic matter
FAME	Fatty acid methyl ester
FMS	Full mass scan
GC	Gas chromatography
Heterotroph	An organism that consumes other living organism to acquire organic matter
MQ	Ultra-pure water
MS	Mass spectrometry
OBIS	Ocean Biodiversity Information System
Oligotrophic	Nutrient poor environment
OVOC	Organic volatile organic carbon
PFT	Phytoplankton functional type
Photoautotroph	An organism that uses light and inorganic carbon to produce organic matter
Phytoplankton	Photoautotrophic plankton
PML	Plymouth Marine Laboratory
PPAO	Penlee Point Atmospheric Observatory
SIM	Single ion monitoring
SML	Sea surface microlayer
SOA	Secondary organic aerosol
SPE	Solid phase extraction
TOC	Total organic carbon
UIB	University of the Balearic Islands
ULW	Underlying water
VOC	Volatile organic compound

Chapter One – Introduction

Atmospheric Structure

The atmosphere of Earth has been forever changing since its formation across geological time with its recent rapid changes being attributed to anthropogenic activity since the industrial revolution. The atmosphere is approximately 78% nitrogen, 21% oxygen and 1% argon with a mixture of remaining trace gases. The next most abundant gas is water vapour whose concentrations are highly variable depending on temperature and levels of evaporation and precipitation. The trace gases also include the greenhouse gases, predominantly carbon dioxide, ozone, methane, and nitrous oxide. These warm the lower levels of the atmosphere by absorbing then re-emitting the infrared radiation emitted from the planet surface when it is heated by the sun, leading to heat dissipation within the atmosphere.
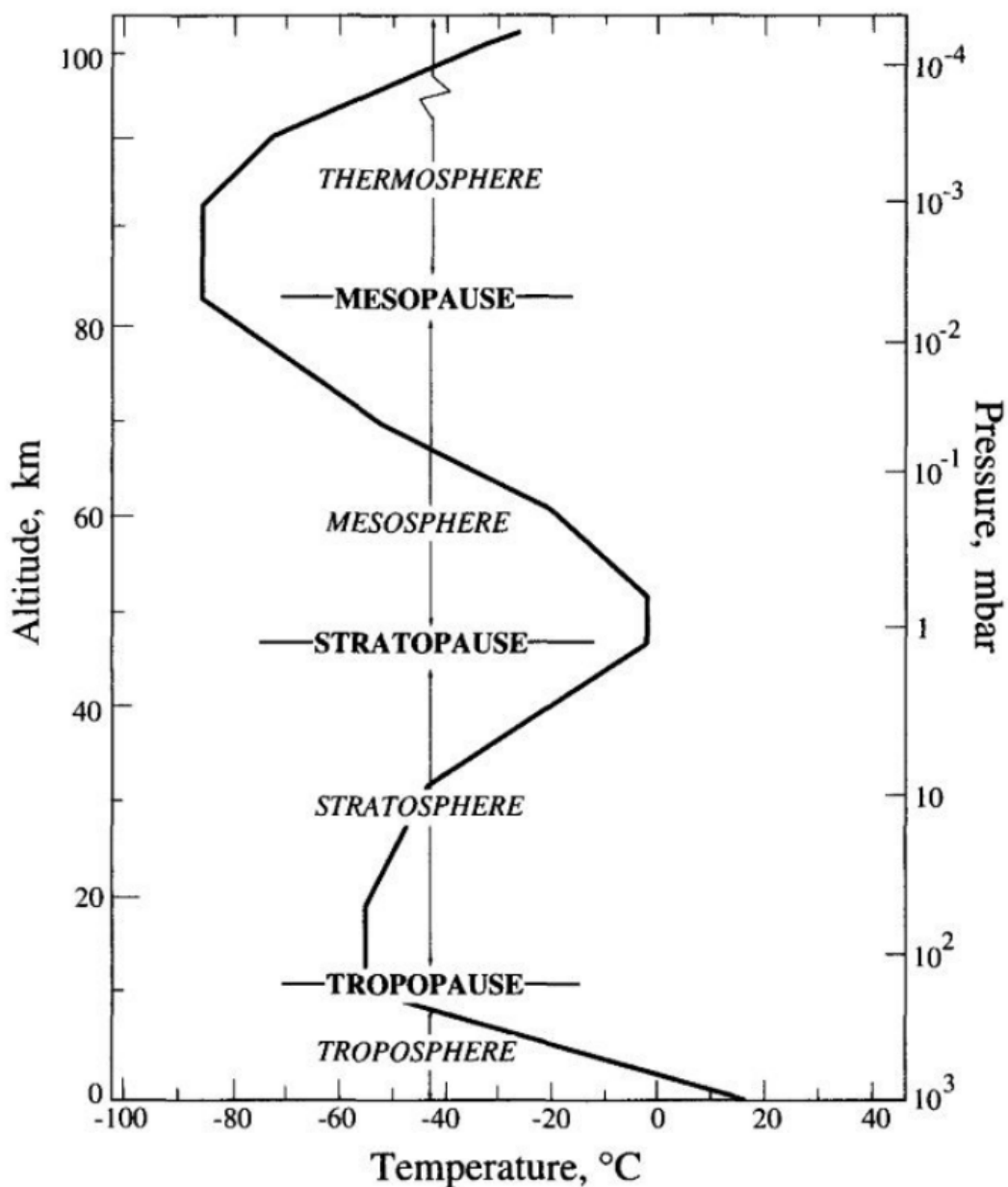
Figure 1 – *Temperature and pressure variations in the distinct vertical layers of the atmosphere. This plot was sourced from the book 'Atmospheric Chemistry and Physics: from air pollution to climate change' by John H. Seinfold.*[4]

The atmosphere itself can be characterised by decreasing pressure with altitude, which is a consequence of gravity, and a temperature profile whose temperature gradient changes depending on the atmospheric layer (see **Figure 1**). These layers include the troposphere, stratosphere, mesosphere and thermosphere. Troposphere is the bottom most layer of the atmosphere, starting at the surface to between 10-15 km altitude. This layer accounts for 80% of the mass of the atmosphere and consists of a boundary layer of a few kilometres and the free troposphere above.[4] This layer is heated by the infrared radiation radiated from the Earth surface and as such the temperature of the troposphere decreases with altitude. This leads to an unstable system due to cold air lying above warm air which means this layer is readily mixed and this mixing is responsible for the weather experienced at the surface. The layer above is the stratosphere, whose altitude is between 11-55 km above the surface. The ozone layer is within this layer which protects living organism from harmful ultra-violet (UV) radiation as it readily absorbs wavelengths of between 240-290 nm and partially absorbs between 290-320 nm.[4] It is this absorption of UV radiation that leads to the inverse temperature profile in comparison to the troposphere, with absorbed radiation being re-emitted as infrared, warming the air with increasing altitude. The mesosphere lies above the stratosphere and is typically between 80-90 km in altitude. Temperature decreases with altitude in this layer with increasing distance from the heat source provided by the UV absorption in the stratosphere. The last significant layer is the thermosphere, where the temperature profile flips again, with temperature increasing with altitude. This is due to absorption of shortwave radiation by nitrogen and oxygen.

Atmospheric Chemistry and Ozone

Much of the chemistry within the atmosphere is dictated by its trace components, with chemical changes occurring either via reactions between the trace gases themselves or being driven by photochemistry. Reactions can occur either completely within the gas phase of the atmosphere, or at the boundaries between the atmosphere and either liquid or solid surfaces. Reactive trace gases typically undergo oxidation reactions, owing to the oxidizing power of the atmosphere. The main oxidising species include the hydroxyl radical (OH), ozone (O_3) and nitrate radicals (NO_3).[5]

90% of the atmospheric ozone is found in the stratospheric ozone layer, while the remaining 10% is in the troposphere.[4] Typical tropospheric concentrations of ozone are around 50 ppb, whereas levels are within the ppm range in the ozone layer.[4, 6] Although some tropospheric ozone comes directly from flux down from the stratosphere, the majority is produced in the troposphere itself.[7]

Broadly, tropospheric ozone is produced by volatile organic compounds (VOCs) and NO_x which includes NO and NO_2. NO is the species that is typically emitted from both natural and anthropogenic sources including directly from soil and in the high temperature environments present in wild fires, lightning, internal combustion engines and powerplants.[4, 8] Production starts with the oxidation of VOCs by any of the three atmospheric oxidants mentioned above or via photolysis (**Equation 1**). Note that in remote areas these reactions are dominated by carbon monoxide and methane, whereas larger organics including aromatic species dominate in polluted, urban environments.[4]

11

$$VOC \xrightarrow{\text{OH, O}_3\text{, NO}_3\text{, } hv} RO_2$$

***Equation 1** – Oxidation of VOCs.*
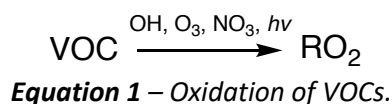
RO_2 in **Equation 1** represents peroxy radicals with R either being hydrogen or a larger organic component. These radicals go on to oxidize emitted NO in **Equation 2**.

$$NO \xrightarrow{RO_2} NO_2$$

***Equation 2** – Oxidation of NO.*
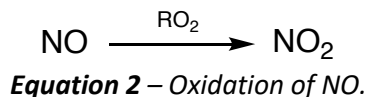
The NO_2 produced readily photolyzes at wavelengths less than 424 nm to produce an oxygen atom.[4] This can then go on to react with O_2 to from ozone. This is shown in **Equation 3**. Note that the excess energy of this reaction is carried away via collision with N_2 or O_2 and is represented by M.

$$O + O_2 + M \longrightarrow O_3 + M$$

***Equation 3** – Formation of ozone.*
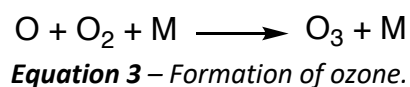
Oceanic Ozone Dry Deposition and the Sea Surface Microlayer

For atmospheric ozone concentrations to remain constant, there must be routes of loss that counter the production previously described. One mechanism of loss is through dry deposition to the Earth surface. Dry deposition is the process of a compound being lost to a surface on contact with said surface. Due to the large surface area of the oceans, much of the global ozone dry deposition is to the ocean surface, thought to account for up to a third of total deposition.[1, 2] Ozone deposition velocity to seawater/saline water is estimated to range from 0.01-0.15 cm s^{-1}.[2] However, ozone itself is very water insoluble so this deposition can only be explained by ozone reacting with species within or at the surface of the water.

Oceanic ozone dry deposition is associated with large uncertainties due the lack of observational data.[1] However, there are two key chemical drivers of deposition: dissolved organic matter (DOM) and iodide. It is thought that these species contribute approximately equally to deposition, although this depends on their relative abundances and the reactivity of organic compounds.[9, 10] For example, in coastal regions, ozone reactivity towards DOM has been found to be 2-5 times higher than towards iodide.[10] Ozone reacts with these species at the surface via a Langmuir-Hinshelwood mechanism, thus the relevant reactions will occur in the sea-surface microlayer (SML).[11] A basic diagram of this process involving the fatty acid component of DOM is shown in **Figure 2**.

Sea Surface Microlayer Organic Matter

The SML represents the top 100s μm at the ocean surface.[12] This layer has been found to be consistently present at the surface of the ocean between 30 °N and 30 °S, with the lack of primary production and high windspeeds outside this zone limiting its formation.[13] The layer is enriched, i.e. being present in greater concentrations in the SML than the bulk, in organic and inorganic matter including carbohydrates, lipids, proteins, amino acids, free fatty acids, alcohols, polysaccharides, humic substances and waxes .[14-17] These compounds are often hydrophobic or are surfactants, hence they accumulate at the phase boundary of the ocean surface.[12] Brewster angle microscopy images of the formation of the SML from a seawater sample from the work by Kozarac *et al.*[18] is shown in **Figure 3**. The organic compounds present in the SML are typically produced *in situ* by marine phytoplankton and bacteria but can also

be brought to the surface by the surfactants adsorbing to the phase boundary of bubbles as they rise to the surface.[12, 17, 19]
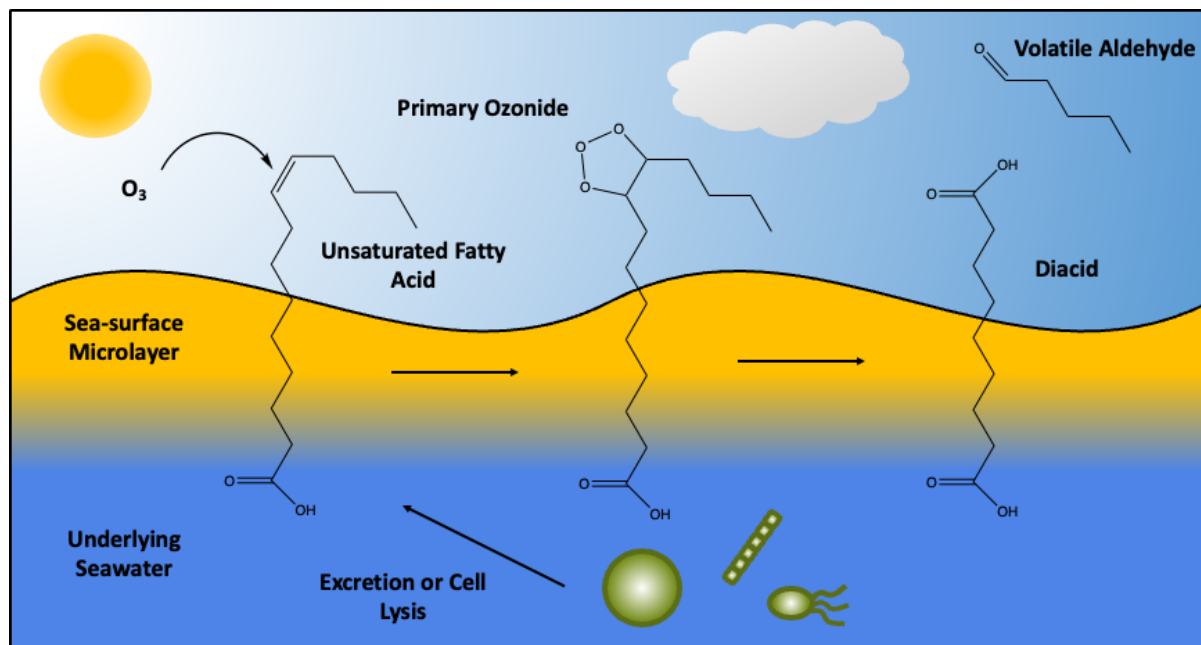
Figure 2 – *Schematic of basic processes involved in the ozonolysis of unsaturated fatty acids in the SML.*
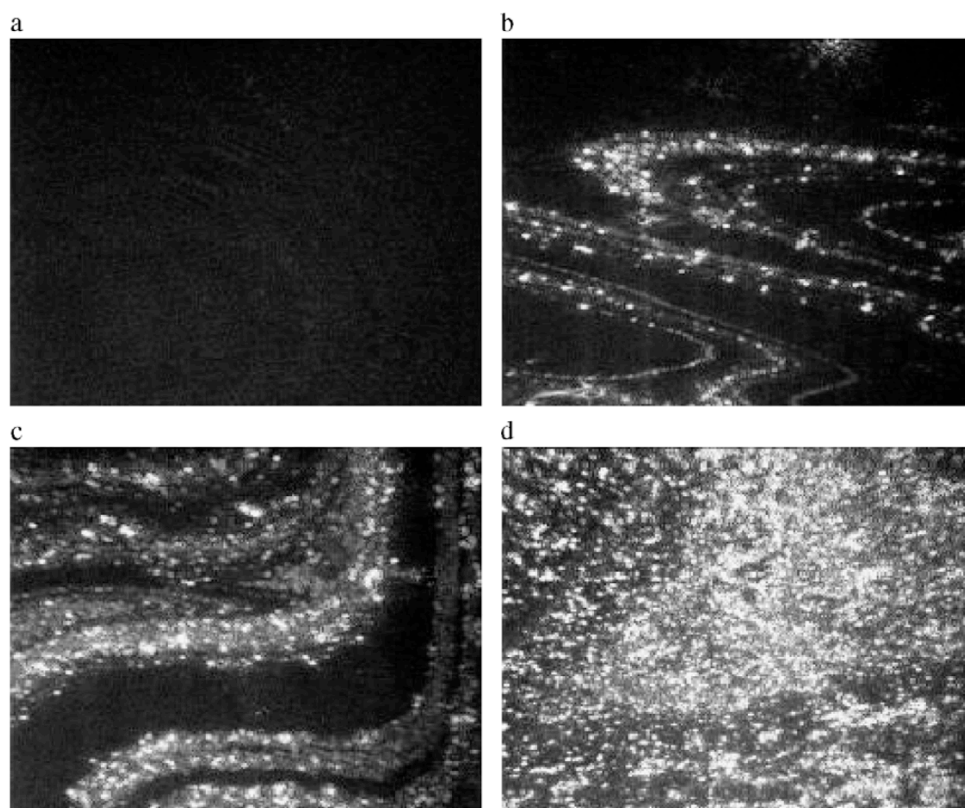
Figure 3 – *Brewster angle microscopy (BAM) image of the formation of a microlayer from a seawater sample as amphiphilic compounds become enriched at the surface at 0 hours (a), 2 hours (b), 10 hours (c) and 24 hours (d) following sample preparation. This figure was taken from the work by Kozarac et al. who used BAM to analyse authentic SML samples and solvent extracts from seawater samples.[18]*

Within the organic component of the SML, ozone can readily react with carbon double bonds, aromatic moieties and amines, with the carbon-carbon double bonds being the focus of this work.[20] Ozone reacts with these bonds through the process of ozonolysis and is therefore lost to the surface as a result. In the context of this study, it is the fatty acids and in particular the unsaturated fatty acids that are of interest. Overall fatty acids make up approximately 10% of the organic matter found in the SML and are typically produced via the primary production of photoautotrophs including marine phytoplankton and bacteria, with aliphatic chain lengths of between 12 to 24 carbon atoms long and levels of unsaturation ranging between 0 to 6 double bonds.[21-23] Marine bacteria also produce branched fatty acids as well as those with 15 or 17 carbon atoms in the aliphatic chain.[17, 24] These fatty acids are released into the surrounding water via processes such as cell lysis, excretion and mucilage formation.[25] Fresh organic material is typically rich in unsaturated fatty acids but as the material ages, saturated fatty acids dominate due to the susceptibility of carbon-carbon double bonds to undergo oxidation.[17, 26] Other, larger fatty acids have also been observed in marine aerosols, which originate from terrestrial vegetation and are typically found in coastal regions.[22] Diacids have also been observed in seawater and typically concentrated at the surface, making up approximately 0.9 to 24 % of dissolved organic carbon (DOC).[27] Diacids range from 2 to 9 carbon atoms long and are also produced by phytoplankton either directly or indirectly from chemical and biological degradation of the organic matter they produce.[27, 28]

Few studies have investigated SML fatty acids, but those who have include Gašparović *et al.*[17], Marty *et al.*[29], Daumas *et al.*[30] and Slowey *et al.*[31]. The results of these studies are summarized in **Table 1**. The amount and type of fatty acid varies greatly between the studies, although the profiles are typically dominated by species of 16 and 18 carbon atoms in their aliphatic chain. This dominance is also seen in marine aerosols.[22, 32] The variety of fatty acids concentrations highlights the many variables that contribute to both their production and loss. Firstly, differences in the microbial community will influence production and subsequent decomposition. For example, Gašparović *et al.*[17] stated that the phytoplankton present in the subarctic fjord they studied were typically very lipid rich, which goes some way to explaining the quantity and variety of fatty acids observed. Highly unsaturated fatty acids are also produced in greater quantities by phytoplankton in colder climates to maintain cell membrane fluidity.[33] The presence and contribution of branched fatty acids with odd numbers of carbon atoms will, as previously mentioned, be driven by bacteria in the microbial community.[26] Because of this intrinsic link with biology, the season in which samples are taken will influence the composition. Fatty acids are typically at their highest concentration following a phytoplankton bloom, i.e. when cells start to die and lyse.[17] During peak biological activity, concentrations may decrease due to heterotrophic consumption and decomposition.[32] Biological activity will also be linked to the region sampled where temperature and nutrient availability will typically be the differentiating factors. In the case of the literature data presented here, Marty *et al.*[29] report concentrations from the open ocean in the North-Eastern tropical Atlantic. These concentrations are comparably lower than the other studies which may be indicative of the oligotrophic nature of the open ocean. Finally, the fatty acids observed will also be a function of sample handling and processing. The length of time between the sample being collected and processed and how it is stored in between these steps will determine the state of the organic matter due to heterotrophic activity and chemical degradation. How the fatty acids are extracted will influence the final profile reported. For example, Gašparović *et al.*[17] carried out a liquid-liquid extraction using

dichloromethane, wheras Slowey et al.[31] used ethyl acetate which may lead to differing results depending on individual fatty acid solubilities in said solvents.

Fatty Acid Ozonolysis

In water, free fatty acids and lipids will orientate themselves so that their polar head group is within the water and their aliphatic chains protruding out of the water, thereby forming a monolayer at the surface, depending on their overall concentration. However, it should be noted that in pure liquids of free fatty acids, the acids can form dimers with each molecule being in a flipped orientation to that next to it at the surface with another layer of molecules below hydrogen bonded via their carboxylic groups.[34] This second surface structure is unlikely in the dilute environment of the SML with regards to fatty acids concentrations but should be noted as a possibility due to the surrounding media in the SML being generally concentrated in other hydrophobic compounds. With the aliphatic chains orientated out of the water, the carbon-carbon double bonds will be exposed to atmospheric ozone and therefore ozonolysis can occur.

Ozone reacts with SML fatty acid double bonds via a Langmuir-Hinshelwood mechanism where ozone adsorbs onto the surface and reacts with the double bond, with ozone spending more time trapped on the SML than it does undergoing ozonolysis.[35] The process of ozonolysis of the model unsaturated fatty acid oleic acid is well established.[36] Ozone reacts with carbon-carbon doubles bonds via addition across the bond to form a primary ozonide. This ozonide is unstable and will break down via the cleavage of the carbon-carbon and oxygen-oxygen bonds to form a carbonyl, either an aldehyde or a carboxylic acid in the case of free fatty acids, and a Criegee intermediate.[36, 37] This Criegee intermediate is an unstable biradical which will either rapidly rearrange or go on to react further.[36, 38] This can include reactions with water to form hydroperoxides; with aldehydes to form secondary ozonides; with acids to form α-acyloxyalkyl hydrogenperoxides; and with themselves to form diperoxides.[36] The hydroperoxides will decompose to form further carboxylic acids and aldehydes while the α-acyloxyalkyl hydrogenperoxides may react with the Criegee intermediates again to form peroxidic polymers.[36] The fate of these ozonolysis products depends on their chemical properties. Taking oleic acid as an example, the species analysed by Vesna et al.[36], the main ozonolysis products are nonanal, nonanoic acid, oxononanoic acid and azelaic acid. Nonanal is a volatile species and as a result, is typically released into the atmosphere following ozonolysis.[36] The remaining species typically remain in solution. This process is shown in **Figure 4**.

Zhou et al.[39] investigated whether the ozonolysis products of fatty acids would be formed from authentic SML samples when exposed to ozone. They tested both SML samples as well as linoleic acid which was used as a proxy for the SML on top of natural seawater. Their linoleic acid experiments produced n-hexanal and 3-nonenal while the SML samples yielded acetaldehyde, propanal, acetone, butanal, butanone, pentanal and pentanone in addition to n-hexanal and 3-nonenal.[39] This study was an important step in putting the well characterised unsaturated fatty acid ozonolysis in the context of the marine environment and oceanic ozone uptake. It demonstrated that fatty acids in the SML could play a key role in driving ozone dry deposition, and it is this which was investigated during this project.

Table 1 – *Literature data of fatty acid concentrations within the SML with the studies represented by the name of the lead author.*[17, 29-31] *Note that the concentrations are averaged across each study. With regards to fatty acid nomenclature, the numerical code refers to the structure of the FAME and therefore fatty acid. The first number is the number of carbon atoms in the aliphatic chain, the number following the colon is the number of double bonds present and the number after ω is the number of carbon atoms the double bond is away from the tail end of the aliphatic chain. Anteiso and iso fatty acids have branched aliphatic chains, with antesio and iso having a methyl group attached to the second and third carbon from the end of the chain respectively.*

Fatty Acid	Code	Fatty Acid Concentration/ µg L^{-1}			
		Slowey	**Daumas**	**Marty**	**Gašparović**
		Gulf of Mexico	Northern Mediterranean Coast	North-eastern Tropical Atlantic	North Norwegian Fjords
Dodecanoic acid	12:0	6.00	7.82	1.20	
Tridecanoic acid	13:0				0.17
Tetradecanoic acid	14:0	16.50	7.55	2.40	6.05
Tetradecenoic acid	14:1	0.00			0.47
Pentadecanoic acid	15:0		1.82	0.40	1.04
Hexadecanoic acid	16:0	27.00	113.18	2.20	11.44
9-Hexadecenoic acid	16:1ω7				4.78
Hexadecenoic acid	16:1	21.00	80.35	0.90	1.58
Hexadecadienoic acid	16:2			0.10	
Heptadecanoic acid	17:0		0.31		0.66
Octadecanoic acid	18:0	63.00	16.94	0.30	26.12
Octadecenoic acid	18:1		18.92	0.60	4.99
9,12-Octadecadienoic acid	18:2ω6				1.36
Octadecadienoic acid	18:2	6.00	33.26		
9,12,15-Octadectrienoic acid	18:3ω3				0.85
Octadecatrienoic acid	18:3	10.50			
Octadecatetraenoic acid	18:4				1.63
Eicosanoic acid	20:0			0.05	37.38
Eicosenoic acid	20:1				0.15
Eicosadienoic acid	20:2				0.06
Eicosatetraenoic acid	20:4				0.33
Eicosapentenoic acid	20:5				4.88
Docosenoic acid	22:1				0.73
Docosahexenoic acid	22:6				2.54
Tetracosanoic acid	24:0			0.05	
Hexacosanoic acid	26:0			0.05	
Ocatacoanoic acid	28:0			0.20	
Triaconoic acid	30:0			0.10	
anteiso-Pentadecanoic acid	*anteiso* 15:0				0.33
anteiso-Heptadecanoic acid	*anteiso* 17:0				0.32
iso-Tetradecanoic acid	*iso* 14:0				0.19
iso-Pentadecanoic acid	*iso* 15:0				0.24
iso-Hexadecanoic acid	*iso* 16:0				0.44
iso-Heptadecanoic acid	*iso* 17:0				0.22
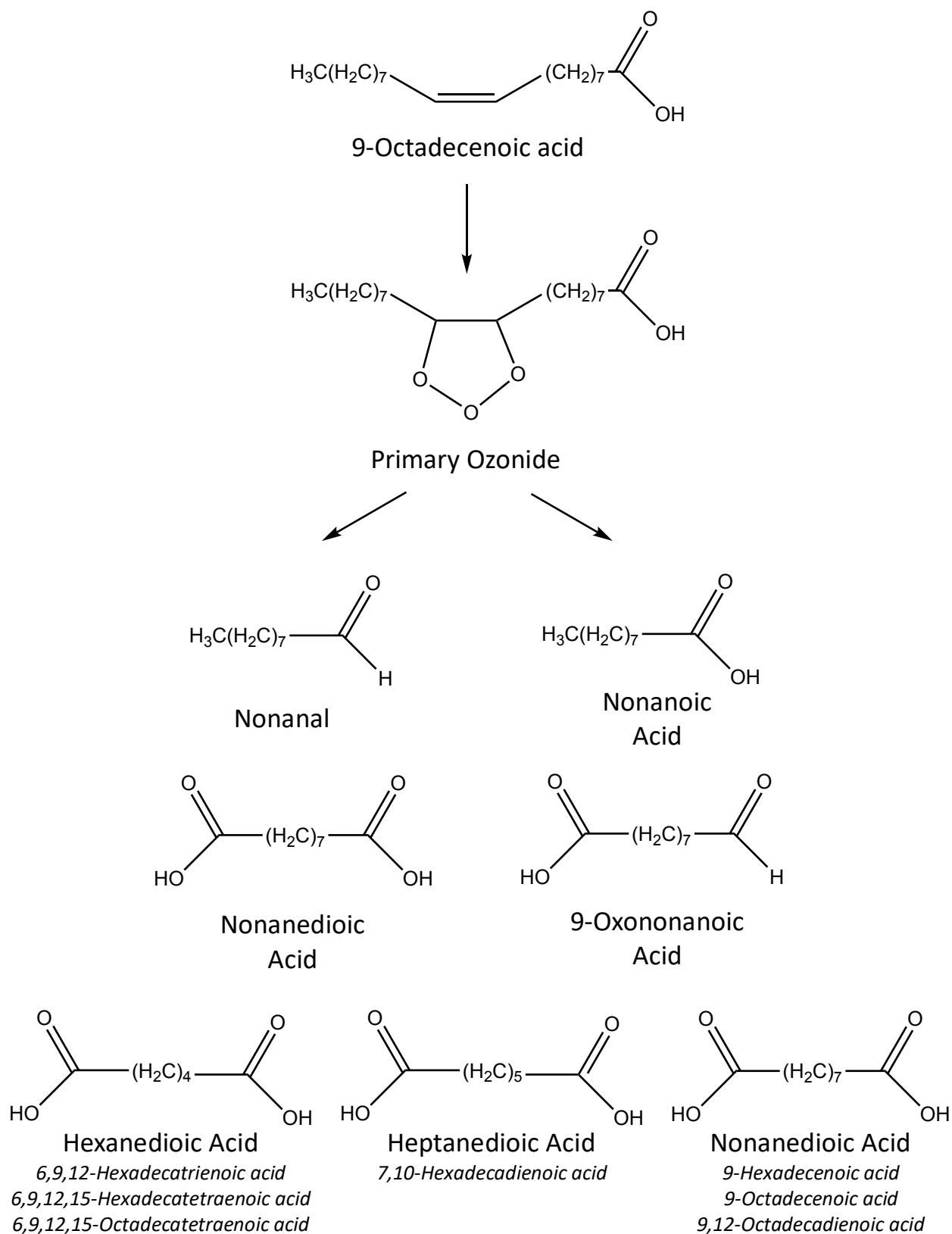
Figure 4 – *Ozonolysis of 9-octadecanoic acid (oleic acid) and its products. Below this reaction scheme are three diacids that have been observed during this study. The compounds in italics are the those that will form these diacids post ozonolysis.*

Project Aims

Few studies have been carried out to investigate seawater fatty acid concentrations and as far as this author is aware, no time series data on these fatty acids has ever been generated. Moreover, no work linking measured fatty acid concentrations to *in situ* ozone flux measurements has to date been carried out. It is this which was the focus of this project.

The initial aim of this study was to develop a method of extracting fatty acids out of seawater which utilised solid phase extraction (SPE) rather than the previously used liquid-liquid extraction. This method was to work in parallel to the DOM analysis already carried out by the research group. This method was then applied to seawater samples collected as part of an 18-month continuous campaign in collaboration with the Plymouth Marine Laboratory. The aim of this campaign was to analyse the physical and chemical properties of the waters surrounding the Penlee Point Atmospheric Observatory and relate these parameters to simultaneous ozone flux measurements, assessing their impacts. In addition to this, fatty acids were also analysed in seawater samples collected on the SO287-CONNECT cruise onboard the RV Sonne. These samples were collected along the cruise track which formed a transect across the Atlantic Ocean, through the Caribbean Sea and into the Pacific Ocean. The aim of this was to investigate how fatty acids changed across this transect and how this related to ozone flux measurements carried out on the ship.

Alongside and following this work, preliminary investigations were made into investigating the phytoplankton fatty acids as these are the primary source of seawater fatty acids. An initial analysis of the literature was carried out with the aim of characterising the variety of fatty acids produced as well as their relative quantities across a range of phytoplankton species. This then fed into analysis of phytoplankton cultures using the SPE method described above to characterise and quantify extracellular fatty acids. The goal of this was to compare the fatty acids observed in these experiments to those detected in the seawater samples, thereby creating a more complete understanding of how fatty acids produced by biology link to seawater fatty acids and ultimately ozone dry deposition.

Chapter Two – Development of a Solid Phase Extraction Method for the Extraction and Analysis of Marine Fatty Acids

Preface to Chapter

The recovery data as well the screen contamination results intend to be published and therefore a portion of this text will be featured in said publication. The text in this chapter was produced by myself with amendments and additions made by Lucy Carpenter and Rosie Chance.

Introduction

Environmental samples often present an analytical challenge due to them containing a complex mix of compounds. The environmental mixture of interest in this study being marine DOM, which contains a variety of biologically produced compounds including carbohydrates, lipids, proteins, amino acids, free fatty acids, alcohols, polysaccharides, humic substances and waxes .[14-17] It is therefore often necessary to separate these mixtures into their components to identify and quantify them. This is often done by utilizing the differences in the physical and chemical properties of compounds to separate them into different phases or media. In this study SPE and gas chromatography-mass spectrometry (GC-MS) are used for this purpose.

SPE has been evolving over the past 70 years to aid the collection and concentration of analytes in bulk media.[40] This is necessary as target analytes may be at low concentrations in unprocessed samples and subsequently below the detection limit of the instrument used for analysis. SPE also provides a way of 'cleaning' a sample by removing species that may interfere with or damage equipment. This is achieved by passing a liquid sample through a solid sorbent which shows greater affinity to the analytes than to the bulk media and the background compounds within.

The typical SPE process is as follows. The sorbent is first activated using a solvent that can be the solvent chosen for sample elution. This is necessary as the functional groups on the polymer backbone may have collapsed on themselves in dry storage, making them less able to interact with the analyte molecules, decreasing the efficiency of the extraction. The cartridge can then be conditioned with a solvent similar to that of the sample solution to wash off the solvent used to activate the sorbent. Note that this was not done in this study due to the relatively large volume of the seawater samples compared to the volume of the activating solvent. The sample is then applied to the sorbent, whereby the analytes will adsorb to the sorbent while the bulk media passes through. Following the sample, any interfering compounds will be removed. This can include adding dilute acids to remove carbonate salts and/or drying the sorbent to remove water. The analytes are then finally removed via elution with a solvent which has a great enough affinity to the analytes to desorb them from the sorbent.

Initial methods of SPE involved granulated activated carbon used for water treatment, whereby organic compounds were removed from the water.[40] Improvements were made by the invention of cross-linked polystyrene resins as well as styrene-divinylbenzene and ethylene-dimethacrylate resins which were eventually followed by silica bonded sorbents

with alkyl groups such as C18, cyclohexyl, diol, cyanopropyl, and phenyl being bonded to the crosslinked polymers.[40] These sorbents were designed to improve the sorption and desorption efficiencies of analytes and can either be compound class specific or more general purpose.

Although SPE presents a much 'cleaner' sample to analyse, in the case of many environmental samples, the sample is still likely a mixture of many unknown compounds. Alone, chromatography can only separate compounds and identification relies on comparing retention times of known compound standards, and although mass-spectrometry allows compound identification from molecular ions and fragments, this is not possible if a mix of compounds enter the spectrometer at the sample time. This is where chromatography combined with mass-spectrometry becomes a powerful tool. Combining the instruments allows for the separation and identification of compounds in complex mixtures.

A typical GC-MS instrument consists of an inlet, where the sample is vapourised, connected to a chromatographic column contained within an oven. The end of the column feeds into a mass spectrometer where the separated components are ionised and analysed. As the sample is transferred to the column via a carrier gas, often helium or hydrogen, compounds become retained by the stationary phase, a liquid film or solid supported material, and only move when they transition back into the carrier gas which is the mobile phase. Compounds become separated from one another due to their different affinities between themselves and the stationary phase as well as their different volatility, allowing them to enter the mobile phase. The more readily a compound is retained by the stationary phase, the longer it spends on the column and the later it elutes off the column. This property is described by the retention factor, k, and is calculated using **Equation 4**.

$$k = \frac{t_s}{t_m} = \frac{n_s}{n_m} = \frac{C_s V_s}{C_m V_m} = K \frac{V_s}{V_m} \; where \; K = \frac{C_s}{C_m}$$

Equation 4 - *Retention Factor*

where t_s and t_m, n_s and n_m and C_s and C_m are the time spent, number of moles of the compound and concentration of the compound in the stationary and the mobile phase, respectively. V_s and V_m are the volumes of the stationary and mobile phases respectively. K is the distribution constant and represents the distribution of the compound between the two phases in terms of concentration. The larger the retention factor of a compound, the more it is retained by the stationary phase, and the later it elutes. In the case of GC, this retention factor can be related to the boiling point of the compound. Using **Equation 4**, the Van't Hoff equation and the assumption that at the boiling point of a compound, the standard enthalpy change is the product of boiling point temperature and the standard entropy change the following equation is given in **Equation 5**:

$$lnk' = \frac{-\Delta S^\theta}{R}\left(\frac{T_{bp}}{T} - 1\right) - ln\frac{V_M}{V_S}$$

Equation 5 - *Substituted Van't Hoff equation relating boiling to the retention factor.*

where, ΔS^θ is the standard entropy change, R is the ideal gas constant, T is temperature and T_{bp} is the boiling point of the compound. From this equation, as the boiling point of a

compound increases so does the retention factor. Also, as the oven temperature increases, the retention factor decreases. By carefully choosing the correct stationary phase, one that is similar in polarity to the target compounds, and altering the temperature ramping within the GC oven, suitable compound separation can be achieved while also keeping run times to a minimum.

Once the compounds are separated and leave the column, they pass into the mass spectrometer. Here they are first ionised and in case of this study, electron ionisation (EI) is used. In EI, a filament is used to generate electrons via thermionic emission of a typical energy of 70 eV. These electrons are accelerated towards an electrode through the compounds emerging from the GC column. This ionises them by the removal of one or more electrons, producing molecular ions. Due to the high energy of the ionising electrons, these molecular ions often fragment into ions and radicals, with the ions being detectable. These fragments are used to then identify the compounds.

In terms of mass analysers, a quadrupole was used for this work. A quadrupole mass analyser uses a combination of four conducting rods, with opposing rods being of the same polarity, either positive or negative. In the case of the positive ions being produced by EI, the positive rods provide a stabilising force by repelling the ions into the central cavity between the rods. The negative rods, however, destabilise the ions as they are attracted to the rods. By repeatedly alternating the polarity of the rods, the ions can be held in the centre of the rods allowing them to pass through to the detector. What ions pass through depends on their mass to charge ratio and is selected for by changing the frequency of the polarity oscillations. If the mass of the ion is too low for the frequency, then it will travel too fast towards the negatively charged rod, colliding with it before the polarity changes. If the mass is too high, then the ions inertia will be too great for its direction to be changed as the polarity is changed, leading to its loss on collision with the rod.

Once an ion is allowed to pass to the detector a signal is produced that is proportional to the number of ions hitting the detector. This is related to the amount of compound ionised and therefore the amount passed from the GC column. The output of a GC-MS system is a chromatogram containing separated Gaussian-shaped peaks, assuming system conditions are optimised for the sample injected, whose peak area is proportional to the amount of the compound. The compound can be identified either by comparing the average mass spectra of the peak to a spectral library or by matching the retention time of the peak to a reference compound standard. Compounds can also be quantified by comparing the peak area to that of a series of calibration standards directly or using an internal standard in both the standards and samples and comparing the peak area ratios of the internal standard to that of the standard compounds.

Overall, the combination of an SPE sample preparation followed by compound separation, identification and quantification via GC-MS provides a powerful tool for comprehensively analysing complex environmental samples. It is these methods which are used for the extraction, identification and quantification of seawater fatty acids in this PhD.

Although the analysis of fatty acids by GC-MS is often standard practise and easily carried out, the extraction of aqueous fatty acids on a large scale is less so. The typical method of

extracting fatty acids and lipids from seawater is via liquid-liquid extraction.[17, 26, 31] Although this leads to high extraction efficiencies, it is not practical for the analysis of multiple, high-volume samples due to the large solvent volumes required. Thus, in this study an SPE method based on a method originally developed by Dittmar et al.[41] to extract DOM from seawater but adapted here for isolation of fatty acids was used.

Description of Chapter

The aim of this part of the project was to develop an efficient method of extracting fatty acids from multiple, large volume seawater samples. The extraction method would also have to be effective at extracting general DOM out of the same samples as parallel DOM analysis was carried out in some instances. Different sections of the method will be discussed, including any changes that were made as the project progressed. At the end of this section, the sampling methodology will also be discussed.

SPE Method Validation

The SPE method that was adapted for extracting fatty acids and lipids was originally developed by Dittmar et al.[41] who found a modified styrene divinyl benzene based SPE cartridge (PPL) to be the most effective at extracting DOM from seawater. Extracting 10 L of seawater per gram of sorbent, they were able to extract DOM at an average recovery of 62%, with a C18 silica-based sorbent only showing two thirds of this recovery. Note that no overloading of the sorbent was observed.[41] Dittmar et al.[41] state that these cartridges are ideal for both polar and nonpolar species present in large volumes of water which make them ideal for this investigation as the target compounds will vary in polarity depending on the nature of the polar head groups and nonpolar aliphatic tails.

The SPE extraction set-up used is depicted in **Figure 5**. This set-up allowed for large volumes of water to be passed through the SPE cartridges, driven by a vacuum pump. The 50 mL syringes used in this setup were initially used as reservoirs to buffer the system from running dry. PTFE caps with O-rings were specifically made for the setup and allowed for the system to be sealed. However, over time these caps wore out and the seals began to fail. To remedy this, a new set of smaller caps were used that attached the sample lines directly to the SPE cartridges as shown in **Figure 6**. The liquid samples were passed through the cartridges held in place by the SPE manifold and the waste liquid was removed from the base of the manifold to the waste liquid trap via the vacuum.

As per the Dittmar et al.[41] method, the samples were first acidified with 37% HCl (analytical reagent grade, Fisher Chemical) to a pH of approximately 2, which was either monitored by a pH probe for the PML samples or pH paper with the CONNECT and Mallorca phytoplankton culture samples. Samples were acidified to ensure the fatty acids were in their non-ionic form to aid retention to the SPE sorbent. Before the samples were extracted, the PPL cartridges were primed with one cartridge headspace of methanol (>= 99.8% HPLC grade, Fisher Chemical); this volume was approximately 6 mL. This was to ensure the correct orientation of the sorbent molecules which may have collapsed in storage. Once the cartridge was primed, the acidified samples were passed through the cartridge, maintaining a drop rate of sample out of the cartridge of about 1 drop a second. Once the sample had passed through the cartridge, the cartridge was washed with approximately 12 mL of 0.01M HCl (analytical reagent grade, Fisher Chemical), i.e. two cartridge headspaces. This was to remove any

22

carbonate salts that may have been deposited on the sorbent. After these washes, the sorbent was dried by detaching any tubing connected to the cartridge and allowing the vacuum to pull air through the cartridge for 5 minutes. Once dry, the cartridges were eluted in 6 mL methanol (>= 99.8% HPLC grade, Fisher Chemical) for the PML and Mallorca phytoplankton culture samples and 8 mL for the CONNECT cruise samples. The eluent was collected in amber glass scintillation vials (EPA, borosilicate glass, 20 mL, Thermo Scientific Chromacol) which had been heated in a muffle furnace at 450 °C for at least 6 hours. These eluents were stored at -18 °C until the FAME conversion step could be carried out.

Figure 5 *- Apparatus used for solid phase extraction. The number labels correspond the following components: **1** is the PPL SPE cartridge; **2** is the reservoir for the sample; **3** is the tube used to fill the reservoir with the sample and **4** is the sample itself.*

FAME Conversion Step

Due to the polar nature of fatty acids, they first need to be converted to their fatty acid methyl esters (FAME) to increase their volatility before they can be analysed by GC-MS. This was done via an acid catalysed esterification, as seen in **Schematic 1**.
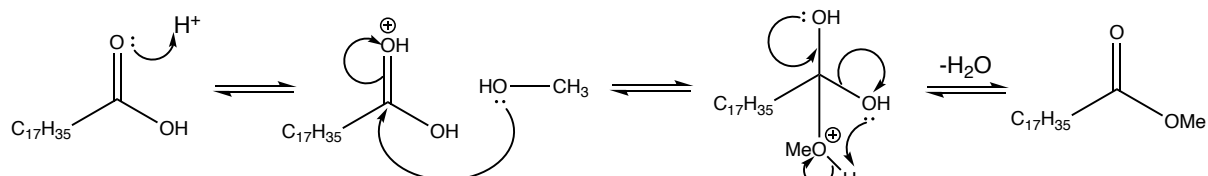
Schematic 1 *– Acid catalysed esterification of the free fatty acid stearic acid (C18:0) to methyl stearate.*
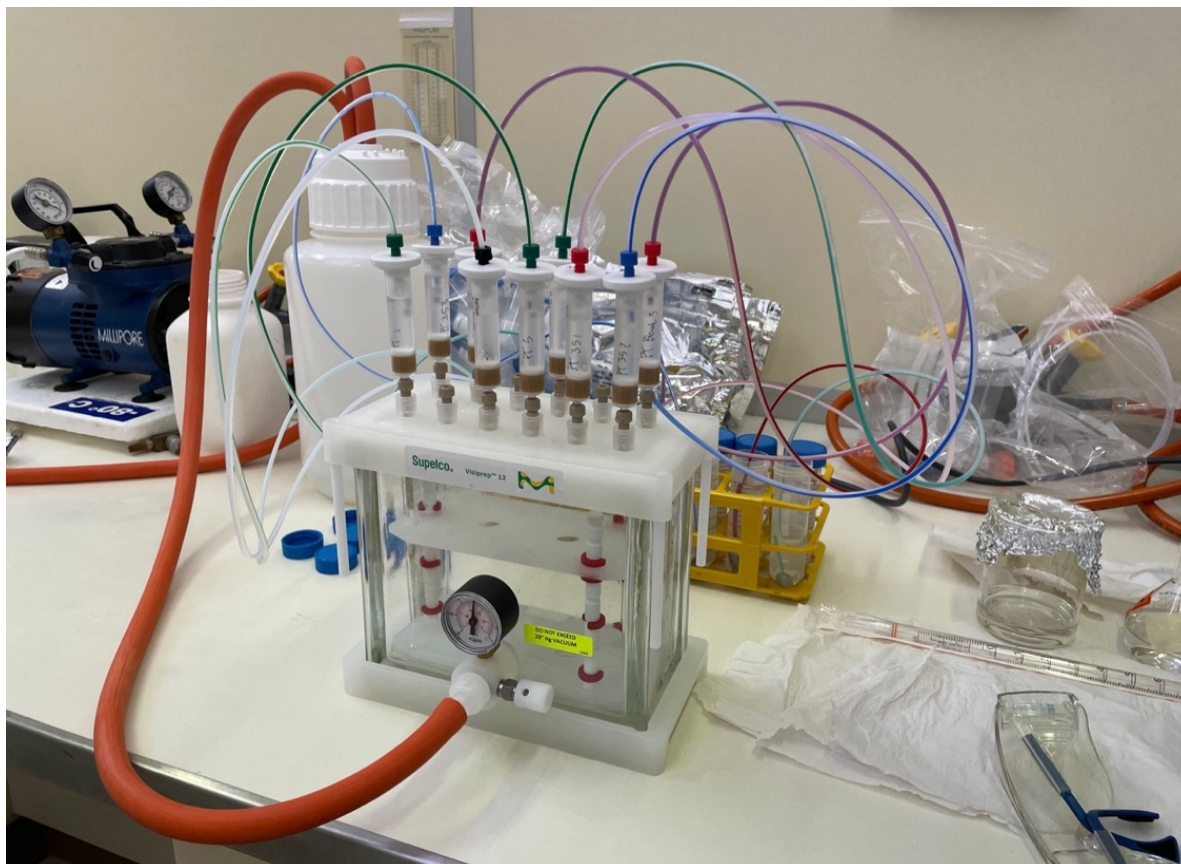
Figure 6 – *Updated apparatus used for solid phase extraction featuring the new cartridge caps.*

A modified one-step method was used based on that developed by Abdulkadir *et al.*[42] with the modification being that the reaction was catalysed by sulfuric acid rather than boron trifluoride.[43] The change in catalyst was to improve the safety of the procedure as boron trifluoride is a high hazard substance. The version of the one step method used in this project is described below.

Prior to the addition of the esterification reagents, an internal standard was added. What was used as the internal standard as well as when and how much was added was changed as the project progressed. For simplicity, the final compound and amount added is used in the following description and the variations in the internal standard usage are described and explained in a later section of this chapter.

An internal standard solution was prepared with ca. 0.1 mg mL^{-1} (actual concentration varied per batch) of methyl nonadecanoate (analytical standard, $\geq$ 98% GC, Sigma-Aldrich) in hexane ($\geq$ 95% HPLC grade, Fisher Chemical). 50 μL of this solution was added to the methanol eluents produced from the SPE (as described in previous section). This was followed by sulfuric acid (puriss., 95-97%, Sigma-Aldrich). For the PML and Mallorca phytoplankton cultures samples (described in Chapters 3 and 4 respectively), 0.156 mL of sulfuric acid was added, whereas 0.103 mL was added to the CONNECT samples (Chapter 3). This was to create a 2.5% sulfuric acid in methanol mixture by volume, with methanol being the reagent in excess for the esterification. 4 mL of hexane ($\geq$ 95% HPLC grade, Fisher Chemical) was then added and the headspace of the vials was flushed with nitrogen and screwed tight. Hexane was used in this

process as an extraction solvent for the FAMEs formed following esterification. The nitrogen atmosphere was added to reduce the risk of oxidation reactions occurring across the double bonds of unsaturated compounds during the esterification. The vials were heated for two hours on a hotplate. A temperature to which the vials were heated could not be given due to the hotplate not having a temperature sensor and that the temperature of the reaction mixture could not be directly measured due to the vials being sealed during heating process. The starting time of the reaction was when the reaction mixture was refluxing off the sides of the vials. Note that at the start of this project, basic paper lined plastic caps were used for the scintillation vials. The vials were subsequently changed for those with a PTFE lined septa which provided a better seal against leakage of gaseous solvents and did not disintegrate during the heating process.

After two hours, the vials were removed from the heat and allowed to cool for 30 minutes. It is possible that the reaction continued after the heat was removed which is why this cooling period was standardised as much as possible. Quenching of the reaction was not possible prior to this time due to the temperature change of the solution causing the reaction media to explode out of the vial. Following this cooling period, approximated 2 mL of distilled water was added to quench the reaction and force the FAMEs into the organic hexane layer. A further 1 mL of hexane was added to the mixture to replace any that may have been lost via evaporation while the vials were heated. The vials were shaken vigorously, and the aqueous layer was disposed of. This was repeated twice more to reduce the sample acidity as acidic samples can damage the GC-MS instrument and breakdown the column. The final aqueous and hexane layers were transferred to a 15 mL centrifuge tube and vortex centrifuged until the layers were adequately separated. The top hexane layer was collected using a glass Pasteur pipette, being careful not to remove any of the aqueous layer. The hexane layers were collected into clean, muffled scintillation vials and reduced in volume using nitrogen. The reduced hexane samples were then transferred to GC-MS 1.5 mL autosampler vials (short thread autosampler vial, amber vial, 11.6 x 32 mm, Supleco) and reduced to dryness using nitrogen. The dried samples were finally redissolved in 100 μL of hexane (≥ 95% HPLC grade, Fisher Chemical). The reason for the samples being transferred to smaller vials before being reduced to dryness was to aid the recovery of the 100 μL final sample as these were pipetted into glass vial inserts (certified glass inserts for 12 x 32 mm, large opening vials, Supelco) prior to analysis due to their low volume. The samples were stored at -18 °C until analysed via GC-MS. The complete experimental process described in the previous two sections is summarised in **Schematic 2**.

GC-MS Parameters
Initial Parameters
The samples were analysed on an Agilent Technologies 6850 GC and 5975C inert XL EI/CI MSD with Triple-Axis Detector. The GC column was a Phenomenex Zebron ZB-FAME column which had a length of 30 m, internal diameter of 0.25 mm and film thickness of 0.2 μm. This column was specifically designed for the efficient separation of FAMEs, including the separation of the stereoisomers of a single species. As per the guidance set by the manufacturer of the column, the following injection and oven parameters were initially used. The injection volume was 1 μL with a split ratio of 5:1. The oven temperature ramped initially from 50 °C to 140 °C at 10 °C min^{-1} then to 190 °C at 3 °C min^{-1}. The oven temperature was finally increased to 260

°C at 30 °C min^{-1} and held at this temperature for 6 minutes. With regards to the MS parameters, the mass spectrometer was set to scan between m/z 50 to 500.

Initial Parameter Assessment

To assess the suitability of the initial GC-MS parameters, a recovery experiment was carried out using the above SPE and FAME conversion methods on artificial seawater made with Instant Ocean salt spiked with fatty acids. The fatty acids were linolenic acid (18:3ω3), oleic acid (18:1ω9), myristic acid (14:0), palmitic acid (16:0), palmitoleic acid (16:1ω7), linoleic acid (18:2ω6), stearidonic acid (18:4ω3), docosapentaenoic acid (22:5ω3) and docosahexaenoic acid (22:6ω3). These fatty acids have been observed in seawater and, from the phytoplankton fatty acid literature data, have been found to be abundant in phytoplankton.[17] In these experiments, Instant Ocean solutions were made by adding approximately 33 g of Instant Ocean salts to 1 L of ultra-pure water. 10 mg of each fatty acid was dissolved in 10 mL of acetone and 20 µL of these solutions were added to the Instant Ocean solutions to give a final concentration of 20 µg L^{-1}. 100 µg of an internal standard of nonadecanoic acid dissolved in acetone was added prior to the SPE step. In addition to the spiked samples, blank Instant Ocean solutions were also analysed that only contained the internal standard. These solutions were either extracted immediately or stored at 4 °C for less than a day before extraction. In the first experiment the final dried samples were redissolved in 1 mL of hexane. Note that the internal standard methodology is different to that described in the final SPE method description given in the previous section. These experiments also provided information on how best to use an internal standard in this project and this will be discussed further in a later section of this chapter.

The GC-MS chromatogram of the first recovery experiment is shown in **Figure 7**. Of the fatty acids added to the Instant Ocean solutions, all were recovered except for 22:5ω3 and 22:6ω3, note that the identity of 18:4ω3 could not be verified for certain due to it not being present in the FAME standard. This was likely due to the FAMEs of these fatty acids could be eluting after 30 minutes, making their presence obscured by the high levels of noise towards the end of the run which is caused by column bleed.

Organics present in the instant ocean salts were also retained by the PPL cartridges, with dodecanoic acid (12:0) being the most notable. Stearic acid (18:0) was also observed both in the sample and blank chromatograms and is a common background signal, alongside 16:0.

Updating the parameters

Following the first recovery experiment in this series, another was carried out to investigate a new set of experimental parameters. In this case, the samples were prepared in the same way as described in the previous section with two changes. The internal standard was dissolved in methanol and added after the SPE step, for reasons explained later, and the final hexane volume was decreased to 100 µL used in the final FAME conversion methodology. This was done to increase the amount of analyte injected onto the column.

To reduce the noise of the chromatograms and increase the sensitivity of the instrument to the FAME of interest, a single ion monitoring (SIM) method was set up with high abundance fragment ions of each FAME group. The fragment ions are shown in **Table 2**. The first radical cation of interest is 74 m/z which is formed from the McLafferty rearrangement given in

Schematic 3. The remaining ions are positively charged alkenes of varying length. Note that the radical cation is not used for the identification and quantification of the unsaturated FAMEs as the double bonds within the species on ionisation can migrate to position 4 of the aliphatic chain making the rearrangement less likely, reducing the signal intensity of this ion.

For the setup of the MS method, it was decided that each of the 8 ions would be scanned with a dwell time of 50 ms. This was done due to the unknown nature of the samples as switching between ion pairs as timed events may have led to some compounds being missed, this was especially a problem for compounds with similar retention times. When quantifying these species, the first major ion is used, while the second was used as a qualifier.

In addition to the MS method changes, the GC oven programme was changed so that the temperature ramp from 140 °C continued to 220 °C rather than 190 °C. This was to allow the later eluting 22:5ω3 and 22:6ω3 time to come off the column. The GC-MS chromatogram of the second recovery experiment is shown in **Figure 8**. With the modified GC-MS and sample volume method, all the fatty acids were observed, although once again the identity of 18:4ω3, 22:5ω3 and 22:6ω3 could not be identified for certain due to the reason previously mentioned. In addition to this, no full mass scan (FMS) data could be generated for 22:5ω3 and 22:6ω3 as these peaks were well within the noise of the FMS chromatograms.

Due to the success of this updated method, it was used for all further quantification of FAMEs in samples going forward. However, as unknowns in samples need to be identified there was a continued need for an FMS per sample. Because of this it was decided that for each sample, one FMS injection would be run followed by three SIM injections. Unknown samples would be identified using the full mass scan data using Agilent MassHunter along with the NIST Mass Spectral Library. These compounds would then be quantified in triplicate again using Agilent MassHunter.
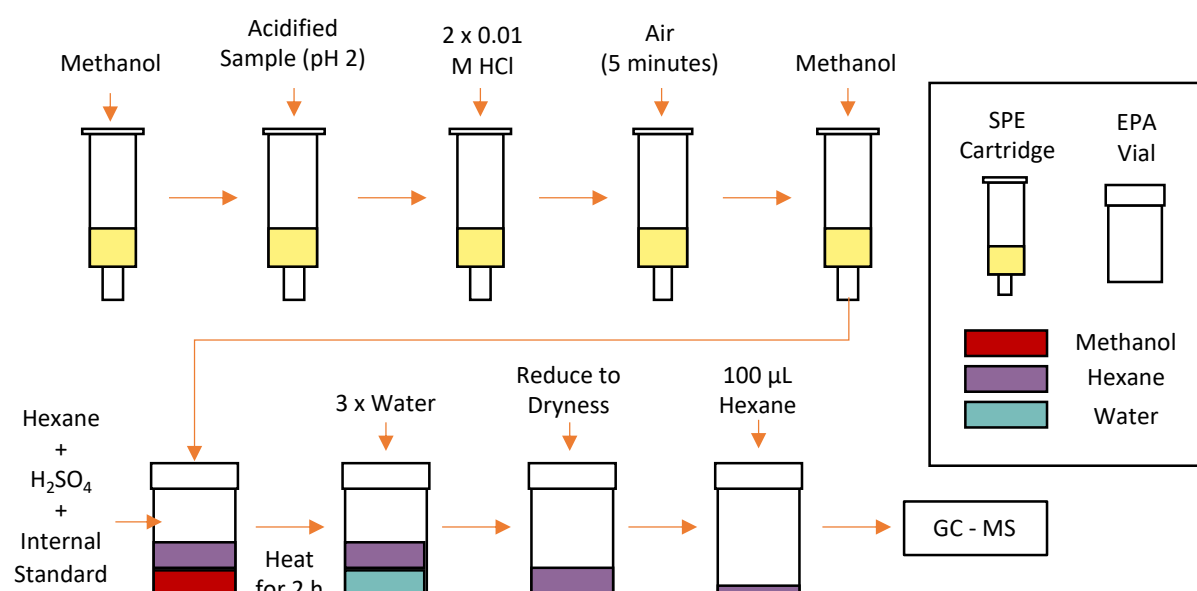
***Schematic 2** – Complete fatty acid extraction, esterification and analysis process.*
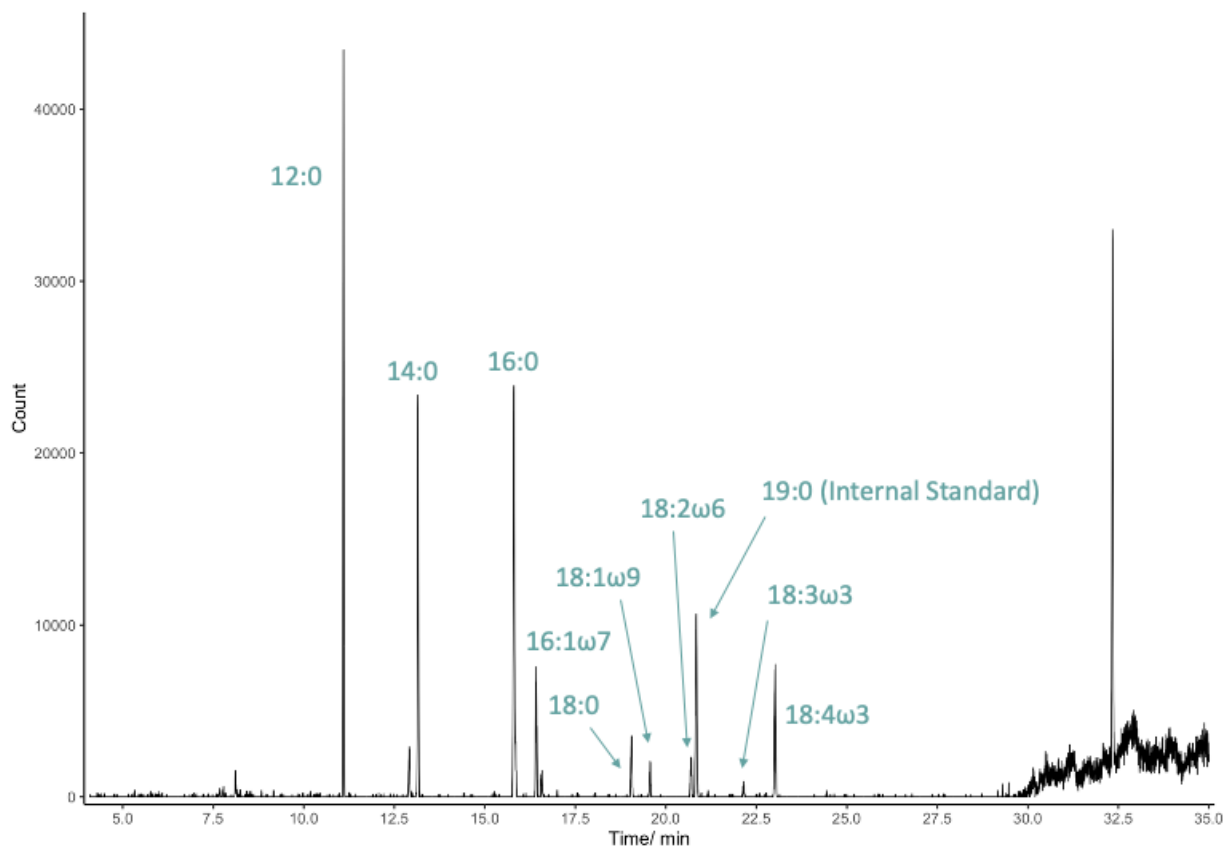
Figure 7 *- GC-MS chromatogram of Instant Ocean spiked with a variety of different fatty acids and analysed using a full mass scan mode.*

Table 2 *– FAME fragment ions.*

FAME Group	1st Major Fragment Ion	2nd Major Fragment Ion	Structure
Saturated	74	87	
Mono-unsaturated	55	69	
Di-unsaturated	67	81	
Poly-unsaturated	79	93	
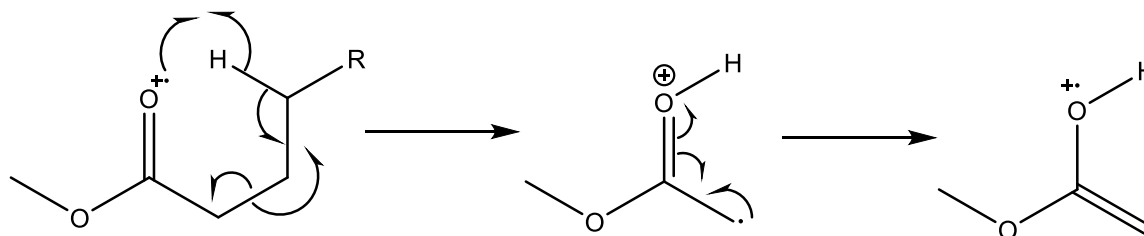
Schematic 3 *– McLafferty rearrangement.*

Choice and Use of Internal Standard

The internal standard used to aid quantify sample fatty acids and therefore FAMEs in the processed samples was methyl nonadecanoate (analytical standard, $\geq$ 98% GC, Sigma-

Aldrich). This compound was chosen as it is not frequently observed in seawater and marine phytoplankton.[17, 26, 29-31, 44]

In the initial stages of this project, as previously mentioned, nonadecanoic acid was dissolved in acetone and added to the sample prior to the extraction step. This would be as per typical use of an internal standard as it should be added as early as possible to account for losses from the earliest stage. However, due to the varying affinities of each individual fatty acid to the SPE sorbent, the loss of nonadecanoic acid is not representative of the general loss of all species. It was therefore decided to add nonadecanoic acid after the SPE stage by dissolving it in methanol and adding it directly to the eluent. It was hoped that by adding the internal standard as its acid, it would account for losses due to any incomplete esterification.

The samples were to be quantified by comparing the peak area ratio of the analyte to the internal standard to the same ratio within calibration standards. As such the internal standard used in the samples must also be used in the standards. Initially this was done by creating a methyl nonadecanoate stock solution at the same concentration as the nonadecanoic acid solution used in the samples and preparing it in hexane so it could be added directly to the standard. However, creating two different standards could lead to inaccuracies in quantification due to slight differences in the concentrations of the internal standard solutions. Because of this, the internal standard solution used in both the samples and standards was switched to, where possible, the same stock solution of ca. 0.1 mg mL^{-1}of methyl nonadecanoate (analytical standard, $\geq$ 98% GC, Sigma-Aldrich) in hexane ($\geq$ 95% HPLC grade, Fisher Chemical). Note that the use of the same solution was not always possible due to the delays in generating linear calibration curves, as described in the next section. In these cases, internal standard solutions were created at the same concentration to the precision of the laboratory balances.
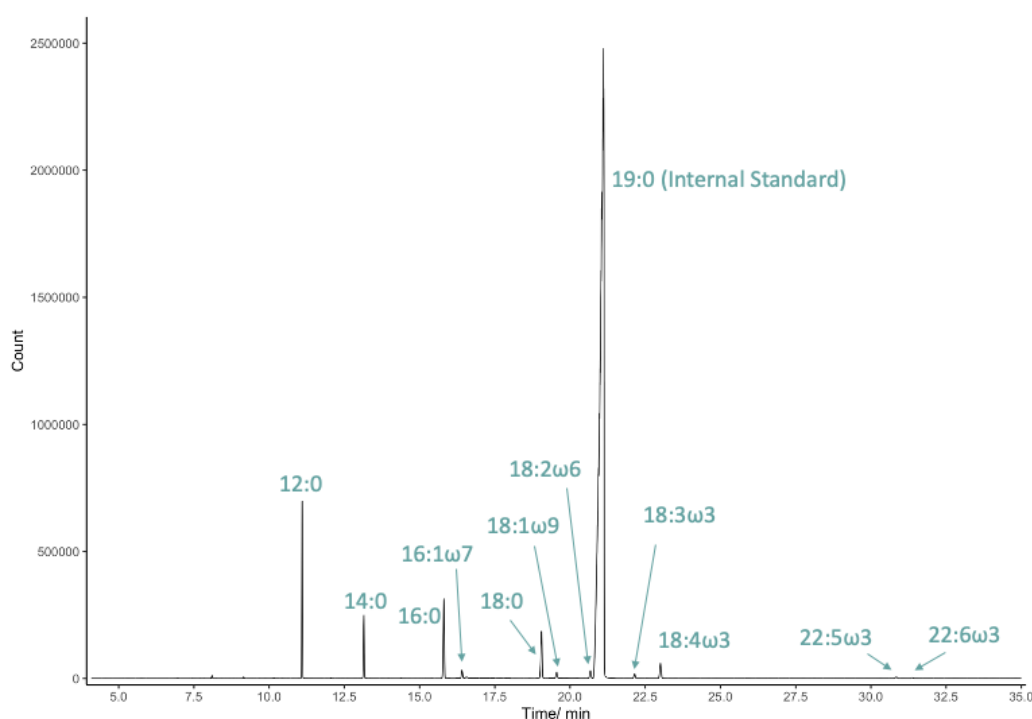
Figure 8 *- GC-MS chromatogram of Instant Ocean spiked with a variety of different fatty acids analysed using a single ion mode (SIM) method.*

29

Calibrations Curves

Improving Calibration Curve Linearity

In the initial stages of this project, calibration standards were made using a Grain FAME Mix (certified reference material, Supelco). This contained a variety of saturated and unsaturated fatty acids dissolved in dichloromethane. Standards were prepared via dilution with hexane (≥ 95% HPLC grade, Fisher Chemical) using micropipettes. Analysing these standards via GC-MS showed poor linearity between concentrations and peak areas as shown in the first plot of **Figure 9**. It was inferred that this was likely due inaccurate pipetting as volatile liquids tend to drip out of the pipette tip leading to inaccurate transfers.

To improve the linearity of the calibration curves a Gerstel MultiPurpose Sampler MPS was used instead to prepare the samples. This instrument consisted of two robotic arms equipped with a 100 μL and a 1 mL syringe which were used to dispense the stock standard solution, internal standard solution and solvent accurately. The improvement in the calibration curve linearity is evident in **Figure 9**. For this reason, all calibration standards used in this project were prepared using the Gerstel MultiPurpose Sampler MPS.

Stock Solution Production

Due to the composition of the samples analysed, the Grain FAME Mix was deemed to be an inappropriate stock. Stocks were instead prepared by creating a ca. 0.04 mg mL^{-1} solution of the following compounds in hexane (≥ 95% HPLC grade, Fisher Chemical) and diluted to within the concentration range of 0.0001 μg mL^{-1} to 10 μg mL^{-1}:

- Methyl octanoate
- Methyl nonanoate
- Methyl decanoate
- Methyl undecanoate
- Methyl dodecanoate
- Methyl tridecanoate
- Methyl tetradecanoate
- Octanedioic acid dimethyl ester (Dimethyl suberate)
- Methyl hexadecanoate
- Methyl palmitoleate
- Nonanedioic acid dimethyl ester (Dimethyl azelate)
- Methyl 9,12,15-octadecatrienoate (Methyl linolenate)
- Decanedioic acid dimethyl ester (Dimethyl sebacate)
- Methyl octadecanoate (Methyl stearate)
- Methyl oleate
- Methyl linoleate

These compounds listed above do not cover all the species observed in the samples as many compounds were either not readily available or prohibitively expensive. As such tetradecenoic acid (14:1), hexadecadienoic acid (16:2), hexadecatrienoic acid (16:3), hexadectetraenoic acid (16:4), octadecatetraenoic acid (18:4), hexanedioic acid (D6), heptanedioic acid (D7), undecanedioic acid (D11), dodecanedioic acid (D12) and tridecanedioic acid (D13) concentrations were estimated using the standard of the most structurally similar compound. Note that when compounds were detected but their peak area

was less than ten times that of the peak areas of the surrounding noise, i.e. below the limit of quantification (LoQ), their concentration was quoted at half the concentration of the lowest calibration standard of the compound used for quantification.
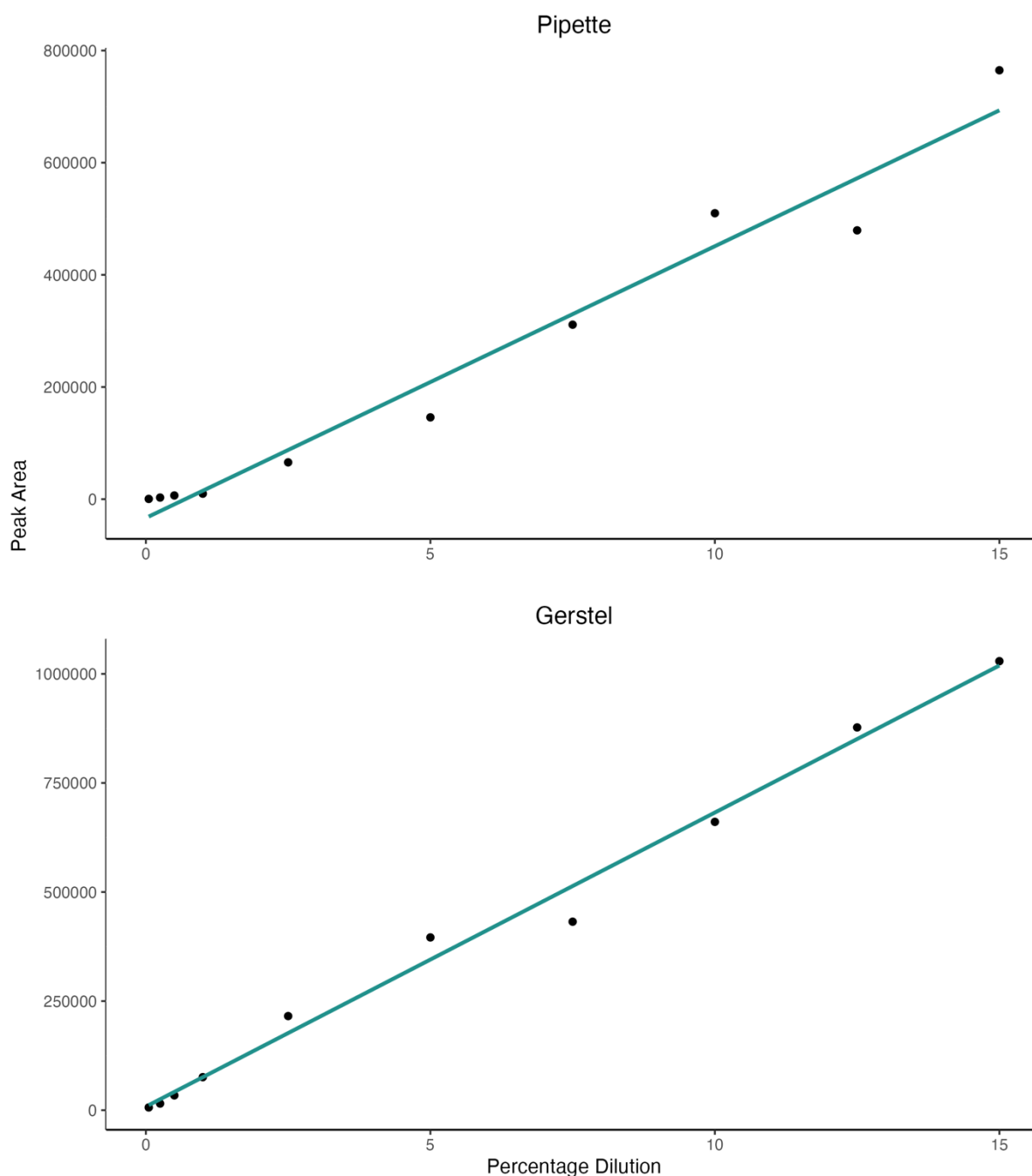
Figure 9 – *Calibration curves of methyl octadecanoate standards produced either via manual pipetting (y = 1.99 x 10^{-5}(± 1.4 x 10^{-6})x + 0.859(± 0.47), r^2 = 0.9644) or by the Gerstel MultiPurpose Sampler MPS (y = 1.47 x 10^{-5}(± 5.1 x 10^{-7})x - 0.068(± 0.27), r^2 = 0.9903).*

Evaluation of the Method

To assess the fatty acid extraction efficiencies of the SPE and FAME conversion methods, a series of aqueous fatty acid solutions were prepared with a salinity that was comparable to that of seawater. 35 g sodium chloride was added to 6 x 1 L MQ water. Into three of these solutions 50 µL of a fatty acid stock solution was added. This stock solution contained

approximately 0.1 mg mL^{-1} of a variety of saturated and unsaturated fatty acids as well as diacids dissolved in acetone. The remaining three sodium chloride solutions were blanks. Two sets of these six sodium chloride solutions were prepared. The first was extracted directly using the SPE method described below, while the other set was filtered through pre-combusted 20 mm GF/F filters prior to extraction to assess any losses to the filters.

The percentage recoveries of the fatty acids from the filtered and unfiltered aqueous fatty acid solutions are shown in **Figure 10**. The greatest extraction efficiencies were observed for C9-C12 (CX representing any fatty acid with X number of carbon atoms) saturated fatty acids as well as the diacids of similar aliphatic chain lengths, with the C10 species overall showing the greatest recovery when only considering the filtered dataset, indicating that these species have optimal adsorption to the sorbent and later elution with this method. The reason for the decreasing recoveries of the increasing molecular weight species may have two explanations. The first is that the affinity between the sorbent and the molecules for them to be adequately captured by the cartridge, or that the affinity is too strong for efficient elution to take place. It is also observed that the recovery increases with number of double bonds for the same number of carbon atoms. This may be due to increased interactions between the double bonds and the vinyl groups of the sorbent while still being soluble enough in the washing solvent to be eluted.

The uncertainties in the recoveries of compounds smaller than and including 12:0 were larger than all the other species and the reason for this is unknown. However, a notable feature of these compounds in their FAME form are their decreased boiling points. Because of the variable amounts of time spent in the reduction of the samples with nitrogen due to the equipment available, it may have led to variable losses of these volatile compounds during this step. This factor may also explain why octanoic acid (8:0) has a relatively low recovery when compared to the other smaller species. However, the strong affinity to sorbent relative to the eluting solvent may also be a factor as previously explained.

When comparing the filtered and unfiltered samples, no trend is observed in the recovery percentages. Most are close to or within the uncertainties of each sample type. There are, however, notable differences between the filtered and unfiltered samples for octanoic acid, nonanoic acid and octadecanoic acid. These compounds seem to exhibit significant losses when filtered. For octanoic and nonanoic acid, it could be that their higher polarity is causing them to adhere to the filters but the cause for the lower octadecanoic acid concentrations in the filtered samples is unknown. For sample quantification reported in this thesis, concentrations were calculated using the recovery efficiencies of the filtered samples, since all seawater samples were filtered prior to extraction.

Overall, the combination of the SPE and FAME conversion methods provides a viable alternative to liquid-liquid extraction for the extraction and purification of fatty acids from large volume aqueous media. The recoveries are lower than those that can be achieved for liquid-liquid extraction, up to 98% for octadecanoic acid, but the fact that there is little sample preparation and extraction can be carried out with minimal manual input makes this method desirable.[31] This method makes the extraction of numerous, large volume samples manageable, which was a requirement for this project. This advantage is clearly demonstrated when considering the volumes of solvent that would be required if this project

was to be carried out using liquid-liquid extraction. Slowey *et al.*[31] extracted fatty acids out of 6 L of seawater using 3 x 600 mL ethyl acetate. During this study approximately 500 L of seawater have been processed, which would equate to around 150 L of ethyl acetate being used if the previous liquid-liquid extraction method was utilised. Not only is this impractical in a laboratory setting, but virtually impossible during field work, such as the cruise that formed part of this study.
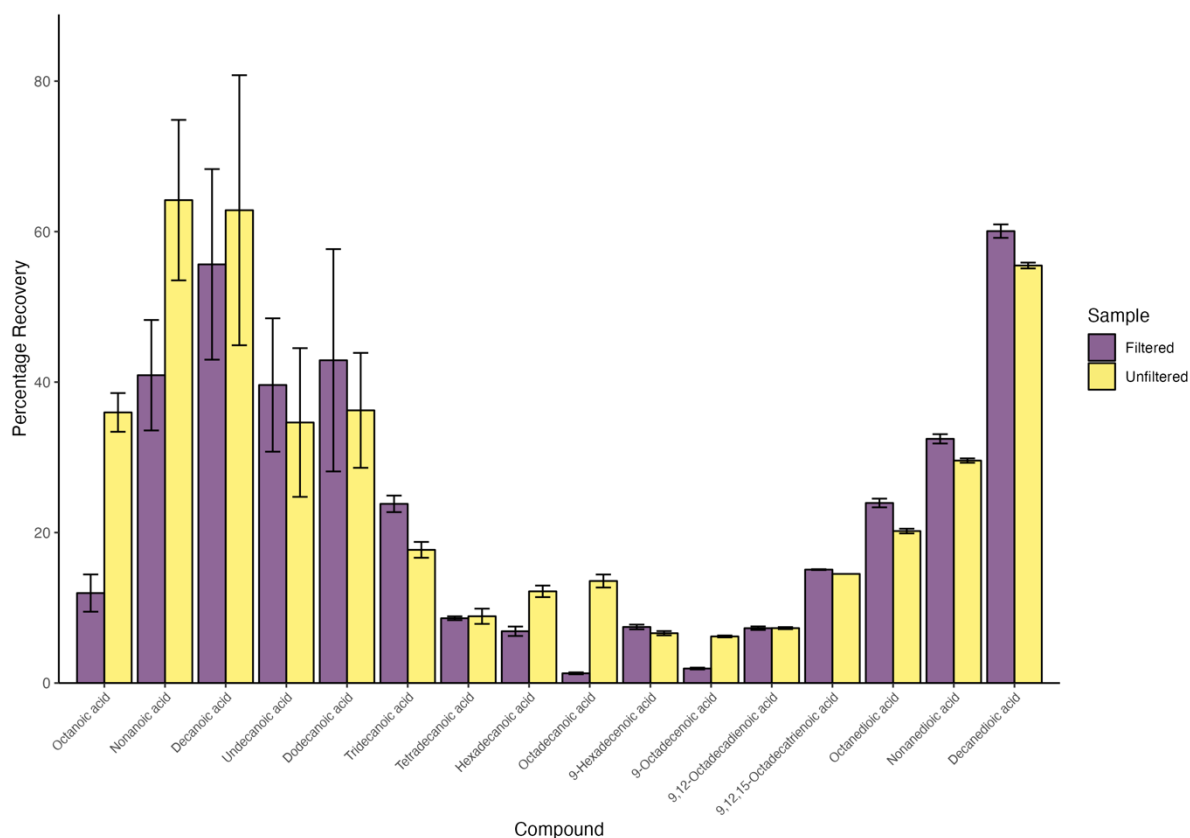
Figure 10 *– Percentage recoveries of filtered and unfiltered*

Evaluation of Sampling Methods

Garrett Screen Exposure Tests

The SML samples collected in this study were collected via a Garrett screen which is a metal mesh within a solid metal frame.[45] This mesh is submerged into the water and then pulled up horizontally so that the top surface layer is collected within the gaps of the mesh due to surface tension. This method was chosen for this study due to the equipment already being readily available. The water collected on the mesh is then collected in glass or HDPE bottles.

While the water is on the screen, the collected surfactants are exposed to the atmosphere where they can potentially react. In the context of this study, it is possible that the unsaturated fatty acids could react with atmospheric ozone, decreasing their concentration during sampling. To assess whether there were any measurable losses of unsaturated fatty acids during Garrett screen sampling due to ozonolysis, screen exposure experiments were carried out. Two separate experiments were carried out and the samples were analysed with the SPE and FAME conversion methods discussed earlier.

For the first test, 41 L of MQ water was decanted into 1 L HDPE bottles. Into these bottles, 200 µL of a stock solution of fatty acids was added. This stock solution was the same as that prepared for the recovery experiments. 8 L of these solutions were decanted into a plastic box from which a surface sample was collected using a Garrett screen, note that these experiments were carried out outside so that atmospheric ozone concentrations were comparable to that observed during environmental sampling. For the first set of samples, the screen was submerged and then immediately drained; this was the 0 s sample. The box was then emptied and replaced with a fresh 8 L of the fatty acid solution and the process was repeated with 15 s, 30 s and 60 s exposure times, replacing the 8 L fatty acid solution for each exposure time. The additional exposure times were achieved by holding the screen above the box for the designated time before draining. For each exposure time, a 1 L surface sample was collected.
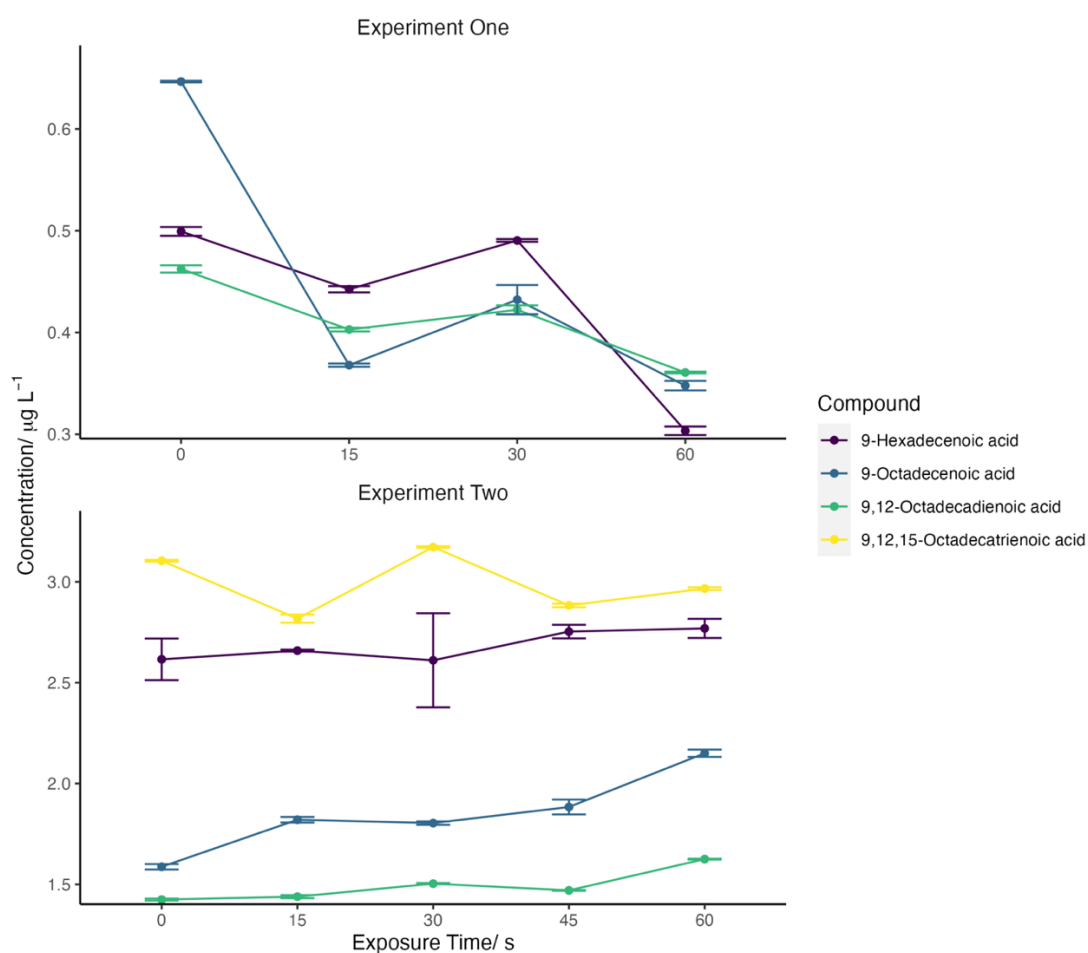
***Figure 11** – Unsaturated fatty acid concentrations following exposure to ambient air at different time intervals. 9,12,15-Octadecatrienoic acid was not quantified in the first screen exposure experiment because of poor recovery pushing the concentrations below the limit of quantification. The first concentration given for 9-Octadecenoic acid in experiment one is likely anomalously high, although the cause of this is unknown so the data point is included in this plot.*
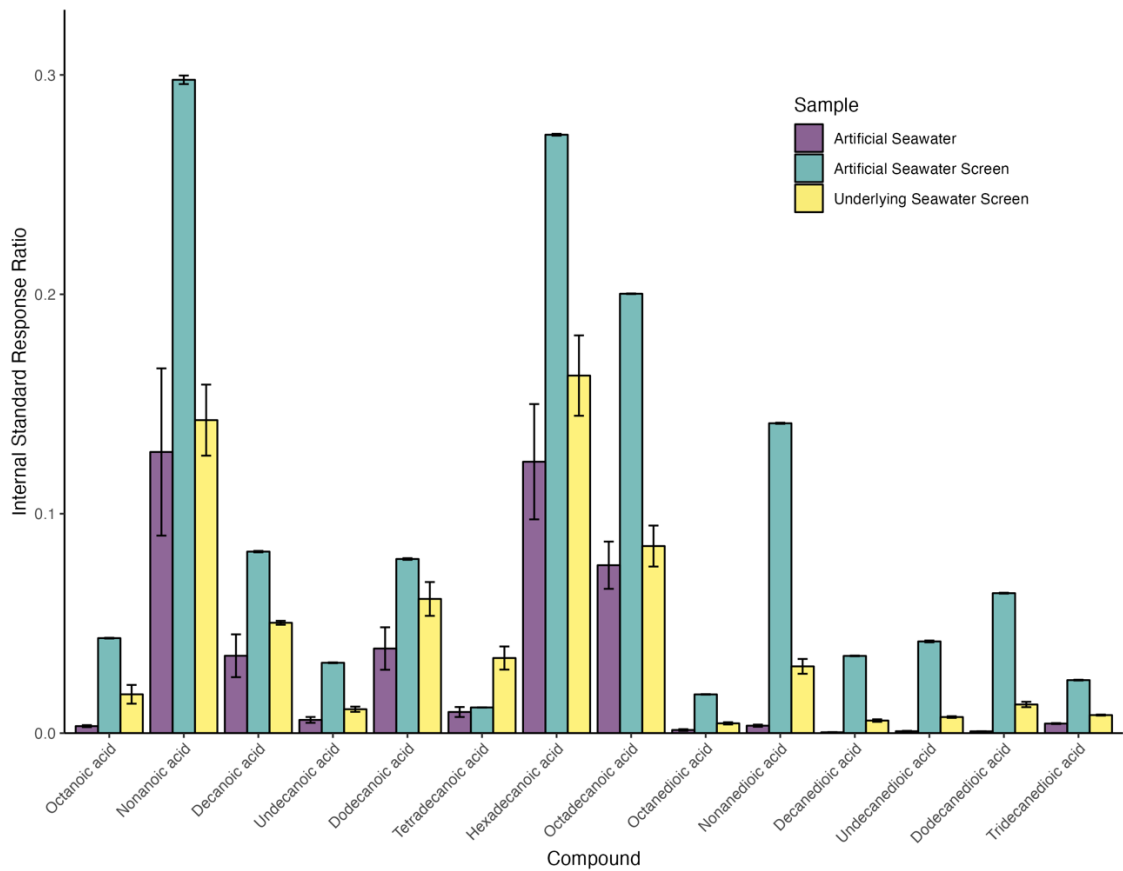
Figure 12 *- Internal standard response ratios for the fatty acids and diacids found in the PML blank test sample.*
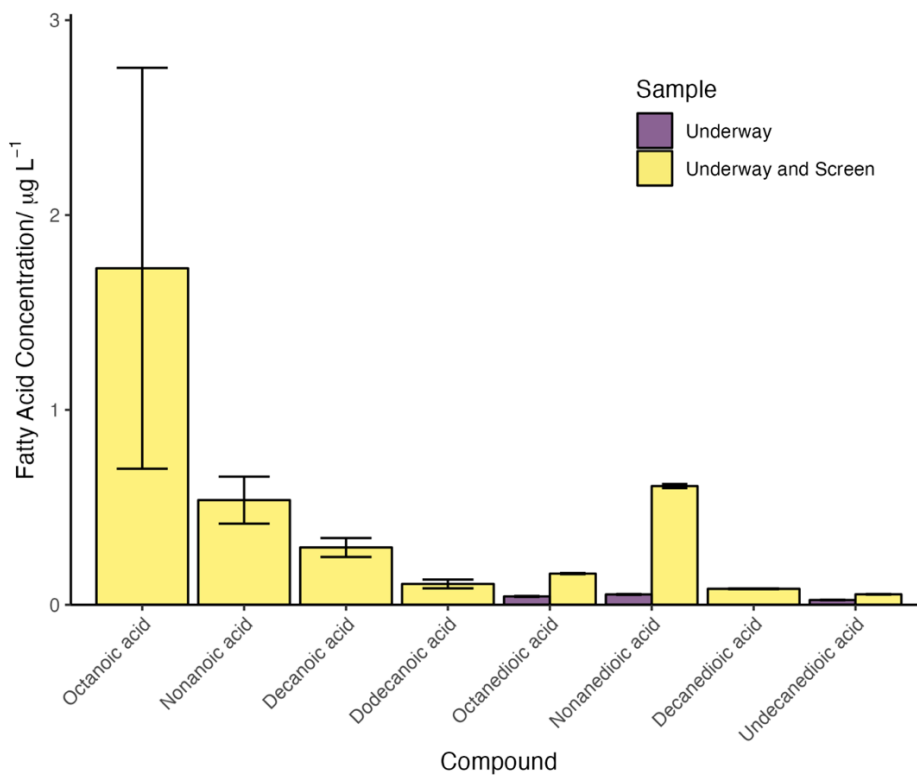
Figure 13 *– Fatty acid and diacid contamination from Garrett screen used on the CONNECT transatlantic cruise.*

For the second test, 9 L of aged seawater from Cape Verde was added to the box followed by 18 mL of the stock fatty acid solution. More of this stock was added for this experiment because only approximately 130 mL would be taken as a sample. The seawater mix was also not replaced and instead mixed, so adding more of stock would reduce the risk of the fatty acids becoming depleted during subsequent sampling of the seawater mix. The above sampling method was repeated with the exposure times of 0 s, 15 s, 45 s and 60 s.

Both screen exposure experiments show that exposure to ozone during Garrett screen sampling has no significant impact on the concentrations of unsaturated fatty acids below 60s (**Figure 11**). There is a drop in concentrations at 60s but this was only observed in the first experiment. It is likely that ozonolysis reaction rates are too slow to have an impact over typical sampling timescales, as these will likely not exceed 60s. It should be noted, however, that ozone concentrations during these experiments were typically 20 ppb and it should not be assumed that there is no impact on unsaturated fatty acids concentrations if ozone concentrations are significantly higher than this in the field.

Bottle and Garrett Screen Contamination
Alongside the SML and ULW samples from PML, procedural blanks were also collected which consisted of artificial seawater that was poured over the Garrett screen used to collect the SML samples. It was later found that these blanks were contaminated with compounds found in the SML so further blanks were also investigated. These included artificial seawater blanks which had not been passed over the Garrett screen, ULW that had been passed over the Garrett screen and ULW that was stored in either plastic bottles or glass bottles. An SML sample stored in glass bottles was also collected. Note that for the glass bottles, some were only acid washed using 4% HCl, as per the bottle washing protocol of the PML campaign, while others were both acid washed and muffled at 450 °C for 2 hours. These blanks were chosen to assess the contamination risk from both the Garrett screen and the plastic storage bottles which were washed and reused throughout the campaign.

Plots of the internal standard response ratios for the fatty acids and diacids found in these blanks are shown in **Figure 12**. The blank which was prepared by passing artificial seawater over the Garrett screen contained the highest amounts of fatty acids and diacids when compared to both the artificial seawater on its own and ULW. It is likely that the Garrett screen retained compounds from the SML sampling and transferred them to the blank, by extension transferring them to other SML samples. The potential reason why the underlying seawater that was passed over the screen did not exhibit such high amounts of fatty acids and diacids as the artificial seawater could be the ordering of which sample was passed over the Garrett screen first, i.e. the artificial seawater washed some of these compounds off the Garrett screen prior to it being exposed to the underlying water. In addition to carry over and regarding the diacids, there is also a possible contribution of manmade lubricants leaching off the Garrett screen as diacids are a known constituent. Contamination was also observed in the CONNECT cruise where the Garrett screen introduced short chain fatty acids and diacids to samples collected from the underway system of the ship (**Figure 13**). When comparing the measured contaminant concentrations to those in the samples, the saturated fatty acids had the potential to contribute 10% to 70% of the respective measured saturated fatty acid concentrations, whereas the diacids contributed 34% to 104% to the diacid sample

concentrations. It was therefore important to consider the influence of these contaminants when SML samples were analysed throughout this study. As a result of these findings, the washing protocol for the Garret screen was improved to include a hot water wash, followed by an ethanol wash and then a final wash is MQ water. This new washing procedure was introduced in March 2021 shortly after the contamination issue was discovered.

With regards to the bottle tests, although the compounds contained within the ULW stored in both types of bottles were similar, the baseline signal below 15 minutes was reduced when glass bottles were used, as seen in **Figure 14**. The baseline of the SML sample stored in a glass bottle appeared to be in between the ULW plastic bottle samples and the ULW glass bottle sample. This could be explained by the increased amounts of organic matter found within the SML sample when compared to ULW. Because of this reduced noise in the baseline when acid washed glass bottles were used, samples collected after this test were stored in glass bottles. Note that there was little difference between the muffled and acid washed bottles compared to bottles that had just been acid washed hence why the glass bottles were only acid washed.
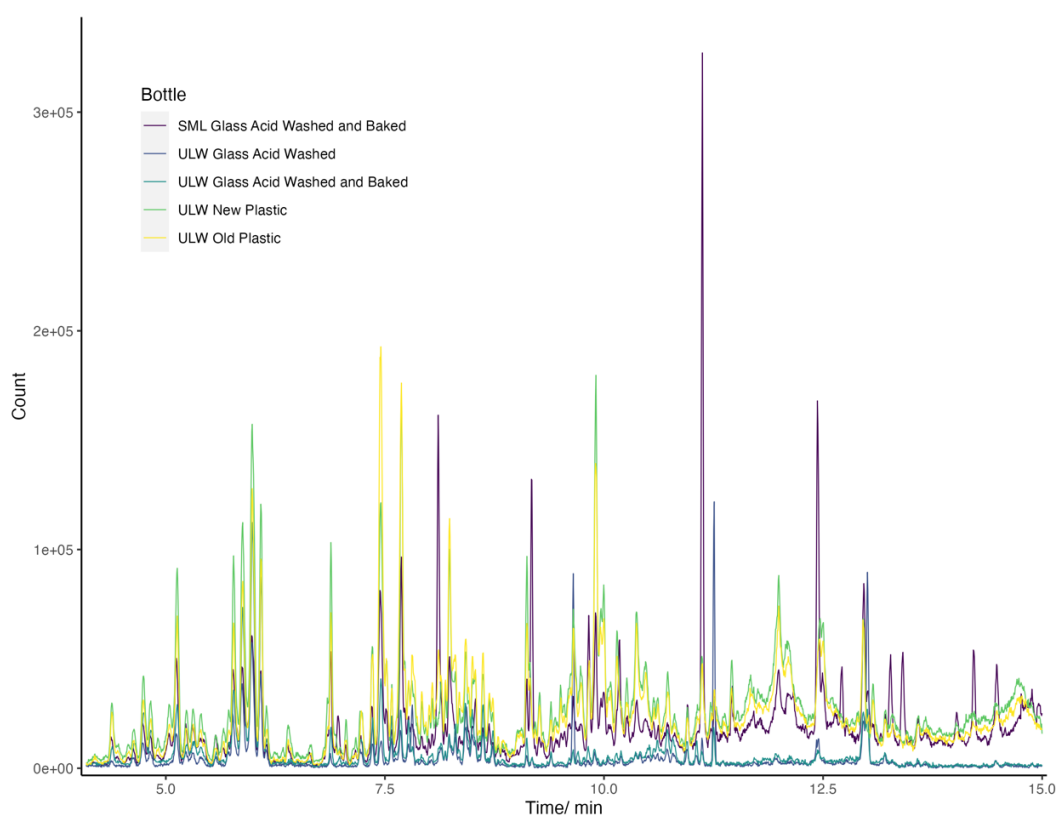
Figure 14 - *Overlayed GC-MS chromatograms of the bottle comparison samples from PML using the full mass scan MS method.*

Conclusions

The SPE method developed during this PhD has proven to be a convenient method of extracting fatty acid compounds from large seawater samples. The extraction efficiencies were not as high as for previous extraction methods, but these methods use litres of solvent per sample which is both costly and inconvenient.[31] The SPE method is more sustainable, utilising only mL of solvent, and is more convenient to deploy on field work where availability of large quantities of solvent may be limited. Extraction efficiencies of the SPE method are

highest for lower molecular weight fatty acids and diacids. In future work, efficiencies could be improved for larger compound by using SPE cartridges with a different sorbent such as C18. However, using the PPL cartridge was advantageous for this study as it allowed for the samples used for non-targeted screening of DOM to be collected using the same method, and as such the samples could be directly compared.

The addition of the FAME conversion step has made it possible to analyse the fatty acids by GC-MS, allowing for both qualitative and quantitative analysis. The choice of GC column as well as moving to a SIM mode of MS analysis proved ideal for the analysis of marine fatty acids in both selectivity and sensitivity. The sensitivity of this MS method could be improved by switching between pairs of fragment ions depending on the FAME expected at that point in the run. This could be done for samples of unknown compounds by splitting the analysis into two sets of runs. The samples would first be analysed via an FMS and the data will be processed. Once compounds have been identified, the samples would be run again in SIM mode. However, this would be time consuming and the compounds within the sample could degrade between those two runs. Also, carrying out FMSs on the samples with the MS used in this study was not optimal as it is a quadrupole system. The sensitivity of the method could be further improved by using a time of flight (ToF) instrument for FMSs. But again, this would be time consuming as two separate instruments would be involved in the analysis.

The evaluation of the sampling procedures provided some insight into how these methods could influence the derived concentrations of fatty acids in the samples. Firstly, the concentrations of reactive, unsaturated fatty acids remain unchanged on the timescales expected for sample collection with regards to SML samples. However, the Garrett screen itself used for sampling is a source of contamination of saturated fatty acids and diacids, although fortunately it does not seem to be a source of unsaturated fatty acids. Care should therefore be taken when considering the concentrations of these species in the SML samples. Finally, although the bottles themselves did not seem to contaminate the samples with fatty acids, they did boost the baseline noise, which is often caused by a mix of alkanes. Switching to the glass bottles therefore slightly increased the sensitivity of this method to the smaller fatty acids that eluted prior to 15 minutes.

Chapter Three – Analysis of Seawater from the Footprint of the Penlee Point Atmospheric Observatory and CONNECT SO287 and Impacts on Ozone Uptake

Preface to Chapter

This chapter alongside the recovery experiment data described in the previous chapter is intended to be published and the majority of this text will be featured in said publication. The text in this chapter was produced by myself with amendments and additions made by Lucy Carpenter and Rosie Chance. The data used in this section was mostly produced by myself except for the chlorophyll data for both sampling campaigns. The PML chlorophyll data was supplied by the team at the Plymouth Marine Laboratory and the CONNECT chlorophyll data was supplied by Alexandra Rosa who was a fellow participant of CONNECT SO287.

Introduction

Ozone is a key tropospheric gas due to its reactivity and infrared absorbing capabilities. It is an atmospheric oxidising agent, a potent greenhouse gas and an air pollutant, all of which make understanding its fate in the atmosphere crucial in order to assess its impacts on climate change and human and ecosystem health.[46] Ozone is produced in the troposphere by *in situ* production from the reactions of VOCs and NO_x and also enters in smaller amounts via transport from the stratosphere. Alongside photolysis, dry deposition is an important sink of tropospheric ozone, with approximately 600-1000 x 10^{12} g of ozone being lost each year via this route, accounting for approximately 25% of total ozone loss.[1, 2, 7, 47]

It is estimated that about one third of ozone dry deposition occurs at the ocean surface but the absolute value of this ozone flux is highly uncertain.[1-3] It is thought that two of the key chemical drivers of oceanic ozone deposition are iodide and DOM.[3, 10] Marine DOM is estimated to amount to 685 x 10^{15} g of carbon, with concentrations ranging from 34-80 μmol kg^{-1}, and is primarily produced from marine photoautotrophic organisms.[48, 49] Surface-active components of DOM can become concentrated at the ocean surface as part of the SML. The SML covers much of the ocean and is enriched in organic and inorganic matter, including proteins, polysaccharides, humic compounds, waxes, free fatty acids, alcohols and glycerides.[13, 16, 50] The presence of an organic-enriched SML is important for a number of reasons. Surfactants can suppress ocean-atmosphere gas exchange through the formation of a physico-chemical barrier or through modifying the turbulent energy transfer, microscale wave breaking and through damping of small capillary waves.[51-55] Reactions of DOM in the SML also result in the formation of volatile reactive gases, and so impact their direct emission.[56] Unsaturated fatty acids and other components of DOM with carbon-carbon double bonds can react rapidly with ozone in a heterogeneous reaction at the ocean surface to produce oxygenated volatile organic compounds (OVOCs) like glyoxal.[39, 57] Aerosolised unsaturated marine DOM is also known produce oxygenated organic compounds such as dicarboxylic acids on photooxidation, whose hydrophilic nature increases the hygroscopicity of aerosols making them more efficient cloud condensation nuclei therefore potentially impacting climate.[58]

With regards to SML fatty acids, marine organisms such as phytoplankton produce fatty acids typically containing aliphatic chains of 12 to 24 carbon atoms long with varying levels of unsaturation; even numbers of carbon atoms are typically favoured by biology.[21, 22] Fatty acids and other lipids can enter the environment either via cell lysis, caused by biotic factors including grazing, viral infection and age or abiotic factors such as temperature and nutrient stress, or by direct excretion and mucilage formation.[25, 59] Being surface active, these compounds will become concentrated in the SML.

While there are a host of studies on fatty acid content of marine phytoplankton, very few studies have investigated dissolved fatty acid concentrations in seawater and to date there are no significant time series studies.[44] Nevertheless, current measurements have observed individual dissolved fatty acids concentrations between 0.039 and 144 µg L^{-1} in the SML and between 0.0007 and 50.8 µg L^{-1} in the ULW, with the highest concentrations being measured in polluted coastal regions.[17, 26, 29-31] In this chapter, the method developed in the Chapter 2 will be applied to open ocean and coastal seawaters samples, with the coastal samples being part of an 18-month time series.

Description of Chapter

The aim of this chapter is to demonstrate how the previously described extraction method can be applied to authentic seawater samples. The samples analysed were SML samples collected off the coast of Plymouth over an 18-month period (referred to as the PML campaign for the remainder of this report) as well as SML and ULW from the SO287-CONNECT cruise.

Experimental

Coastal Water Sampling

Coastal SML samples were collected at and around the marine monitoring station L4 in the English Channel (**Figure 15**). Station L4 is part of Western Channel Observatory of the Plymouth Marine Laboratory.[60] Samples were collected approximately weekly from the RV *Plymouth Quest* from 11/11/19 to 12/07/2021; the majority were collected from a near shore site in the footprint of the Penlee Point Atmospheric Observatory[61] (referred to as PPAO samples hereafter), while one in six samples were collected from the L4 site itself (referred to as L4 samples hereafter). SML samples were collected using a Garrett screen. To facilitate rapid (<40 minutes) collection of large volumes of microlayer, a screen with a mesh size of 1.44 m^2 void space was used, which resulted in an SML sampling thickness of ~500-800 µm. The average exposure time of the screen to air during sampling was (33 ± 5) s per dip. Note that the previously described exposure tests, which involved exposing a stock fatty acid solution on the Garrett screen to air, showed no losses of fatty acids on the Garrett screen for exposure times up to at least 45 s.

Initially, 1 L samples were collected for fatty acid analysis, but this was increased to 2 L on 04/05/2020 to improve sensitivity. All samples were filtered through GF/F filters and then frozen at -20°C until extraction and analysis. SML samples collected up to the end of April 2020 were found to be contaminated with di-acids, thought to arise from residual manufacturing greases on the Garrett screen. Because of this, these early samples were removed from the results presented here. As mentioned in the previous chapter, an improved

cleaning protocol was introduced part way through the campaign to reduce contamination from the Garrett screen.

Open Ocean Sampling

Open ocean samples were collected during the SO287-CONNECT cruise on board the RV *Sonne* from 11/12/2021 to 11/01/2022. The cruise transected the Atlantic Ocean from Gran Canaria to the Caribbean Sea, migrating upwards to the Sargasso Sea between 11/12/2021 and 11/01/2022, and ended in the Pacific. Sampling was carried out daily across the Atlantic and there were also two stations in the Pacific Ocean (**Figure 15**). For each sampling event, three seawater samples were taken. The first, termed 'Underway' hereafter, was taken from the underway pump (~6 m depth) at approximately 9 am local time each day as the ship was moving towards the station of that day. Underway samples were also collected on days when no stations took place, primarily in the Caribbean Sea. While the ship was on station, at the solar zenith, a second sample from ~ 5-6 m depth was taken from a Niskin bottle on one of the CTD rosettes. These samples are termed 'CTD'. The final sample was an SML sample collected using a Garrett screen with the same design as described above. Depending on the weather conditions, the screen was either deployed off the side of the ship using a crane, or by hand from a Zodiac motorboat approximately 100 m or further forward of the ship. At some stations, unsuitable weather conditions prevented SML sampling. All samples collected were 5 to 8 L in volume and prior to SPE, each sample was filtered through pre-combusted 90 mm GF/F filters using a negative pressure vacuum pump. SPE extractions were carried out on board ship within 1 hour of sample collection, and the methanol extracts were frozen at -20°C for return to the UK.
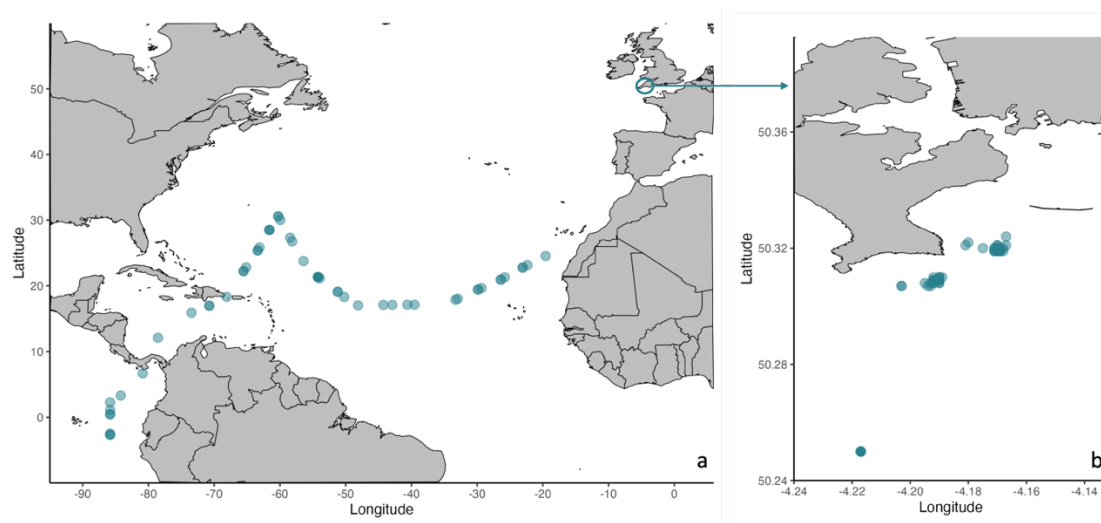
Figure 15 *– Seawater sampling locations indicated by the blue markers. The CONNECT samples are shown in plot a and the PPAO samples are shown in plot b. The geographical data for plot b was sourced from the Office for National Statistics licensed under the Open Government Licence v3.0. Contains OS data © Crown copyright and database right [2022].*

Solid Phase Extraction and FAME Conversion

For the seawater samples collected from both the PML campaign and CONNECT SO287, the fatty acids were extracted and processed using final SPE and FAME conversion methodology described in Chapter 2. There are, however, differences of note between the sample processing of each study.

Two different types of PPL SPE cartridge were used during these two campaigns. For the PML samples and the CONNECT underway samples 21/12/21 and 06/01/22, cartridges containing 0.5 g of sorbent were used. Whereas the remaining CONNECT samples, 1 g cartridges were used.

All concentrations were corrected with the filtered percentage recoveries calculated in Chapter 2 and blank subtracted using extracted ultra-pure water blanks processed in the same way. Note that for the CONNECT samples where a 500 mg PPL cartridge was used, the blanks for the PML campaign were used as they too used the 500 mg cartridge. A separate ultrapure water blank was carried out during the cruise for the 1 g cartridges.

Dissolved Organic Carbon Analysis
During both the coastal and open ocean campaigns, aliquots of filtered (GF/F) samples were frozen (-20 °C) for determination of dissolved organic carbon (DOC) once returned to the University of York. For this analysis, 9 mL of sample, ultrapure water blank or standard was transferred to a 12 mL acid washed glass vial and the vial covered with tin foil. Each vial was acidified with 10 % HCl to purge any inorganic carbon and analysed using an Elementar Vario TOC cube instrument. Standards were prepared using a commercial TOC standard (TOC standard 50 mg L^{-1}, 76319 – 250ML – F, Supelco) diluted with ultrapure water (MQ).

Chlorophyll-a Analysis
During the coastal time-series campaign, samples for extracted chlorophyll-a determination were collected by filtering between 0.1 and 1 L of water through a 47 mm diameter GF/F filter paper. The residue was extracted using 90% acetone, and chlorophyll-a measured by fluorescence using a Turner Trilogy fluorometer. During the CONNECT cruise, chlorophyll-a was measured using a fluorometer monitoring the continuous underway intake.

Results and Discussion
Concentrations of Dissolved Fatty Acids in the Coastal and Open Ocean
A typical chromatogram of a SML sample is shown in **Figure 16**, demonstrating the ability of the method to selectively resolve a broad range of fatty acids. Concentrations of the saturated and unsaturated fatty acids frequently observed in SML samples collected in the English Channel and Atlantic Ocean are shown in **Figure 17**, alongside measurements made in comparable previous work,[17, 26, 29-31] and summarised in **Table 3**. The marine fatty acids reported in the literature typically have aliphatic chain lengths of 12 to 30 carbon atoms, [17, 26, 29-31] whereas the fatty acids observed in this study tend towards shorter chain lengths (8 to 18 carbons). Similarly, branched fatty acids were also not observed in this study but have been reported previously. This may be a consequence of the different extraction methods used, as the SPE method with methanol elution used here will favour the smaller polar species relative to the liquid-liquid extractions with dichloromethane or ethyl acetate used previously.[17, 31] Note that this only affects the range of different compounds for which data is reported, not the concentrations themselves, as differences in recovery for detected species are corrected for.

Median total, saturated and unsaturated SML concentrations were 29.56, 11.22 and 5.56 µg L^{-1}, respectively, for the coastal samples and 15.69, 12.76 and 0.73 µg L^{-1} for the open ocean.

Individual fatty acid concentrations spanned several orders of magnitude, from 0.0005 to 46 µg L^{-1}. The individual compound median SML concentrations were 0.40 µg L^{-1} (0.0018 µM) for the PML study and 0.27 µg L^{-1} (0.0013 µM) for the CONNECT cruise. The equivalent median CTD and underway concentrations were 0.074 µg L^{-1} (0.00037 µM) and 0.063 µg L^{-1} (0.0003 µM) respectively.

Concentrations of SML fatty acids observed in the English Channel (PPAO and L4) are comparable to the previous observations made in other coastal regions including the Norwegian fjords and the northern Mediterranean coast (Gašparović et al.[17] and Daumas et al.[30]) (**Figure 17**). Average concentrations of the lowest molecular weight saturated fatty acids were substantially higher at the near-shore PPAO site compared to the L4 site, but this effect diminishes with increasing carbon number approaching 12, and concentrations are comparable for compounds with 12 carbons or more (**Table 3**).

With the exception of 8:0, the CONNECT SML samples have saturated fatty acid concentrations broadly similar to those observed at L4. 8:0 has a much higher average concentration, but this may be due to screen contamination (see Chapter 2). In contrast, concentrations of unsaturated fatty acids were substantially higher in the coastal SML samples (PPAO and L4) than the open ocean (CONNECT; **Table 3**). This may be due to the lower biological productivity of the tropical Atlantic relative to temperate coastal waters, as indicated by lower chlorophyll-a concentrations along the CONNECT cruise track compared to the PPAO and L4 sites (**Figure 18** and **Figure 19**). Despite the lower productivity in the tropical Atlantic, DOC concentrations are broadly similar when comparing the CONNECT and PML samples. Of the organic matter present in the open ocean, a greater proportion is likely to be aged due to the distance from regions of high primary productivity where these compounds are produced, and hence this fraction will have lower concentrations of compounds with short lifetimes such as unsaturated fatty acids.[17]
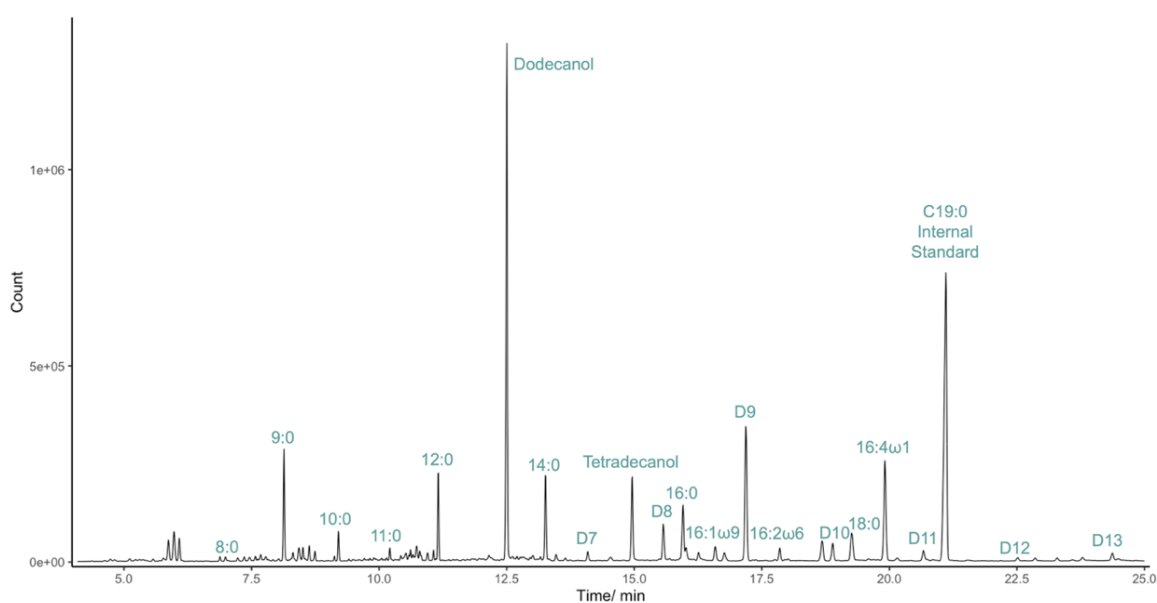
Figure 16 *– GC-MS chromatogram of a 2 L SML sample collected on 13/07/2020 in the footprint of the PPAO. See the caption for **Table 1** for the explanation of the compound codes. In addition to this nomenclature, the D used in these labels denotes a diacid with the number following corresponding to the number of carbon atoms in the aliphatic chain.*

43
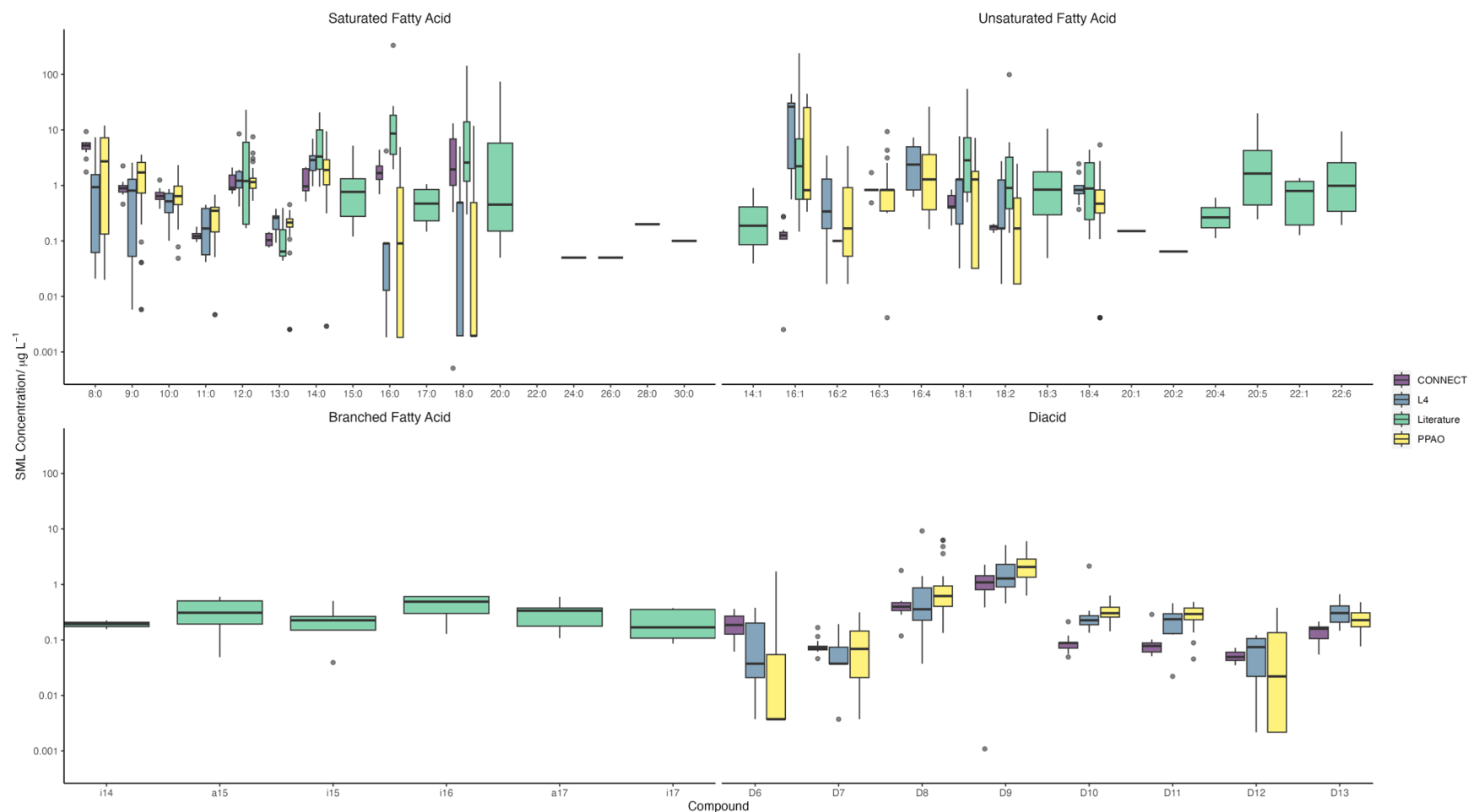
*Figure 17 – Fatty acid and diacid concentrations of the SML samples collected in the footprint of PPAO, at L4 and from the CONNECT cruise alongside literature SML concentrations, with the boxplots representing the first quartile, median and third quartile.[17, 26, 29-31] The boxes represent the interquartile range with the median shown within. Whiskers show the largest/smallest value smaller/greater than 1.5 times the interquartile range from upper/lower quartile. Values outside this range are marked as outliers. See the captions for **Table 1** and **Figure 16** for the compound code explanation. In addition to these codes, the codes starting with 'a' or 'i' represent branched fatty acids, with 'a' standing for anteiso and 'i' representing iso compounds. The number following the letters corresponds to the number of carbon atoms in the aliphatic chain.*

Table 3 – *Mean $\pm$ standard deviation (SD) and well as median fatty acid concentrations for PPAO, L4 and CONNECT seawater samples. These values were calculated across the entirety of dataset for each sample type. The 'n' number following the sample type description gives the total number of fatty acids quantified for each replicate injection of each sample. See* *Table 1* *and* *Figure 16* *for the fatty acid code nomenclature.*

Compound	PML SML Fatty Acid Concentrations/ µg L^{-1}				CONNECT Fatty Acid Concentrations/ µg L^{-1}					
	PPAO (n = 3916)		L4 (n = 620)		CTD (n = 913)		SML (n = 832)		Underway (n = 816)	
	Mean $\pm$ SD	Median	Mean $\pm$ SD	Median	Mean $\pm$ SD	Median	Mean $\pm$ SD	Median	Mean $\pm$ SD	Median
8:0	4.12 $\pm$ 4	1.95	1.58 $\pm$ 2	0.78	1.65 $\pm$ 0.2	1.64	5.14 $\pm$ 1.7	5.27	1.58 $\pm$ 0.11	1.58
9:0	1.69 $\pm$ 1.1	1.71	0.90 $\pm$ 0.9	0.75	0.31 $\pm$ 0.08	0.29	0.96 $\pm$ 0.4	0.89	0.30 $\pm$ 0.04	0.29
10:0	0.75 $\pm$ 0.5	0.65	0.51 $\pm$ 0.3	0.56	0.14 $\pm$ 0.02	0.13	0.69 $\pm$ 0.2	0.64	0.13 $\pm$ 0.011	0.13
11:0	0.30 $\pm$ 0.17	0.35	0.21 $\pm$ 0.17	0.17	0.09 $\pm$ 0.03	0.09	0.12 $\pm$ 0.02	0.12	0.05 $\pm$ 0.04	0.08
12:0	1.35 $\pm$ 1.1	1.13	2.10 $\pm$ 3	1.49	0.10 $\pm$ 0.05	0.07	1.18 $\pm$ 0.5	0.91	0.08 $\pm$ 0.04	0.07
13:0	0.21 $\pm$ 0.09	0.21	0.23 $\pm$ 0.10	0.25	0.05 $\pm$ 0.02	0.05	0.11 $\pm$ 0.03	0.10	0.04 $\pm$ 0.02	0.05
14:0	2.42 $\pm$ 2	1.87	2.99 $\pm$ 1.8	3.34	0.27 $\pm$ 0.3	0.15	1.29 $\pm$ 0.6	0.96	0.17 $\pm$ 0.06	0.15
16:0	0.60 $\pm$ 1.5	0.09	0.65 $\pm$ 1.5	0.09	1.14 $\pm$ 1.2	0.66	1.83 $\pm$ 0.9	1.68	0.40 $\pm$ 0.5	0.31
18:0	0.58 $\pm$ 2	0.00	0.88 $\pm$ 2	0.49	8.00 $\pm$ 13	2.94	4.38 $\pm$ 5	2.00	3.06 $\pm$ 3	2.58
16:1	9.83 $\pm$ 15	0.86	20.38 $\pm$ 17	25.74	0.11 $\pm$ 0.08	0.12	0.15 $\pm$ 0.07	0.13	0.07 $\pm$ 0.06	0.10
16:2	0.85 $\pm$ 1.3	0.17	1.00 $\pm$ 1.2	0.42	-	-	-	-	-	-
16:3	1.10 $\pm$ 1.5	0.83	0.90 $\pm$ 0.4	0.83	-	-	-	-	-	-
16:4	3.68 $\pm$ 6	1.60	3.12 $\pm$ 2	2.63	-	-	-	-	-	-
18:1	1.63 $\pm$ 2	1.28	1.84 $\pm$ 3	1.28	0.41 $\pm$ 0.14	0.42	0.52 $\pm$ 0.2	0.46	0.32 $\pm$ 0.17	0.36
18:2	0.52 $\pm$ 0.8	0.17	0.88 $\pm$ 1.1	0.17	0.16 $\pm$ 0.02	0.16	0.18 $\pm$ 0.02	0.18	0.13 $\pm$ 0.05	0.15
18:4	0.73 $\pm$ 0.9	0.47	1.04 $\pm$ 0.7	0.83	-	-	-	-	-	-
D6	0.11 $\pm$ 0.3	0.00	0.12 $\pm$ 0.13	0.04	0.08 $\pm$ 0.04	0.07	0.19 $\pm$ 0.09	0.18	0.08 $\pm$ 0.04	0.08
D7	0.10 $\pm$ 0.10	0.04	0.07 $\pm$ 0.07	0.04	0.04 $\pm$ 0.02	0.05	0.08 $\pm$ 0.03	0.07	0.05 $\pm$ 0.02	0.05
D8	1.01 $\pm$ 1.4	0.62	1.63 $\pm$ 3	0.41	0.05 $\pm$ 0.010	0.05	0.48 $\pm$ 0.4	0.40	0.04 $\pm$ 0.011	0.04
D9	2.32 $\pm$ 1.3	1.99	1.85 $\pm$ 1.4	1.29	0.06 $\pm$ 0.04	0.06	1.17 $\pm$ 0.6	1.09	0.06 $\pm$ 0.03	0.06
D10	0.33 $\pm$ 0.13	0.31	0.46 $\pm$ 0.7	0.24	0.06 $\pm$ 0.07	0.04	0.09 $\pm$ 0.04	0.08	0.04 $\pm$ 0.03	0.03
D11	0.30 $\pm$ 0.10	0.29	0.23 $\pm$ 0.13	0.24	0.02 $\pm$ 0.006	0.02	0.09 $\pm$ 0.06	0.08	0.02 $\pm$ 0.007	0.02
D12	0.07 $\pm$ 0.11	0.02	0.07 $\pm$ 0.05	0.08	0.03 $\pm$0.012	0.03	0.05 $\pm$ 0.011	0.05	0.03 $\pm$ 0.02	0.02
D13	0.24 $\pm$ 0.11	0.23	0.35 $\pm$ 0.2	0.26	0.04 $\pm$ 0.04	0.03	0.14 $\pm$ 0.05	0.16	0.04 $\pm$ 0.02	0.04
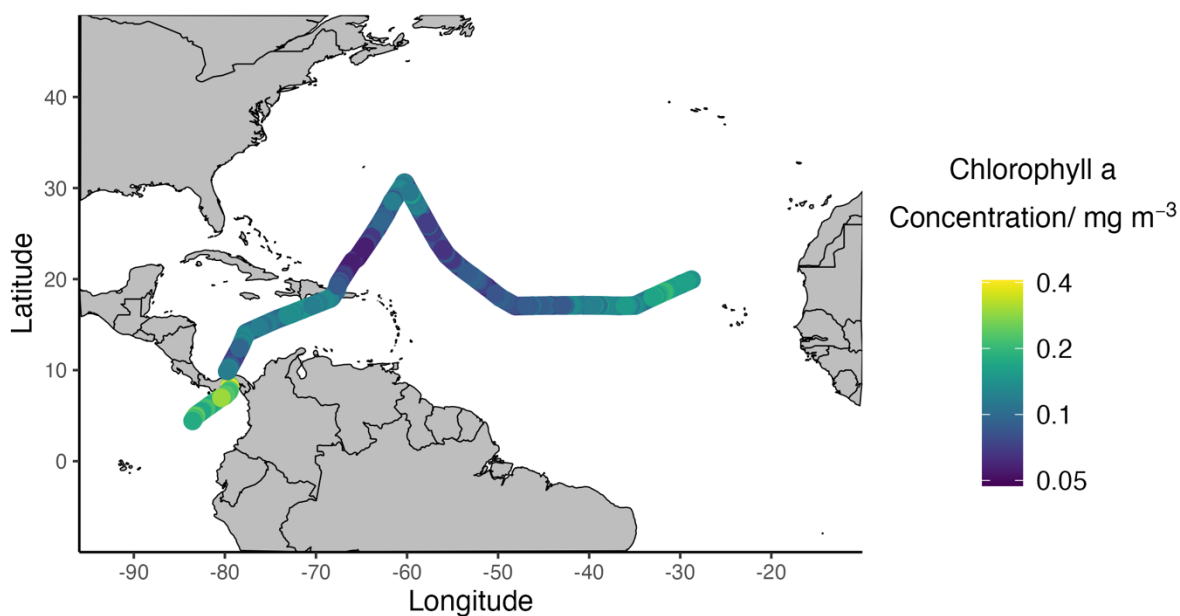
Figure 18 *– Spatial distribution of chlorophyll a concentration measured in the underway system of the CONNECT SO287 cruise. Note that the latitude, longitude, and concentration values were averaged hourly.*

During the CONNECT cruise, SML concentrations of almost all fatty acids were higher than those in the underlying water (**Table 3**), with enrichment factors of the total fatty acid concentrations ranging from 0.50 to 6.91 (**Figure 20**). The consistent fatty acid enrichment is expected given the surface-active nature of these compounds and demonstrates that SML rather than bulk concentrations are more applicable when considering air-sea exchange processes. Saturated fatty acids were substantially enriched compared to the underlying seawater, while unsaturated fatty acids were only slightly enriched (**Table 3**). A key factor in this is likely due to the short lifetime of unsaturated fatty acids relative to their saturated equivalents.[39] Only SML samples collected in the Pacific Ocean and one collected on 26/12/2021 (in the Sargasso Sea), were not enriched with this driven by higher than normal concentrations of saturated fatty acids in the underlying water. The Pacific samples coincide with higher chlorophyll *a* concentrations. It is hypothesised that high biological activity at these stations led to high levels of fatty acid production, but were accompanied by enhanced microbial utilisation and degradation of fatty acids in the SML and hence a lack of surface enrichment.[32] This could possibly be accompanied by the transfer of refractory material including saturated fatty acids to the underlying water via the sinking of particulate matter.[13]
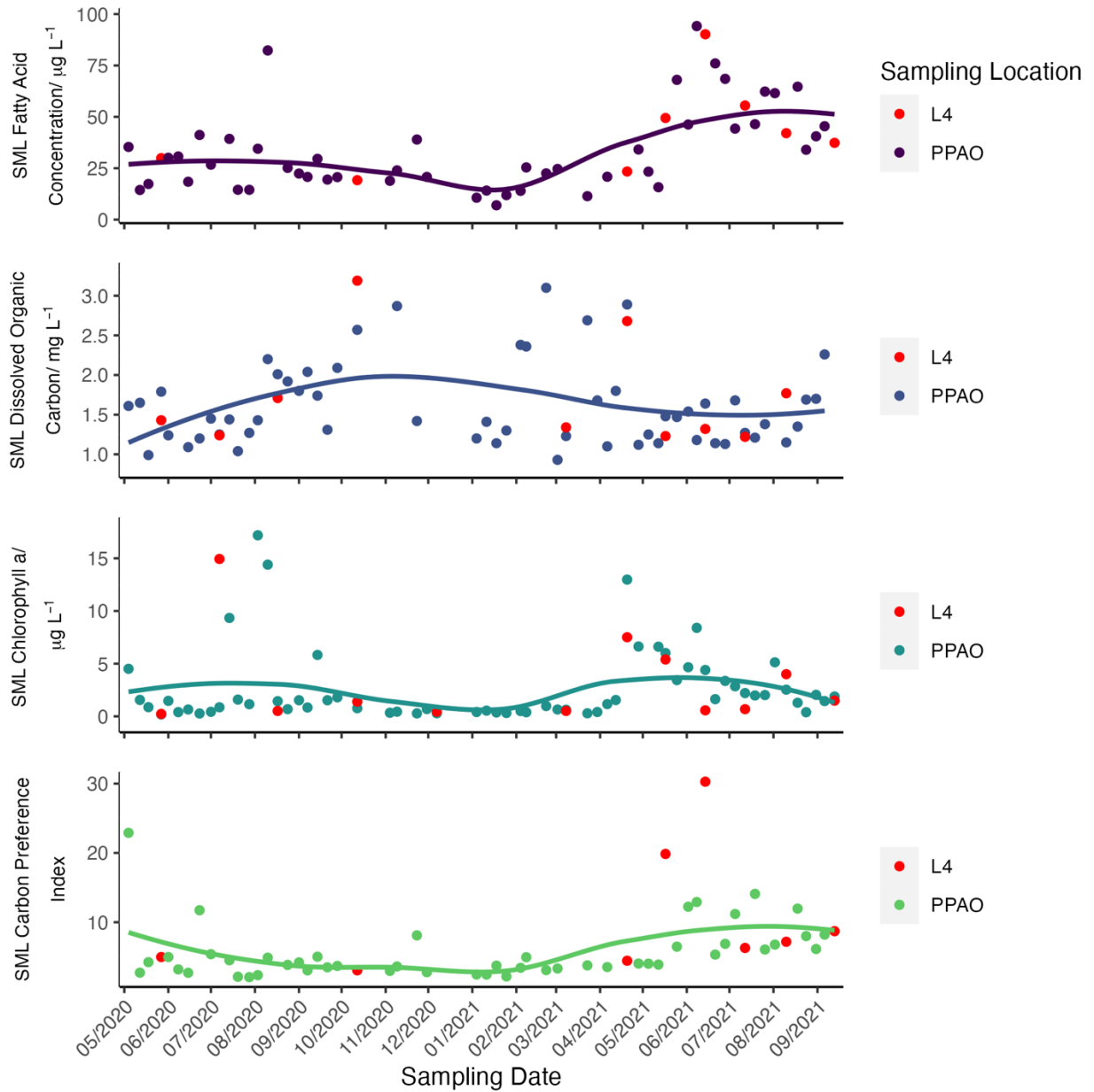
Figure 19 – *Time series of total SML fatty acid concentrations in addition to SML, DOC and ULW chlorophyll a concentrations. The carbon preference index was determined by the ratio of the total concentration of saturated fatty acids with even numbers of carbon atoms to those with odd numbers of carbon atoms.[32] The trend line is LOESS smoothed trendline.*
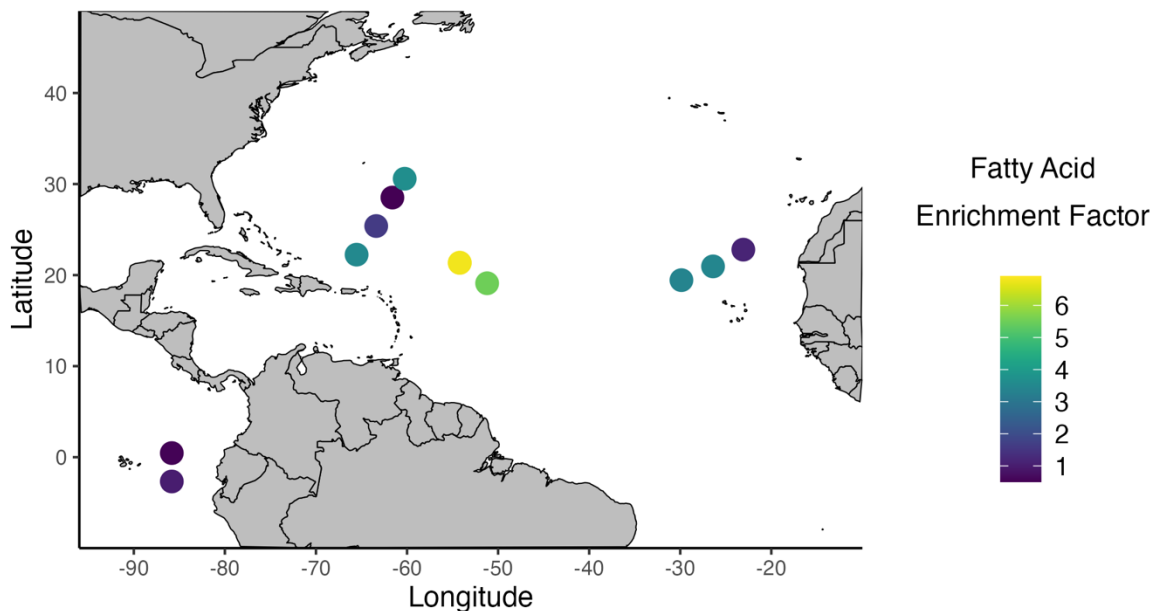
Figure 20 *– Enrichment of total fatty acids in the SML compared to the CTD samples.*

Temporal Variation of Fatty Acids in Coastal Waters

The coastal sampling sites (PPAO and L4) are subject to a strong seasonal cycle of biological activity, with pronounced increases in chlorophyll-a during the spring and summer (**Figure 19**).[59, 62] SML concentrations of unsaturated fatty acids at these locations exhibited elevated values during these periods relative to the cooler months (**Figure 21**). As the lifetime of unsaturated fatty acids in seawater is low, at minutes to hours (e.g. the lifetime of oleic acid (18:1) exposed to 50 ppb of ozone at the air-water interface is approximately 1.3 hours[6]) this is consistent with a local biogenic source of unsaturated fatty acids.[6, 26, 32, 39, 63] In contrast, saturated fatty acids did not show a clear seasonality, possibly reflecting their longer lifetime and sources other than biological activity, with one possible source being, as mentioned in the previous chapter, contamination from the Garrett screen itself.

DOC in the SML at PPAO and L4 displayed a different seasonal cycle to fatty acids (and chlorophyll-a), exhibiting highest concentrations during the late autumn and late winter/early spring (**Figure 19**). The combined fatty acids at PPAO contributed only a small fraction (0.4 to 8%) of the DOC concentrations, with the highest contributions being in the summer months when DOC concentrations were low. Thus, fatty acids were not significant drivers of the seasonal change in DOC concentrations. Instead DOC concentrations could be driven more by proteins and carbohydrates which make up a greater percentage of the organic matter produced by phytoplankton.[44] The difference in seasonal behaviour and distribution between bulk DOC and the fatty acids highlights the importance of characterising the reactive fractions of DOC individually in the context of evaluating the potential of the SML to contribute to ozone uptake or marine trace gas and secondary organic aerosol (SOA) production. For example, Sarwar *et al*. used a single value for the rate constant for the reaction of DOC and ozone to model oceanic ozone deposition.[64] This value is unlikely to be representative of the true reactivity of the organic matter present in the SML because the abundances of reactive components can vary independently of the overall DOC concentration.
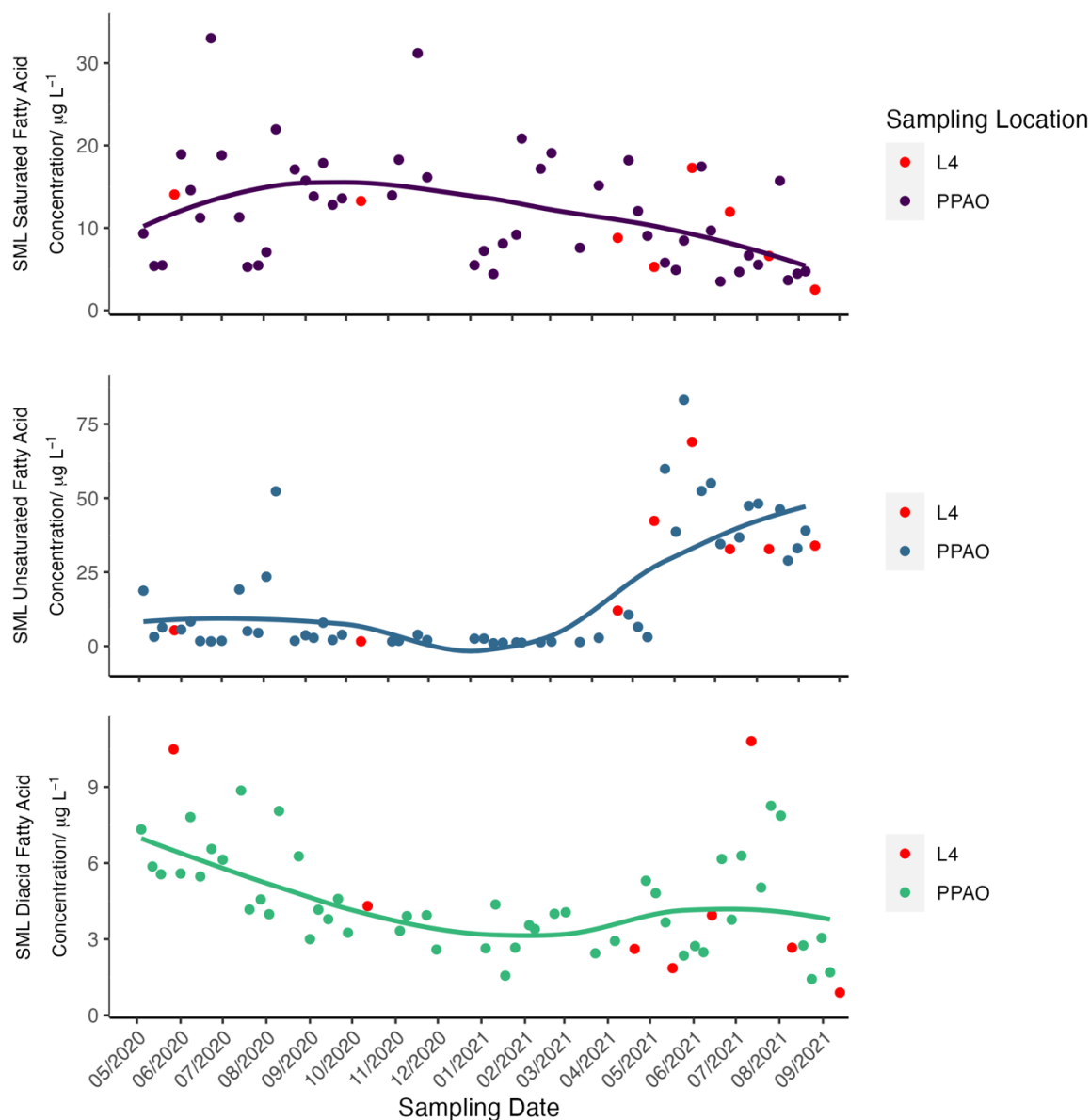
Figure 21 *– Seasonal variation of saturated and unsaturated fatty acids as well as diacids found in the SML. The trend line is LOESS smoothed trendline.*

CONNECT Cruise Track

As previously discussed, saturated fatty acid concentrations were similar during the CONNECT cruise and the PPAO time series, while unsaturated fatty acids were much less abundant in the open ocean. Chlorophyll-*a* levels during the CONNECT cruise were also much lower than observed at the PPAO and L4 sites (typically <0.1 ug L^{-1} vs. 5 – 30 ug L^{-1} respectively), as is expected for the oligotrophic tropical ocean. Concentrations of saturated fatty acids increased from east to west, peaking in the Sargasso Sea (**Figure 22**), but no such trends were observed in the unsaturated fatty acids, although this may have been due to these compounds typically being close to the limit of detection in these samples. The saturated fatty acids followed a similar distribution to that of chlorophyll *a* (**Figure 18**), which also showed slightly elevated levels in the Sargasso Sea, though chlorophyll *a* concentrations remained more than an order of magnitude lower than observed in the English Channel. In contrast to

the observations made in the coastal English Channel, elevated biological activity in the Sargasso Sea did not correspond to an observed increase in unsaturated fatty acid concentrations.
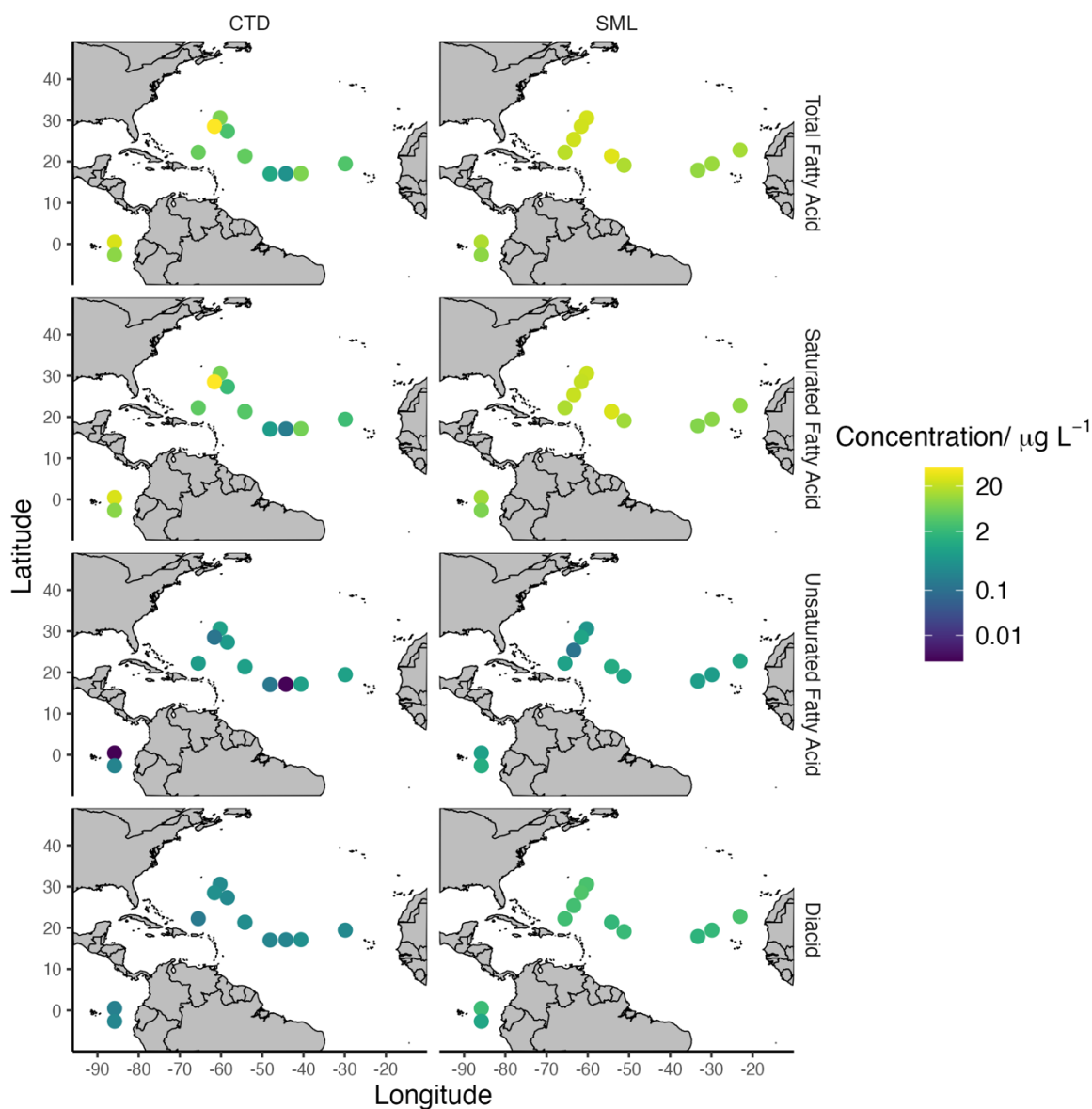
***Figure 22** – Spatial distribution of fatty acid concentrations along the cruise track of CONNECT SO287.*

The dominance of more refractory saturated fatty acids throughout the CONNECT cruise (**Figure 22**, **Table 3**), is indicative of aged organic material.[17] The saturated fatty acids observed may be the remnants of organic matter produced by the previous spring bloom in this region, that had been partially consumed over the following summer and autumn. Such blooms have been observed at the nearby Bermuda Atlantic time series study station by Carlson *et al*.,[65] but it should be noted that the biogeochemistry at BATS does not necessarily apply to the whole Sargasso Sea region.[66] Alternatively, DOC from the east coast of Africa is transported across the Atlantic as far as the Sargasso Sea, and may include saturated fatty acids.[67] However, the DOC reaching this far west is typically found 100 to 200 m deep,[67] and

does not appear to influence DOC in the surface ocean as there is no corresponding longitudinal trend in surface concentrations (**Figure 23**).

Average DOC concentrations in the Sargasso Sea were 2.37, 1.87 and 1.7 mg L^{-1} for the SML, CTD and underway samples respectively. These values are higher but within the same order of magnitude to previous winter DOC measurements made in the North-Western Sargasso Sea (approximately 0.75 mg L^{-1}; Carlson *et al.*[65]). Fatty acids comprised only 0.002-3.6% of the total DOC, which is considerably lower than in the PPAO samples. This is driven by lower fatty acid concentrations in the open ocean, as previously described, which may be linked to lower primary productivity and a more aged DOC pool.
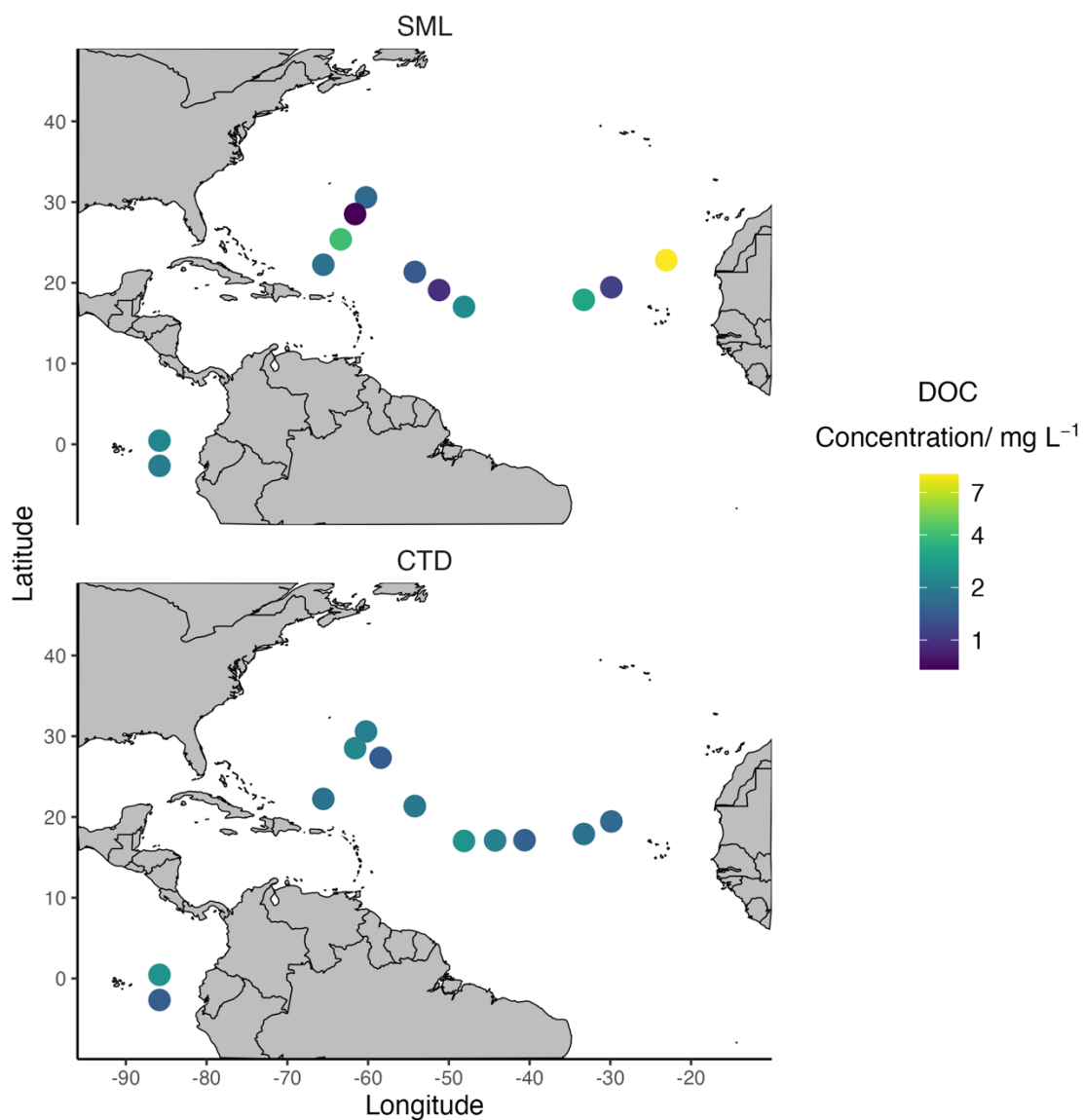
Figure 23 *– Spatial distribution of DOC concentrations along the cruise track of CONNECT SO287.*

Biogenic Contribution to Fatty Acids

Phytoplankton are the dominant source of dissolved fatty acids in the oceans, releasing them either by direct excretion or cell lysis.[25] The dissolved fatty acids observed in this study are

typical of those found in phytoplankton cells, with even numbers of carbon atoms being favoured, and carbon chain lengths ranging from 8 to 22 with lengths above 14 most common.[44, 68, 69] The biological contribution to the fatty acid inventory may be assessed using the carbon preference index (CPI), which is calculated as the ratio of the total concentration of even carbon numbered saturated fatty acids to the total for odd carbon numbered saturated fatty acids, see **Equation 6**.[32] High values of CPI are indicative of a biogenic fatty acid source.

$$CPI = \frac{\sum[C_{Even}]}{\sum[C_{Odd}]}$$

Equation 6- Carbon Preference Index

The CPI was consistently above 1 throughout both campaigns (**Figure 24**), suggesting biogenic production of the fatty acids. The CPI values of the PPAO and L4 samples were generally lower than those calculated for other coastal locations (**Figure 24**). The L4 summer samples were an exception to this, with a CPI of 27.3, very similar to that calculated for Norwegian Fjords (31.4; Gašparović *et al.*)[17] At PPAO and L4, CPI increased from autumn/winter to summer (4; **Figure 24**), which is consistent with increased biological activity in the warmer months releasing fatty acids to the water column. The summer CPI value was notably higher at L4 compared to the PPAO samples when using only 10:0 to 30:0 saturated fatty acids, but only 25% higher when calculated using all the saturated fatty acids observed. The chlorophyll *a* concentrations show that the biological activity of the sites is broadly similar (**Figure 19**), suggesting that the lower CPI at the PPAO sampling site is instead due to a higher contribution of non-biogenic fatty acids to the total. This is evident in the higher levels of C11:0 and C9:0 at PPAO; note 8:0 was also higher, and while these would not cause a decrease in CPI they are known to have non-biogenic sources. The PPAO site is closer to the shore, and has higher levels of nitrate (Jones et al., submitted), and so is expected to be subject to greater anthropogenic and terrestrial inputs. However, it should be noted that chlorophyll *a* concentrations are a proxy for biological activity and only provide an estimate due to its concentration being influenced by other independent factors such as differences in phytoplankton species present.

Despite having lower chlorophyll-a levels, the CPI for the CONNECT cruise samples was substantially higher than for the PPAO and L4 samples (**Figure 24**). This indicates a much greater biological contribution to the fatty acid concentrations in the open ocean relative to coastal waters. The CPI of 37.3 for the CONNECT samples was higher than those calculated for the North-Eastern Tropical Atlantic (Marty *et al.*)[29] and North Mediterranean open ocean (Daumas *et al.*)[30] (16.4 and 14.0 respectively). This could indicate a lesser anthropogenic influence on the remote open ocean locations sampled during CONNECT compared to these locations.
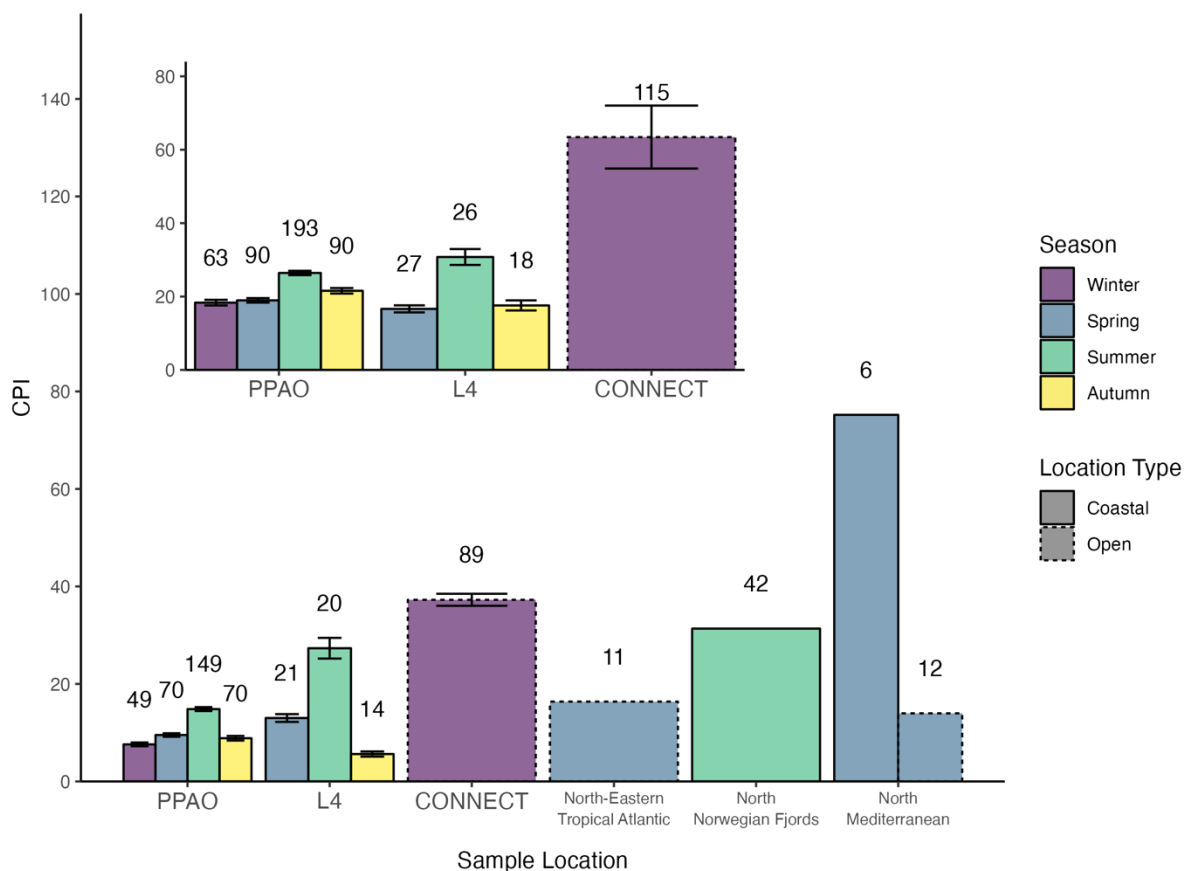
Figure 24 *– Carbon Preference Index (CPI) by season (winter being December, January and February, spring being March, April and May, summer being June, July and August and autumn being September, October and November) across the entire dataset of this campaign as well as those of other studies.*[17, 29, 30] *The numbers above the bars represent the number of individual fatty acids that contribute to the calculated CPI value. Note that to make valid comparisons, only saturated fatty acids between C10:0 and C30:0 were used in the calculations as these compounds were in the observable ranges across all studies. The inset plot shows the CPI values of this study calculated using all the saturated fatty acids observed.*

Diacids and Short Chain Fatty Acids in the SML

As discussed above, phytoplankton typically produce fatty acids with chain lengths above 14.[44, 68, 69] During this study, smaller (< C10) fatty acids and diacids (C6 to C13) were also found to be abundant in the SML (**Figure 17**, **Table 3**). Rather than being produced directly by phytoplankton, these compounds are formed by the biotic and abiotic breakdown of larger fatty acids.[27, 28, 70, 71] For example, nonanoic acid and nonanedioic acid (which was consistently observed throughout the PML campaign) can be formed from ozonolysis of oleic acid at the ocean surface (**Figure 4**).[36] Additional pathways for the formation of low molecular weight carboxylic acids include oxidation and breakdown of DOM by sunlight or bacteria, [70, 71] and the photooxidation of anthropogenic aromatic hydrocarbons.[72] Diacids also have anthropogenic sources such as synthetic lubricants and grease. However, with the data collected during this study, it is not possible to differentiate between diacids produced via different pathways.

The molecular size range of diacids observed in this study falls within that previously measured in seawater and in sea spray aerosols (C2 to C22).[27, 32, 58, 72] Mean di-acid

concentrations ranged from 0.07 to 2.32 ug L^{-1} in SML from PPAO and L4, and from 0.05 to 1.17 ug L^{-1} in SML collected during the CONNECT cruise (**Table 3**). Concentrations of D6 and D7 diacids observed in this study were within an order of magnitude of those observed in seawater by Tedetti *et al.*[27] In the PPAO, L4 and CONNECT samples D8 and D9 diacids were most abundant (**Figure 17**). Similarly, Cochran *et al.*[32] found the dominant saturated diacids in sea spray to be D4, D8 and D10, and Kawamura *et al.*[72] found that C9 was the third most abundant diacid in polar marine aerosols after D4 and D2 diacids (which are not measured by our analytical method).

For the PPAO dataset, none of the fatty acids and diacids measured in this study exhibited statistically significant correlations with their ozonolysis precursors ($p > 0.05$ Kendall's Rank Correlation Test), suggesting ozonolysis was not a dominant source of these compounds. However, the complex reaction pathways involved and differing lifetimes of reactants and products mean ozonolysis cannot be entirely dismissed as a potential source of the smaller fatty acids and diacids.

In the English Channel, di-acids did not exhibit the same seasonal trends as unsaturated FAs, suggesting again that their sources cannot solely be linked to biological activity and that there was a role for anthropogenic input and/or sampling contamination. Di-acid concentrations were broadly similar across the PPAO and CONNECT datasets, except for D12 and D11 diacids where concentrations were lower in the CONNECT samples. SML concentrations were also significantly higher than those in the underlying water; while this in part may reflect enrichment due to their surface-active nature, it could also indicate that the Garrett screen used for sampling was a source of contamination.

Early SML samples from the coastal time-series were suspected to be contaminated with diacids arising from the Garrett screen and so were excluded from the data set. Contamination was suspected because of the steep decline in diacid concentrations as sampling progressed. It is possible the screen contamination also contributed to the diacid concentrations reported for the coastal time-series (**Figure 21**), as concentrations continued to decline from May 2020. A procedural sampling blank collected during the CONNECT cruise also indicated that the screen introduced additional 8:0-12:0 saturated fatty acids and D8-D11 diacids to the samples. Levels of saturated fatty acid contamination measured in this test were sufficient to account for up to 10 – 63% of the respective concentrations measured in the SML samples, whereas diacid contamination could potentially contribute up to 34 – 100+% of the sample concentrations. Sample concentrations were not corrected by subtraction of the sampling blank, as the blanks collected during the time-series study indicated that contamination levels were likely to vary over the course of the cruise, and likely decline. Because of the potential influence of screen contamination, SML concentrations of lower molecular weight fatty acids and diacids measured during the CONNECT cruise have high uncertainty and should be considered as maximum values.
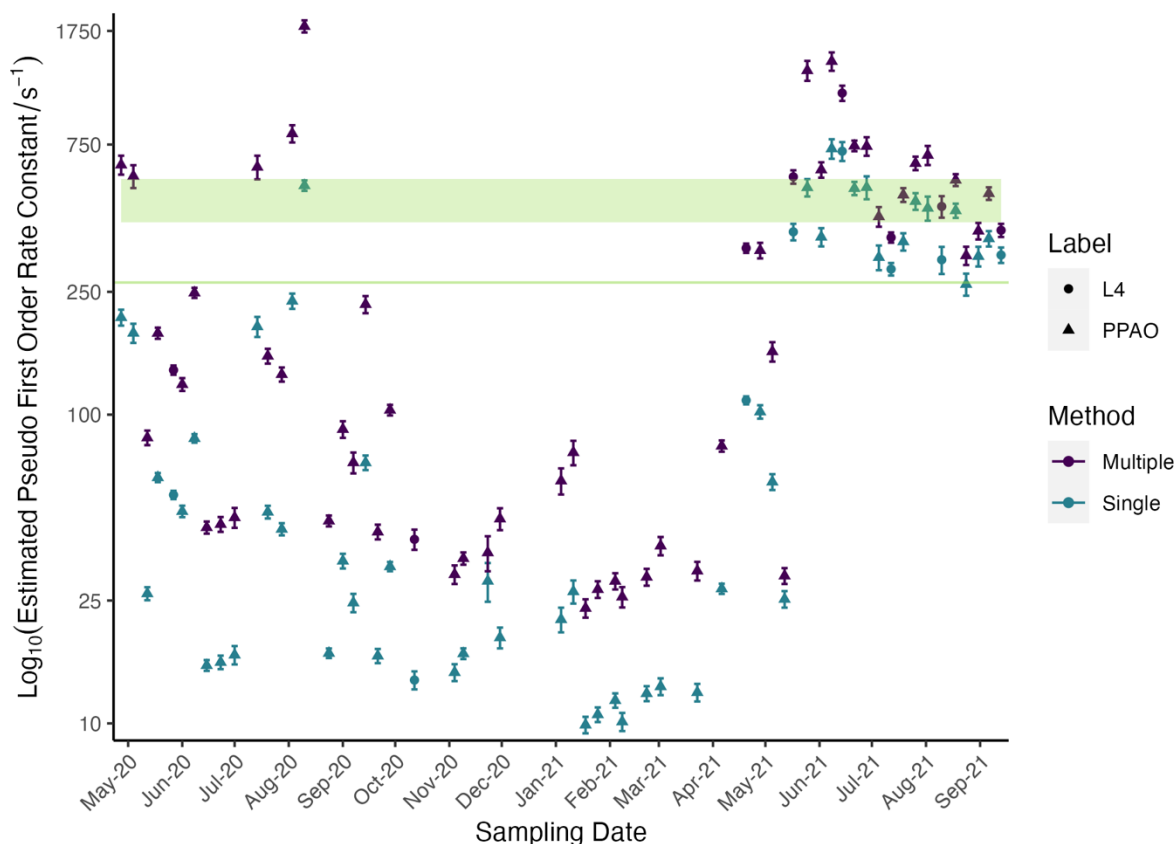
Figure 25 *– Estimated pseudo first order rate constants of the reaction of ozone with unsaturated fatty acids in the SML. The rate constant was estimated either via assuming all unsaturated compounds had the same rate constant as the reaction of oleic acid and ozone (single method) or multiplying this constant by the number of double bonds within the fatty acid (multiple method).[6, 73] The filled rectangle represents the estimated range of pseudo first order rate constants for the reaction of ozone and ocean DOM calculated by Shaw et al.[10] The line shows the estimation of the same rate constant but calculated by Sarwar et al.[64]*

Fatty Acid Contribution to Ozone Uptake

To demonstrate the importance of the impact of the seasonality of unsaturated fatty acids on ozone uptake, the pseudo first order rate constant for the reaction of ozone with the unsaturated fatty acids in the SML was estimated. The surface coverage of each compound was first calculated assuming the total SML sample volume was spread evenly over the surface occupying up to the sample depth calculated. For this study sample depths ranged from 507 µm to 727 µm. The area occupied by each fatty acid was assumed to be the same as oleic acid which has been estimated as 3.5×10^{-19} m^2.[74] The number of molecules per cm^2 was then multiplied by the a value of the rate constant using two different assumptions. For the first method each unsaturated fatty acid was assumed to have the same rate constant as oleic acid and, in this study, an average literature value of 6.1×10^{-11} cm^2 molecule^{-1} s^{-1} was used.[6, 73] In the second method, the rate constant was multiplied by the number of double bonds, using the assumption that reactivity scales with the level of unsaturation.[75] This assumption is supported by the work of King *et al.* who found that the rate of reaction of dienes with non-conjugated double bonds towards ozone can be accurately estimated by multiplying the rate constant of the equivalent monoalkene by the number of double bonds.[75] The calculated pseudo first order rate constants, as shown in **Figure 25**, were then summed for each sample to give an overall pseudo first order rate constant. The uncertainties shown

represent the uncertainty associated with the fatty acid concentrations within the samples. The green rectangle and line in **Figure 25** represent the estimated pseudo first order rate constants for DOM in seawater Shaw *et al.*[10] and Sarwar *et al.*[64] respectively.

There are two key take away messages from this analysis. The first is that unsaturated fatty acids appear to represent a major constituent of DOM reactivity towards ozone, especially during the summer months. The second is the seasonal variability of this reactivity, which increases well above the estimated value of DOM during the summer months calculated by Shaw *et al.*[10] and Sarwar *et al.*[64]. This highlights that using a single numerical value for the reactivity of ozone towards DOM, the method used previously by Sarwar *et al.*[64], is not appropriate due the variable composition of DOM. Even if the seasonal variability of DOM is factored in, the seasonality of the individual reactive components needs to be investigated for the reactivity to be truly represented.

Conclusions

This study has demonstrated that SPE using PPL sorbent is a viable method for extracting fatty acids from high-volume seawater samples, offering a more convenient method of extraction over traditional liquid-liquid methods. The substantially lower volumes of solvent required for the SPE method compared to liquid-liquid extraction make it possible to extract large numbers of samples even in remote field environments such as research cruises, and offer practical, environmental and safety benefits. Use of this method has allowed the measurement of fatty acids and related compounds in two much larger marine sample sets (61 samples for CONNECT and 89 for PML) than any previously investigated (n≤ ~20), and so has substantially increased the available observations of these compounds in seawater.

Unsaturated fatty acids are of particular interest because they can react with ozone at the sea surface, and so contribute to the marine ozone sink. The dominant unsaturated fatty acids observed in the SML were C16 and C18 compounds. SML samples from high chlorophyll coastal waters contained higher concentrations of unsaturated fatty acids than samples collected in low chlorophyll open ocean waters. In the coastal waters unsaturated fatty acid concentrations increased in the spring and summer months, mirroring increases in biological activity. CPI values also indicated a biological source of these compounds. Fatty acids did not follow the same seasonality as overall DOC concentrations and represented only a small but variable proportion of DOC (0.4-8% and 0.002-3.6% for PPAO and CONNECT, respectively). This highlights the need to characterise individual reactive components of organic matter relevant to ocean-atmosphere interactions, including the oceanic uptake discussed here, rather than use bulk DOC concentrations as a proxy.

In the Atlantic, saturated fatty acid concentrations followed a similar pattern to chlorophyll *a* and both were highest in the Sargasso Sea. However, no such trends were seen in unsaturated fatty acids, which were present at much lower levels. The dominance of saturated fatty acids in these samples, and the relatively high CPI values, are consistent with the presence of aged, biogenic organic material in the open ocean.

Diacids were analysed as part of this study and have not previously been analysed on this scale. Although they may be produced directly by marine biota or by degradation of biogenically produced organic matter, there was evidence of sampling contamination that

could have artificially increased their concentrations in the samples and prevented a detailed interpretation of these results. Therefore, alternative sampling strategies are needed if these compounds are to be studied further. An alternative sampling method could include the use of a glass sheet to collect the SML.[76] This would eliminate potential sources of manufacturing greases which can contain diacids. The sheet itself can be easily cleaned with both solvents and acids, with the latter not being practical for Garret screens due to corrosion, and also baked to remove residual organics.

Chapter Four – Analysis of Phytoplankton Fatty Acids

Introduction

Phytoplankton are single celled, photosynthetic autotrophs between 0.4 and 200 μm in size who typically inhabit aquatic environments.[77] It is thought eukaryotic phytoplankton emerged following an endosymbiosis event in which a heterotrophic eukaryote engulfed a cyanobacterium, allowing the eukaryote to photosynthesize.[77] Eventually, much of the genetic material of the cyanobacteria in this symbiosis was lost, with their remaining structure becoming a chloroplast of the eukaryote cell.[77, 78] Marine phytoplankton are ubiquitous across the oceans and, being photosynthetic, are usually found between the surface and a depth of 200 m. The dominant groups are diatoms, dinoflagellates and haptophytes which are most abundant around the continental shelf, with diatoms being the most abundant out of this group.[77, 78] Other prominent groups include green algae, picoplankton and cyanobacteria.[77]

In the marine environment, phytoplankton are the dominant primary producers, with primary producers being organisms that derive their energy and organic matter from non-living sources. Their primary production is roughly equal to that of terrestrial photoautotrophs and is estimated to be approximately 48.5 x 10^{15} g or carbon per year.[79] Despite this, the pool of biomass generated only represents 1% of that present on the planet.[77] The organic matter produced is eventually released into the surrounding water either by being excreted directly or released via cell lysis caused by environmental stressors including grazing or viral infection. Much of this organic matter is biologically labile and will be scavenged and reprocessed by other marine organisms within hours or days of release.[48]

The organic matter produced by phytoplankton can be divided into three dominant groups: proteins, carbohydrates and lipids whose amounts are approximately split 5:3:2 as a percentage of organic matter.[44] Other compound classes include hydrocarbons, free fatty acids, sterols and pigments.[44] The lipids themselves can be split into two categories: polar and neutral lipids. The neutral lipids contain compounds like triacylglycerols and diacylglycerols and the polar lipids contain galactolipids and phospholipids (**Figure 26**).[44, 80] Lipids provide numerous cellular purposes including storage, cell structures and pigments.[44] More specifically, polar lipids are typically found in membranes whereas triacylglycerols are storage lipids.[80]

Generally, a lipid is a compound that consists of one or more fatty acids chains bonded to a head group via the acyl group of the fatty acid, or existing as a free fatty acid (see **Figure 26**). The synthesis of these lipids starts with the formation of single fatty acid chains and begins with the glucose produced from photosynthesis. Glucose initially undergoes glycolysis to form pyruvate which itself is subject to oxidative decarboxylation via coenzyme A to form acetyl-CoA.[44] Acetyl-CoA is converted to malonyl-CoA via acetyl-CoA carboxylase and the two compounds combined to form the first four carbons of the aliphatic chain of the fatty acid attached to an acyl carrier protein (ACP).[44, 81] The carbon chain is then elongated two carbon atoms at a time, typically to chain lengths up to eighteen, by the addition of malonyl-ACP via a cyclic condensation reaction using fatty acid synthase.[81] At this point, the fatty acid-ACP compounds will either pool in the cytosol or move onto the endoplasmic reticulum.[44, 81] In the endoplasmic reticulum, various desaturase and elongase enzymes further extend and modify the fatty acids to varying lengths and levels of unsaturation.[44, 81] Once the fatty acids are

synthesised, they either remain as free fatty acids or go on to form structural or storage lipids. This starts with the formation of phosphatidic acid from the addition of acyl-CoA to glucose-6-phosphate via acyl transferase.[44] This acid and its hydrolysis product diacylglycerol then used to form the head group of lipids.[44]

When these lipids are released into the marine environment by phytoplankton, through the mechanisms previously stated, they will be readily scavenged and exposed to biotic and abiotic decomposition. Enzymatic digestion of lipids will lead to the release of the fatty acid chains from the headgroups where they can be consumed and broken down further.[32] Even the most unreactive saturated fatty acids have been known to be consumed by bacteria.[32] In the context of this study, it is the abiotic decomposition of lipids that is of interest, namely the ozonolysis of unsaturated fatty acids. Given the abundance of marine phytoplankton and their ability to produce a wide variety of fatty acids, understanding how differences in community structure, species distribution, environmental stressors as well has how intracellular fatty acids relate to what is present in the surrounding medium are important when considering ozone deposition to the ocean surface. It is this that will be investigated in this chapter.
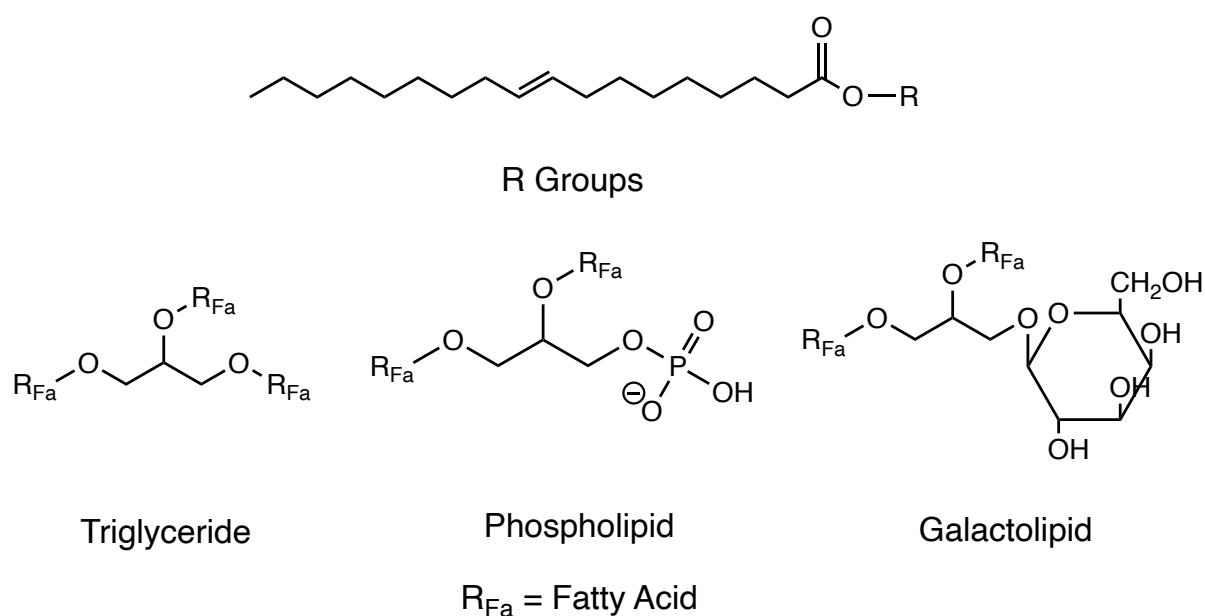
Figure 26 – Examples of key lipid structures. Note that in the case of free fatty acids the R group is a hydrogen atom.

Description of Chapter

This chapter describes both the literature based and experimental work carried out on the fatty acids produced by marine phytoplankton. This was done to establish the links between the fatty acids observed in seawater, as described in Chapter 3, and those known to be produced by phytoplankton. A meta-analysis of the literature on phytoplankton fatty acids was first carried out and the data generated was used to assess the overall fatty acid profile of a variety of phytoplankton species as well as the environmental factors impacting fatty acid production. These results then fed into culture experiments where fatty acids released by

different phytoplankton species were analysed directly using the previously developed SPE and FAME conversion method.

Experimental

Literature Searching

Literature data was taken from two previous meta-analyses by Jónasdóttir[44] and Galloway *et al.*[82], as well as from a literature search of low temperature polar species which were not heavily featured in these publications. For each species reported, the percentage fatty acid composition per cell and/or the absolute mass of individual fatty acids per cell were recorded. In addition, where possible, the phytoplankton functional type (PFT), species name, culture origin (culture collection or sample area), strain number, light duration and light intensity, temperature, culture growth stage at the time of harvesting, culture media and nutrient levels were also recorded using the same method as Galloway *et al.*[82] Overall, 34 publications were sampled yielding 401 percentage composition fatty acid profiles and 135 fatty acid mass per cell profiles.[23, 25, 68, 69, 83-113] To add locational information, i.e. latitude and longitude data, to the fatty acid dataset, data from the Ocean Biodiversity Information System (OBIS) were retrieved for the phytoplankton species available using the R programming package Robis, as used previously by Righetti *et al.*.[114, 115] The OBIS database provided locational information of reported observations of different phytoplankton species and were combined with average fatty acids profiles generated by the meta-analysis for each species.

Characterising the Growth and Fatty Acid Analysis of Proof-of-Concept Phytoplankton Cultures

Following the analysis of the literature data, three species were chosen to be proof of concept species (see results and discussion of this chapter). These species were *Skeletonema costatum* (RCC70), *Thalassiosira pseudonana* (RCC950) and *Emiliania huxleyi* (RCC1265) which were obtained from the Roscoff Culture Collection, France. The cultures obtained for these species were non-axenic. The phytoplankton cultures were grown in ESAW media enriched with K + Si nutrients for *S. costatum* and *T. pseudonana* and K/2 for *E. huxleyi*.[116, 117] The composition of ESAW and the K nutrients can be found in **Table 4** and **Table 5** respectively. Note that for the experiments involving *S. Costatum*, the trace metal stock used contained ten times more $CuSO_4.5H_2O$ than in other experiments in error. However, due to the high concentration of Na_2EDTA, which strongly chelates the metal ions within the media making them less biologically available, this was not detrimental to phytoplankton growth.

Before use, the ESAW media as well as the trace metals, nitrate, ammonium, phosphate, selenium, tris-base and silicate solutions were autoclaved, and the vitamin stock was sterilized via filtration through a sterile 0.2 μm filter. The nutrient solutions were added to 4 x 200 mL of ESAW in sterile 250 mL conical flasks using the amounts shown in **Table 5** for each of the species giving one blank and three replicates. Three of the four solutions were inoculated with 20 mL of their respective stock cultures in a biosafety cabinet. The *T. pseudonana*, *E. huxleyi* and *S. costatum* cultures were placed in 15 °C, 17 °C and 20 °C controlled temperature rooms respectively under a blue-red 50 W LED light with a 12-hour light-dark cycle. To monitor the growth of the cultures, the *in vivo* fluorescence was measured using a Turner Designs Trilogy Laboratory Fluorometer using the CHL-A-INVIVO blue module. Prior to analysis, the ~2 mL aliquots used to take the measurement were dark adapted by isolating them from light for at least 30 minutes in their respective controlled temperature

room. Because the observed fluorescence is variable with respect to time due to the Kautsky effect whereby the photosynthetic system becomes saturated and start to decay via non-photochemical quenching, the first five readings were taken for each sample so that the readings were consistent across each sample. Fluorescence readings for each of the blanks and replicate cultures were taken every 2-3 days. Only *S. costatum* was taken forward for SPE extraction and this process is described below.

2 x 100 mL of a stock *S. costatum* culture were added to 2 x 1 L of sterile ESAW K + Si media and each was approximately split in half in a biosafety cabinet. The separation of the culture into ~500 mL volumes was to allow for suitable gas exchange between the culture and the headspace above it in the 1 L conical flasks used to hold the cultures. The cultures were placed into the 20 °C controlled temperature room under a blue-red 50 W LED light with a 12-hour light-dark cycle alongside 4 x ~500 mL sterile ESAW K + Si solutions used as blanks. The cultures and blanks were left for 8 days, allowing the cultures to reach the end of their logarithmic growth phase as determined by the *in vivo* fluorescence measurements. An image of the cultures on the day of harvesting is shown in **Figure 27**.

The cultures and blank solutions were separated into 100 mL, 200 mL, 300 mL, 400 mL and 500 mL aliquots and filtered through GF/F glass microfibre filters under a low vacuum. Varying culture aliquots were analysed to assess the appropriate samples size if cartridge overloading was found to be a problem in these experiments. The low vacuum was used to minimise cell lysis. Cells may also lyse when exposed to air following filtration but this was unlikely to influenced these samples as there was no rinsing step following filtration.[118] The filtrate was stored in acid washed HDPE bottles at 2-4 °C until extraction one day later and analysis via the same SPE GC-MS method covered in Chapter 2.

Figure 27 *– S. costatum cultures 8 days post inoculation prior to filtration.*

Table 4 – *Composition of ESAW media used for phytoplankton growth.*

Salt	Concentration/ g L^{-1}
NaCl	20.7580
KCl	0.5870
$NaHCO_3$	0.1700
KBr	0.0870
$Na_2SO_4.10H_2O$	5.5000
H_3BO_3	0.0225
NaF	0.0027
$MgCl_2.6H_2O$	9.3950
$SrCl_26H_2O$	0.0210
$CaCl_2.2H_2O$	1.3160

Table 5 – *Composition of K + Si nutrients used for phytoplankton growth.*

Stock Solution	Amount used in K + Si media/ mL L^{-1}	Amount used in K/2 media/ mL L^{-1}	Chemicals	Concentration/ g L^{-1}
Nitrate	1	0.5	$NaNO_3$	75
Ammonium	1	0.5	NH_4Cl	2.67
Phosphate	1	0.5	Na_2 β-glycerophosphate	2.16
Selenium	1	0.5	H_2SeO_3	0.000129
Tris-base	1	0.5	Tris-base	121.1
Trace Metals	1	0.5	$Na_2EDTA.2H_2O$	41.6
			$FeCl_3.6H_2O$	3.15
			$CuSO_4.5H_2O$	0.0025
			$ZnSO_4.7H_2O$	0.023
			$CoCl_2.6H_2O$	0.01
			$MnCl_2.4H_2O$	0.178
			$Na_2MoO_4.2H_2O$	0.0063
Vitamin	0.5	0.25	Cyanocobalamin (B_{12})	0.001
			Thiamine HCl (B_1)	0.2
			Biotin	0.001
Silicate	1	0	$Na_2SiO_2.9H_2O$	15.35

Table 6 – *Composition of f/2 nutrients used for phytoplankton growth.*

Stock Solution	Amount of Stock/ mL L^{-1}	Chemicals	Concentration/ g L^{-1}
Nitrate	1	$NaNO_3$	75
Phosphate	1	$NaH_2PO_4.2H_2O$	5.65
Trace Elements	1	Na_2EDTA	4.16
		$FeCl_3.6H_2O$	3.15
		$CuSO_4.5H_2O$	0.01
		$ZnSO_4.7H_2O$	0.022
		$CoCl_2.6H_2O$	0.01
		$MnCl_2.4H_2O$	0.18
		$Na_2MoO_4.2H_2O$	0.006
Vitamin Mix	1	Cyanocobalamin (B_{12})	0.0005
		Thiamine HCl (B_1)	0.1
		Biotin	0.0005

Because no fatty acids were observed in the growth media of *S. costatum* (see the Results and Discussion section of this chapter), further phytoplankton culture experiments were carried out whereby the cultures were subject to environmental stresses, which may lead to the release of cellular fatty acids. This work was carried out at the University of the Balearic Islands (UIB) with *Phaeodactulum tricornutum, Synechococcus* and *Ostreococcus* cultures, which were all non-axenic. Note that work was also carried out on *Prochlorococcus,* but the sample extracts were lost in shipping.

Cultures were grown in 300 mL conical flasks. These flasks were first soaked in 1% HCl (aq) overnight, rinsed with MQ water and autoclaved prior to use. Cultures were grown in 100 mL volumes of f/2 (**Table 6**), plain artificial seawater (ASW) and K media for *P. tricornutum, Synechococcus* and *Ostreococcus* respectively.[119] Note that the base media for f/2 and K solutions was seawater collected off the coast of Palma which was filtered and autoclaved. All cultures were grown at 22 °C under continuous illumination by cool white light, except for those who were undergoing heat stress which were moved to a 35 °C incubator after an initial growth period. This temperature was chosen due to it being the set point of the equipment available in the laboratory. In case of the *Synechococcus* viral stress test, the virus was added after the initial growth phase of 15 days. Inoculation dates, stress dates and extraction dates of the cultures and media blanks are described in **Table 7**.

On the day of collection, an aliquot of each culture replicate (10 μL for *Synechococcus* and 100 μL *P. tricornutum* and *Ostreococcus*) was fixed in 4% glutaraldehyde and 0.01% pluronic acid (made up in filtered seawater) for cell counting. This counting was carried out by Dr Joseph Christie at UIB via flow cytometry. The remaining culture material was transferred to two 50 mL Falcon centrifuge tubes and centrifuged at 4000 rpm for 10 minutes to separate the cells from the growth media. The supernatant was separated and acidified to a pH of approximately 2.0 and extracted with the SPE and FAME conversion method described in Chapter 2. Note that the SPE step was carried out at UIB and the methanol extracts were stored frozen and shipped back to the UK for the FAME conversion step.

Results and Discussion

General Phytoplankton Fatty Acid Profiles from the Literature

The full fatty acid profiles generated from the literature are summarised in **Figure 28** and **Figure 29**, representing both fatty acid percentage contribution and mass per cell. [23, 25, 68, 69, 83-113] As expected the profile ranges from C8 to C28, with even numbered species being favoured.[21, 22] C14, C16 and C18 compounds are dominant on account of the number of different levels of unsaturation observed for these chain lengths, hence why they are typically considered markers for marine biota.[120] Despite the high contributions of 20:5ω5 and 22:6, fatty acids of C20 and above contribute less to the profile, with acids above C22 typically being produced by terrestrial plants as opposed to marine phytoplankton.[17, 121]

When comparing this literature fatty acid profile (**Figure 28** and **Figure 29**) to the observed seawater fatty acids found in this study and the literature (**Figure 17**) in the previous chapter), the distribution is broadly similar with regards to the dominance of the C14, C16 and C18 species. Although not typically seen in this study, for reasons discussed in Chapter 2, fatty acids larger than C18 have also been observed in seawater.[17, 26, 29-31] There is a notable

absence in the phytoplankton fatty acid literature data on diacids as these species were not the target of the studies sampled. Overall, the generation of this literature data set highlights the link between marine biota and seawater fatty acids. However, these data only represent the intracellular fatty acids whose profile may therefore not entirely match those that are released into the surrounding media, which are seen in the later phytoplankton culture experiments carried out in this study.

Table 7 – *UIB phytoplankton stress test experimental parameters.*

Culture	Sample	Repeat	Stress	Start Date	Stress Date	Collection Date	Centrifuged Volume/ mL
Phaeodactulum tricornutum	Stress	1	Temperature	12/07/2022	19/07/2022	22/07/2022	87.5
		2					99
		3					85
	Control	1	NA	12/07/2022	NA	22/07/2022	92.5
		2					97.5
		3					87.5
	Blank	1	NA	12/07/2022	NA	22/07/2022	100
		2					81.25
		3					100
Synechococcus	Stress	1	Temperature	07/07/2022	22/07/2022	25/07/2022	99
		2					100
		3					100
	Stress	1	Virus	07/07/2022	22/07/2022	25/07/2022	100
		2					100
		3					100
	Control	1	NA	07/07/2022	NA	25/07/2022	100
		2					100
		3					100
	Blank	1	NA	11/07/2022	NA	25/07/2022	100
		2					100
		3					100
Ostreococcus	Culture	1	NA	15/07/2022	NA	27/07/2022	100
		2					100
		3					100
	Blank	1	NA	15/07/2022	NA	27/07/2022	95
		2					83
		3					100

Figure 28 – *Percentage contribution of the intracellular fatty acids by mass of a variety of phytoplankton species studied in the literature.* [23, 25, 68, 69, 83-113] *401 individual fatty acid profiles are represented here. The boxes represent the interquartile range with the median shown within. Whiskers show the largest/smallest value smaller/greater than 1.5 the interquartile range from upper/lower quartile. Values outside this range are marked as outliers.*
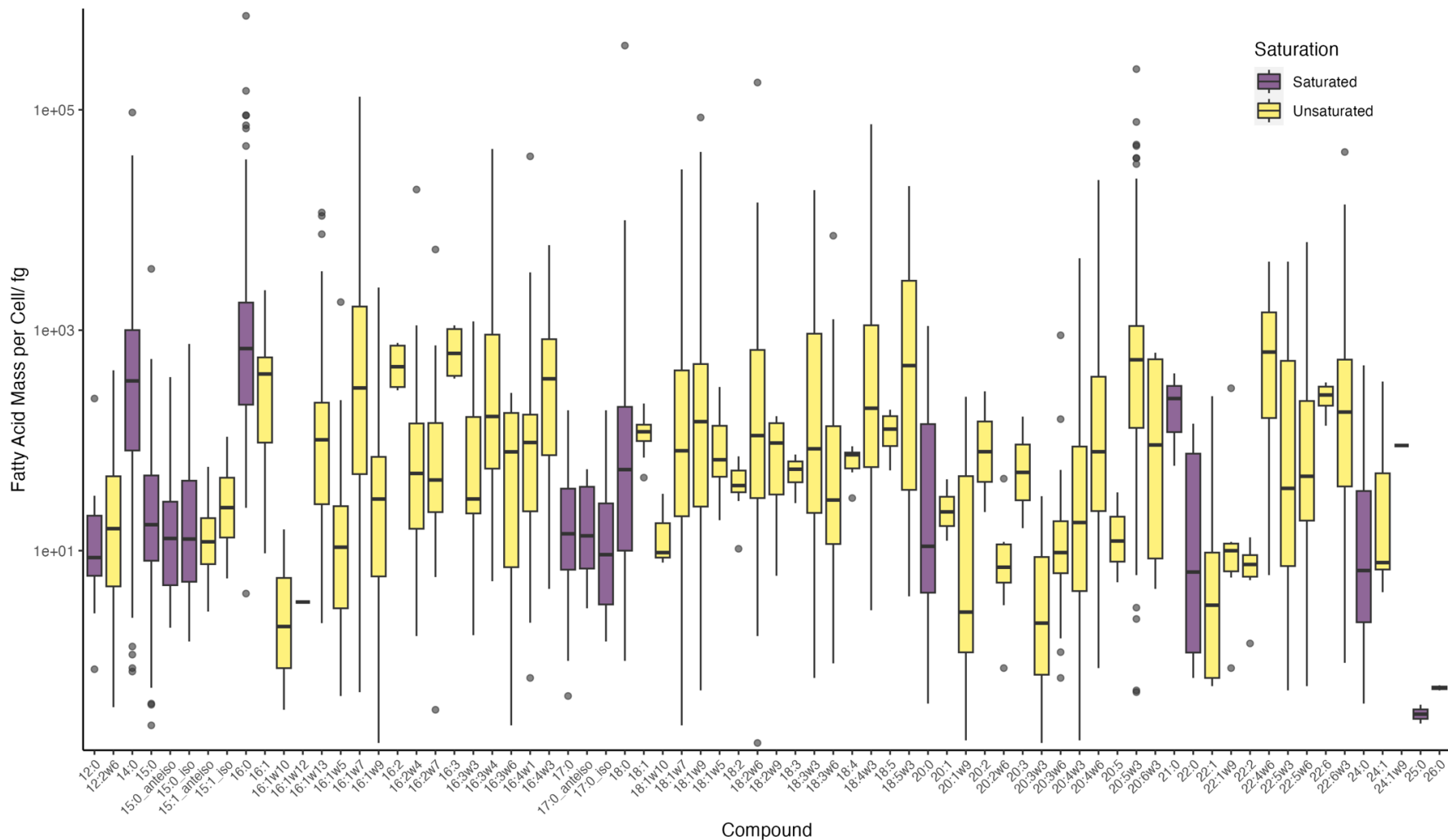
Figure 29 *– Mass per cell of intercellular fatty acids of a variety of phytoplankton species representing 135 individual fatty acid profiles studied in the literature.* [23, 25, 68, 69, 83-113] *The boxes represent the interquartile range with the median shown within. Whiskers show the largest/smallest value smaller/greater than 1.5 the interquartile range from upper/lower quartile. Values outside this range are marked as outliers.*
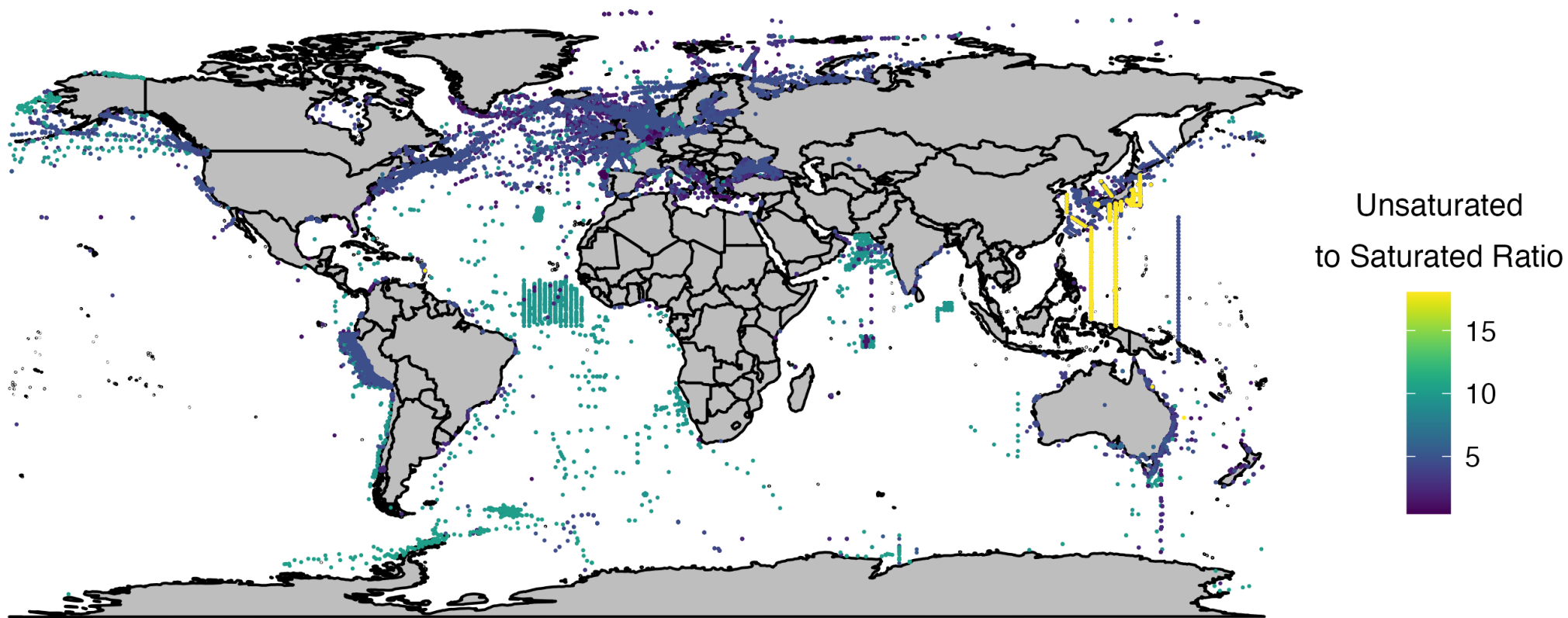
Figure 30 – Global distribution of the unsaturated to saturated ratio of the percentage composition of fatty acids found in a variety of phytoplankton species.
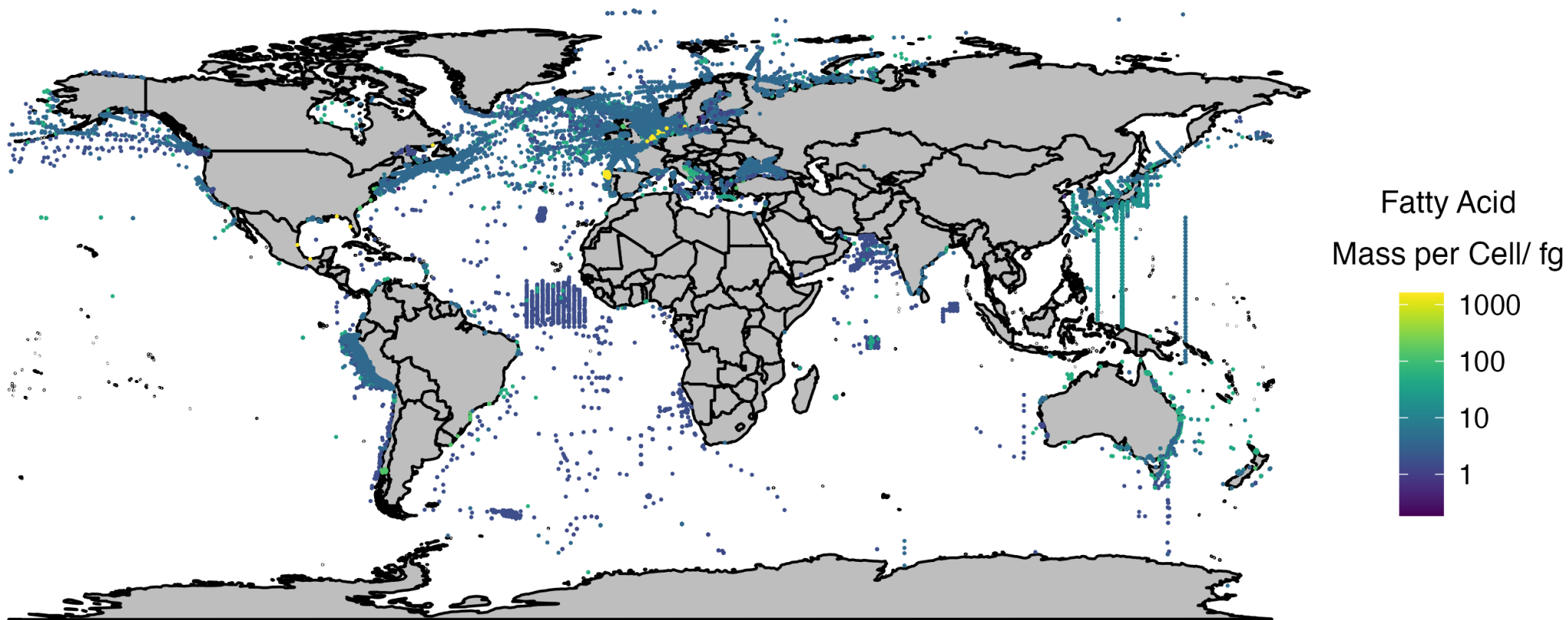
Figure 31 – *Global distribution of the mass of fatty acids per phytoplankton cell for a variety of phytoplankton species.*
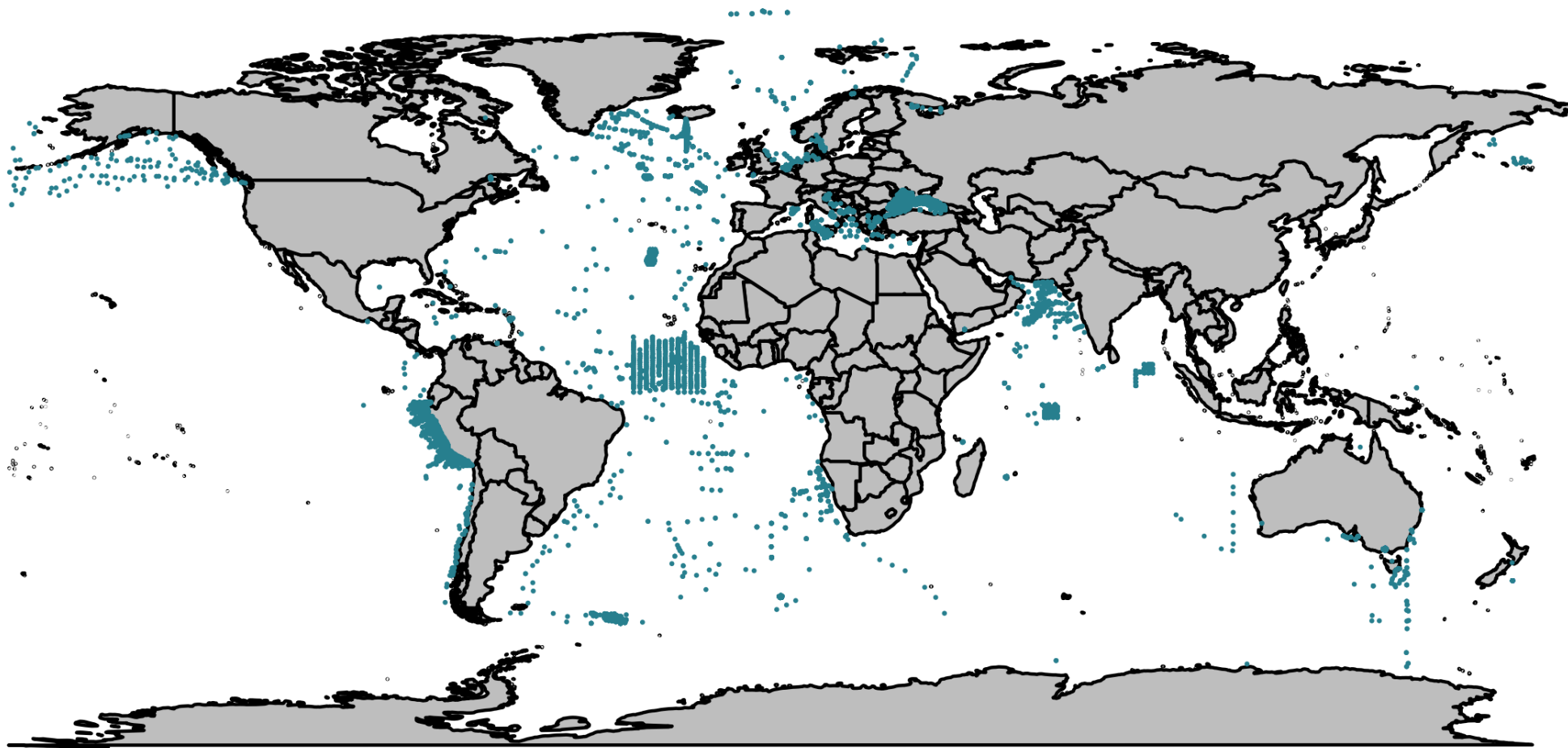
Figure 32 *– Global distribution of Emiliania huxleyi consisting of the individual worldwide observations made of the species recorded in the OBIS database.*[114]
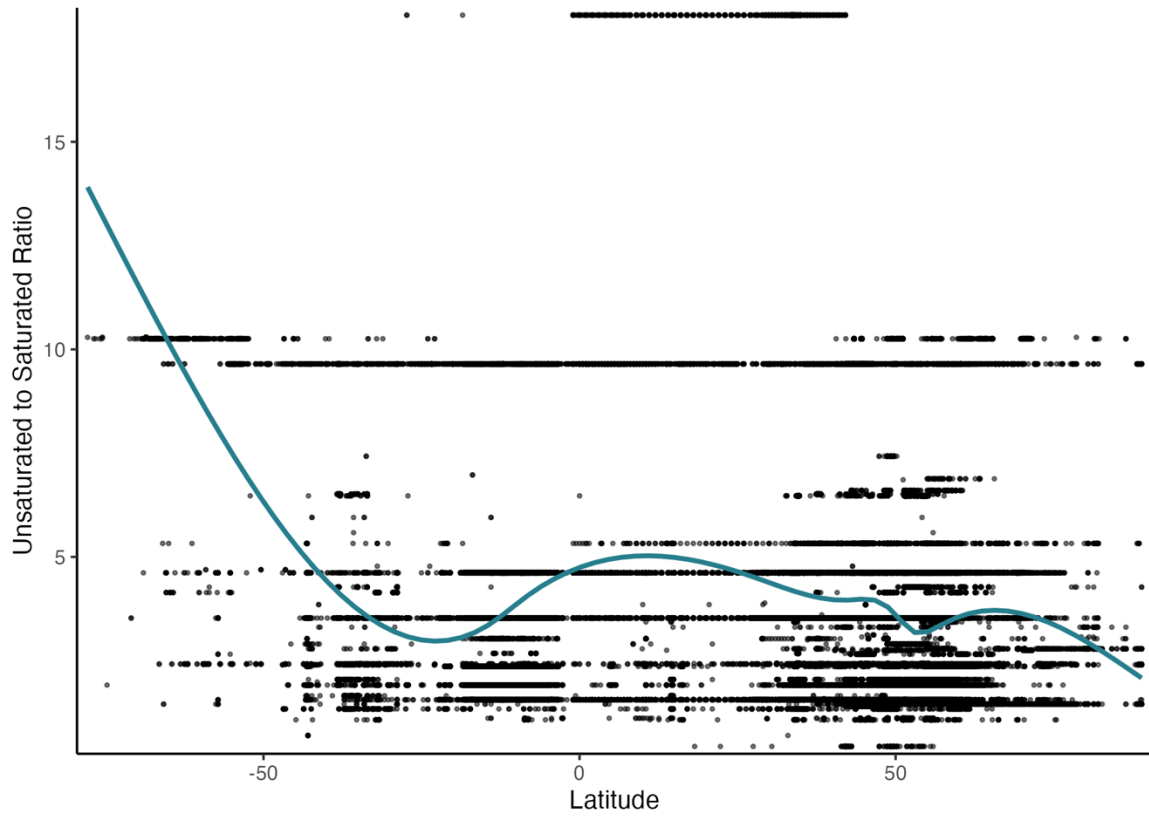
Figure 33 – Latitude distribution of the unsaturated to saturated ratio of the percentage composition of fatty acids found in a variety of phytoplankton species.
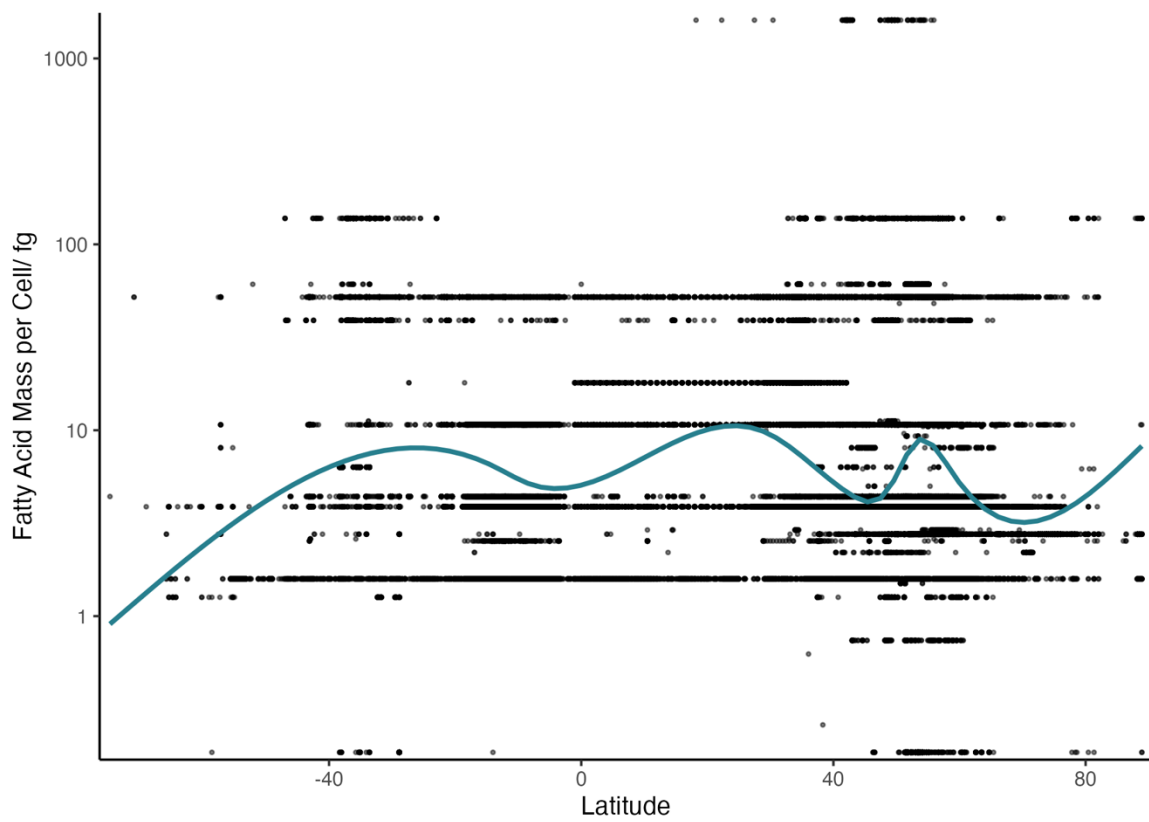
Figure 34 – Latitude distribution of the mass of fatty acids per phytoplankton cell
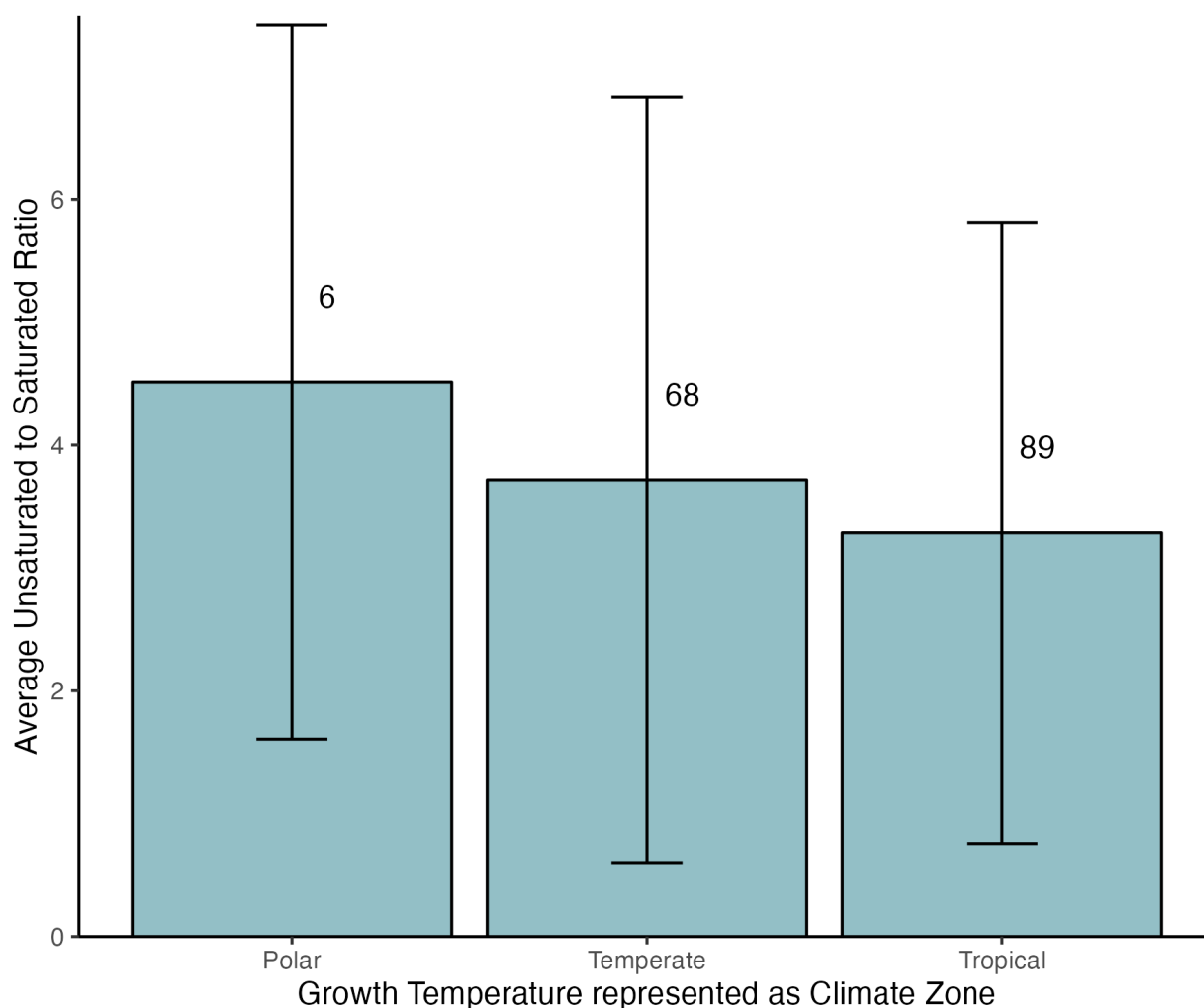
Figure 35 *– Variability of phytoplankton fatty acids with regards to their intracellular unsaturated to saturated ratio under different growth temperature regimes. The numbers above the bars show the number of species that contribute to each average.*

Global Distribution of Phytoplankton Fatty Acids from the Literature Meta Analysis

To plot the global distribution of phytoplankton fatty acids, an average of the unsaturated to saturated ratio by mass per cell as well as the average fatty acid mass per cell was calculated for each species. This was then plotted on a world map using the OBIS locational data for each species.[114] This was done for the sake of simplicity and it is a metric of potential interest with regards to ozone reactivity. From the global plots seen in **Figure 30** and **Figure 31**, no observable trend for both the unsaturated to saturated ratio and the fatty acid mass per cell with relation to global position could be found. This, however, could be a product of the data plotting method giving a poor representation of the actual global distribution of phytoplankton fatty acids. Over-plotting is an issue with these plots due to many species being observed in similar regions and within the same samples collected to generate OBIS dataset. This is particularly evident in the waters surrounding Europe. In addition, although averaging the data for each phytoplankton species simplifies the plots, this may not be appropriate for all species. This is the case for *E. huxleyi* seen in **Figure 32**, this species is globally distributed with different strains isolated from different regions. Averaging the fatty acid data means any differences between strains from different climatic zones are lost. In addition to this, some of

the species that are globally distributed, including *E. Huxleyi*, can be very abundant thereby dominating the plot, further diminishing any potential trends. Overall, this method of plotting the global distribution of fatty acid data is too simplistic for the purposes of this study. Another more simplistic approach was to instead plot these variables against latitude as this provides a basic representation of the changing climatic zones across the globe from pole to pole (**Figure 33** and **Figure 34**). However, once again no trend was observed across global latitudes.

Impact of Culture Conditions on Phytoplankton Fatty Acids
The culture conditions which were collected and analysed in this study were the temperature, culture growth stage, light duration, light intensity and nutrient availability within the culture media. The impact of changing these variables on the phytoplankton fatty acid unsaturated to saturated ratio was assessed using the percentage fatty acid composition data. This dataset was chosen due to it containing more fatty acid profiles than the mass per cell dataset, making it more representative of general phytoplankton fatty acids. Of the culture conditions that were analysed, observable differences and trends in phytoplankton fatty acid unsaturation were seen for changes in temperature, light intensity and nutrient availability. The data for growth stage and light duration was heavily biased towards the logarithmic stage and 12 hours respectively, making statistical tests invalid.

When comparing culture growth temperatures, the temperatures were grouped into their characteristic climate zones. Any temperature below 5 °C was labelled polar, temperatures above 5 °C and below 20 °C were labelled temperate and temperatures above 20 °C are considered tropical. The average unsaturated to saturated ratios for each climate zone is shown in **Figure 35**. The uncertainties associated with these averages are large and stem from the large species inter-variability as well as other culture growth conditions that were not controlled for here. The percentage composition data was analysed using a Kruskal-Wallis[122] test which found that there were no statistically significant (p = 0.06297) differences between the unsaturated to saturated ratios of the different climate zones. The accuracy of this assessment is questionable as it is known that cold water phytoplankton produce more unsaturated fatty acids to maintain membrane fluidity.[84] The number of polar species, however, is low relative to temperate and tropical species in this dataset meaning this data may be too limited to be representative of all phytoplankton species.

The nutrient availability was split into the following categories: replete (no limitation), moderate limitation, strong limitation, iron-limited, phosphorus-limited and the nitrogen source either being ammonia, nitrate or urea, as defined by the parameters set in the literature. The average unsaturated to saturated ratio of the phytoplankton species exposed to these nutrient regimes are shown in **Figure 36**. Once again, the uncertainties are large within the different nutrient regimes. There is also a bias towards replete nutrient levels which is a product of the type of studies sampled. A Kruskal-Wallis[122] test followed by a Dunn[123] test on this data shows that the only statistically significant difference was between the unsaturated to saturated ratio of the species exposed to an alternative nitrogen source to that of all the other nutrient regimes (all p values <0.05). However, drawing the conclusion that these alternative nitrogen sources lead to phytoplankton producing fewer unsaturated fatty acids would not be justified. Firstly, many of the other studies which report the nutrient regime to be replete use culture media such as f/2, PES and GSe. These media all use nitrate

as their source of nitrogen so it would be expected that, on average, the phytoplankton grown using nitrate as their nitrogen source in the study by Lourenço *et al.*[94] would produce fatty acids of a similar unsaturated to saturated ratio to that of the species with replete nutrients.

Secondly, all of the fatty acid profiles that contribute to the average US ratios for the alternative nitrogen source data come from a single study by Lourenço *et al.*[94] where certain experimental parameters such as, fatty acid extraction efficiencies and differences in instrument sensitivity, may make comparisons between the data generated by individual studies difficult. This highlights the difficulty of comparing fatty acid profiles when the data is heavily biased towards certain culture conditions.

Finally, from the plot seen in **Figure 37**, an inverse relationship can be seen between the unsaturated to saturated ratio and the light intensity the phytoplankton cultures are exposed to. This is confirmed with a Kendall rank correlation test ($p = 2.2 \times 10^{-6}$). This result has been observed in previous studies, including the similar phytoplankton fatty acid meta-analysis carried out by Galloway *et al.*[82], who found that the percentage contribution of ω3 and ω6 fatty acids decrease as light intensity increases. The decrease in the proportion of unsaturated fatty acids within the cell is thought to be an light intensity induced acclimatisation to modulate the process of photosynthesis.[124]
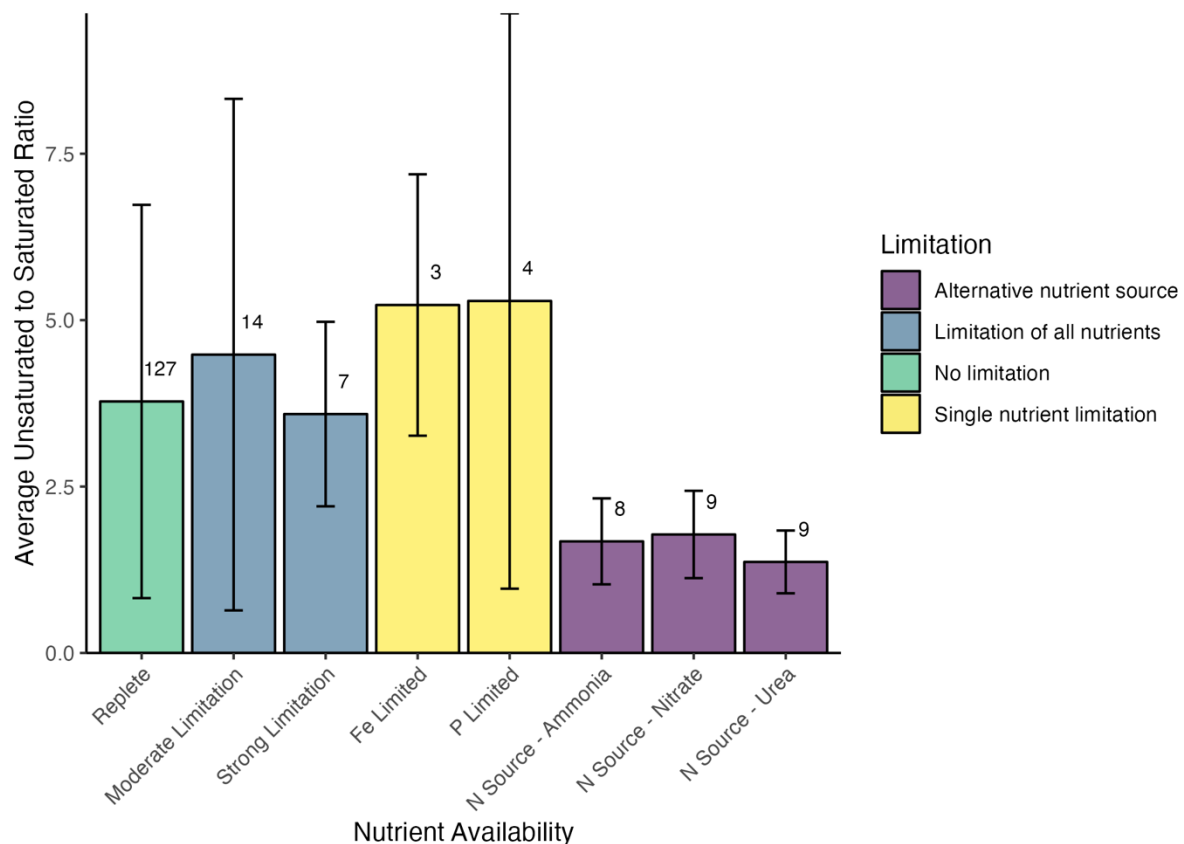
Figure 36 *– Average unsaturated to saturated ratio of phytoplankton species under different nutrient regimes. The numbers above the bars show the number of species that contribute to each average.*
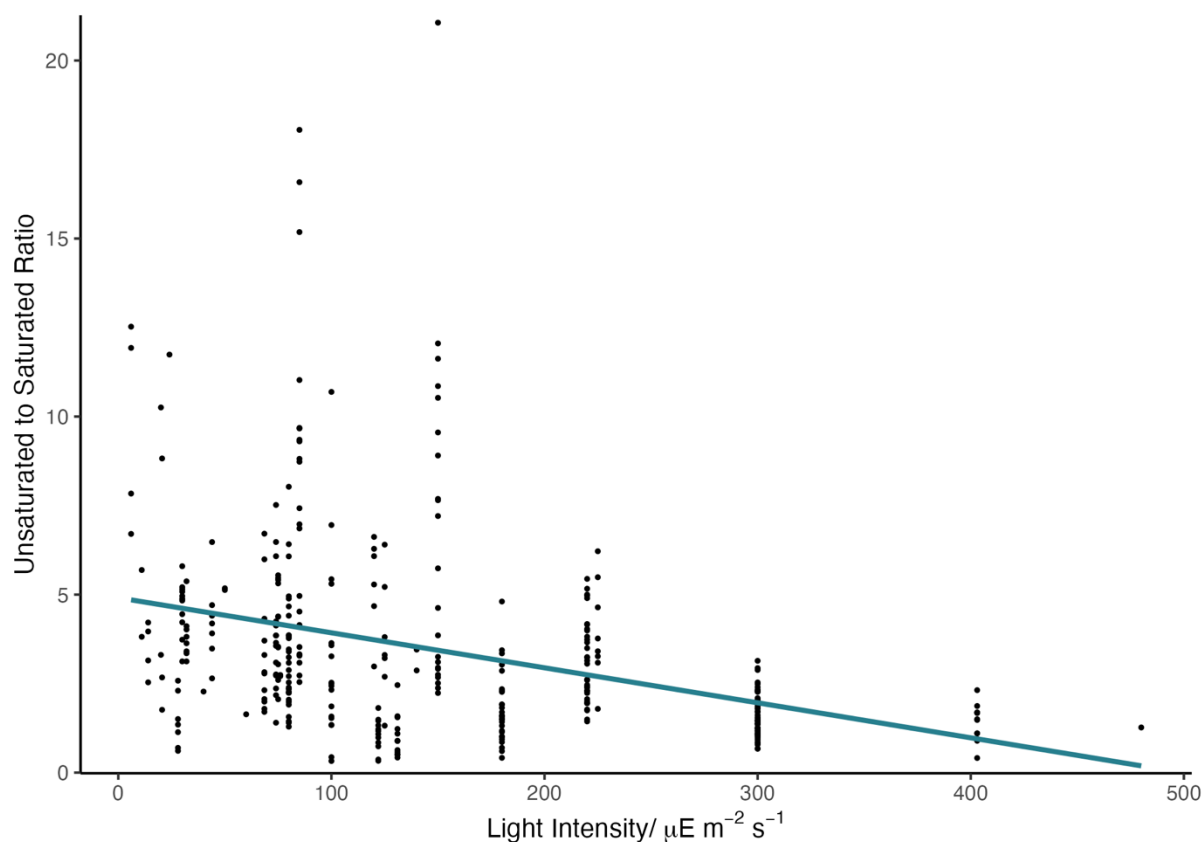
Figure 37 *– Light intensity dependence of the unsaturated to saturated ratio of phytoplankton fatty acids.*

Phytoplankton Species Determination for Proof-of-Concept Experiments

Following on from the direct analysis of the literature phytoplankton data, this data was then used to determine phytoplankton species ideal for proof-of-concept experiments. In the context of this research project, the proof-of-concept culture experiments involved species that were known to produce relatively large amounts of unsaturated fatty acids which, if released by the cells, would readily react with ozone at the ocean surface.

To identify these proof-of-concept species, the dataset containing fatty acid mass per cell information was ranked according to the average unsaturated to saturated ratio of the fatty acids found within the phytoplankton cell; the average total mass of fatty acids found within the cells and the number of species observations obtained from the OBIS database as a proxy for abundance. The observational data was included in this ranking to eliminate species that are not readily observed in the oceans as these species would not have a major impact on ocean ozone uptake under normal circumstances. In this instance the fatty acid mass per cell dataset was used as it contained information about the amount of fatty acids produced rather than the relative percentage amounts given by the percentage composition dataset. This information gives a more realistic prediction of ozone uptake potential as this will depend on the absolute amount of organic matter produced. Four species that were deemed most appropriate can be seen in **Table 8**, with considerations being made with regards to culture and strain availability. Note that the OBIS observations only apply to the species and not the specific species strain.

Table 8–- *Phytoplankton species for proof-of-concept experiments. The values given here are means with their respective standard deviations.*

Species	Strain	Average Unsaturated to Saturated Ratio	Average Fatty Acid Mass per Cell/ pg	Unsaturated Fatty Acid Mass per Cell/ pg	Observations in OBIS Database
Emiliania huxleyi	RCC1265	8.90 ±3.07	1.59 ±2.53	0.93 ±0.90	20515
Skeletonema costatum	RCC70	7.69 ±6.55	3.88 ±2.23	2.80 ±1.90	59348
Rhodomonas salina	CCMP1319	7.05 ±2.85	6.33 ±3.07	4.67 ±1.78	766
Thalassiosira pseudonana	CCAP 1085/12	5.85 ±2.23	1.26 ±0.67	0.96 ±0.48	316

Fatty Acid Analysis of Proof-of-Concept Phytoplankton Species

Of the five species that were identified, the three that were chosen were *Skeletonema costatum* (RCC70), *Thalassiosira pseudonana* (RCC950) and *Emiliania huxleyi* (RCC1265) due to culture availability. Prior to any extractions, attempts were made to characterise the growth curves of these species in culture, as described in the experimental of this chapter. The growth of these cultures can be seen in **Figure 38**.

S. costatum had the most typical growth curve out of the three, with a logarithmic growth phase up to around day 8, a short stationary phase of around 4 days and a long senescence phase thereafter. *T. pseudonana* has a sharp logarithmic phase of two days, after which the culture exists in an extended stationary phase before declining into a senescence phase around day 40. Due to the short nature of the logarithmic growth phase, it is poorly characterised, and it is unclear whether the unusually high fluorescence reading on day 3 is erroneous. The growth curve of *E. huxleyi* shares a similar trend as *S. costatum*, except with the stationary phase being elongated to around day 20. The reason for the decline in fluorescence in the middle of the stationary phase is uncertain. A possible explanation is the tendency of this species to adhere to the sides of the flask they are cultured in. The process of swirling the cultures before aliquots are taken was not standardised and could have led to variable amounts of cellular material being resuspended into the media. As it is the cells suspended in the media that are used to give the fluorescence reading, this could lead to an unrepresentative result. The unpredictable growth of this species may also be explained by the LED light not being ideal for its growth. It was observed in this study and in the work of Dr. Alison Webb (currently a PDRA in the Carpenter group) that many cultures purchased did not survive or grow favourably in these lighting conditions, including many *T. pseudonana* cultures that failed prior to the work shown here. The LED lights emit light at two specific red and blue wavelengths, and it was postulated that some species require a wider spectrum for optimal growth. Due to *S. costatum's* ideal and predictable growth curve, this was the only culture chosen to go through fatty acid extraction as no further growth curves could be generated in the study time available.

SPE of Skeletonema Costatum Culture Filtrate

The chromatograms of a 500 mL culture filtrate and a blank are shown in **Figure 39**. The results of this experiment show that saturated fatty acids and diacids were seen in both the phytoplankton filtrate samples and the culture media blanks. No additional compounds beyond those found in the blanks were found even in the highest volume of phytoplankton filtrate of 500 mL. There are several possible reasons why *S. costatum* did not seem to

contribute any additional material to the filtrate. The first could be that the volume of culture filtrate extracts was too low to see any measurable contribution of the phytoplankton organic matter. The second was that at the end of logarithmic phase, very little organic matter had been released into the media due to there being limited cell death at this stage. Although it is known that more organic matter is released when phytoplankton blooms start to die off, organic matter is readily released during the early stages of phytoplankton growth so this explanation seems unlikely.[125, 126]

There are multiple potential sources of the fatty acids and diacids in the culture media blanks. The first could be the salts used to prepare the media. As seen previously with the artificial seawater (Chapter 2), these salts can be contaminated with saturated fatty acids. This, however, does not explain the presence of the diacids and may not be the only source of the fatty acids. Another potential source could be the equipment used to culture the phytoplankton and subsequently filter these cultures. The glassware was frequently used in phytoplankton culture work prior to this experiment and was either washed by rinsing with deionised water or by a laboratory dishwasher. The filter manifold was washed with deionised water. This could have led to carry over into the blanks and the samples for this experiment. In addition to this, another source of potential contamination could be the PTFE-coated silicone seals used during the esterification step. These had been acid washed and reused for the experiments involving the PML seawater samples. Given that the fatty acids and diacids that were present in the phytoplankton filtrate experiments were also present in the PML samples, there could be carry over on these seals.
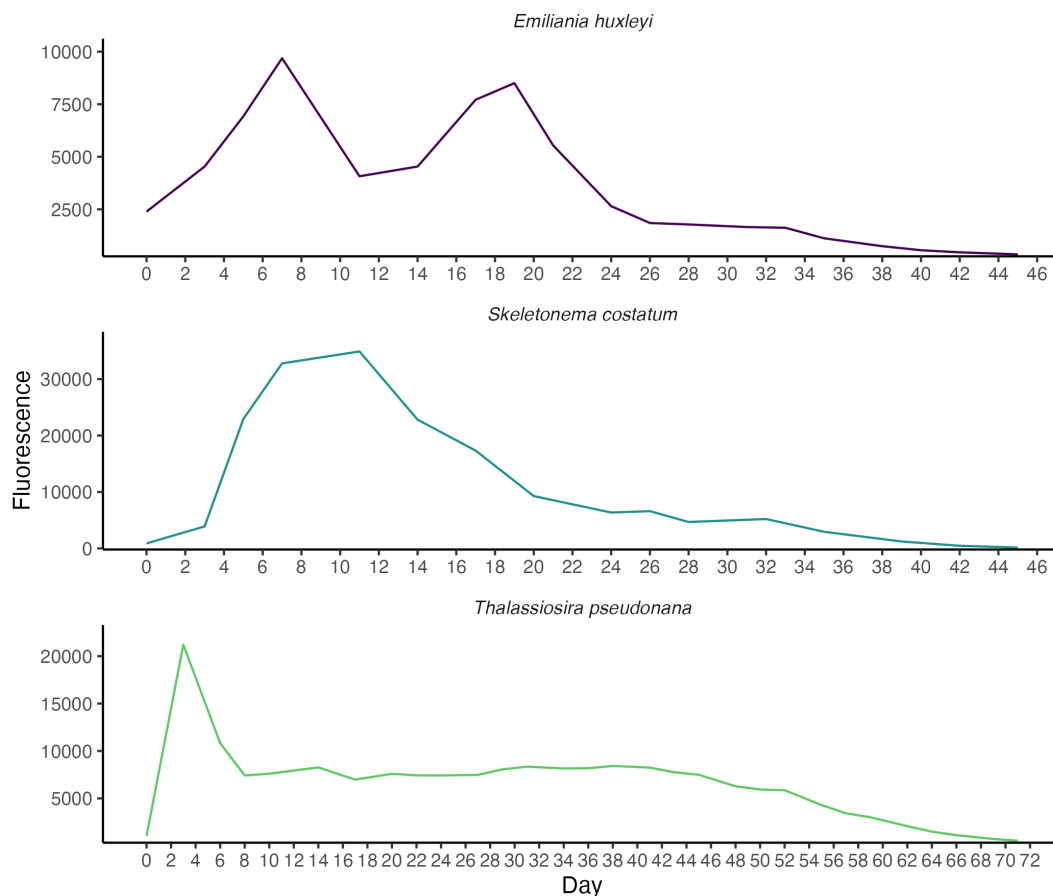
Figure 38 – *Growth curves of proof-of-concept phytoplankton cultures, characterised by in vivo fluorescence.*
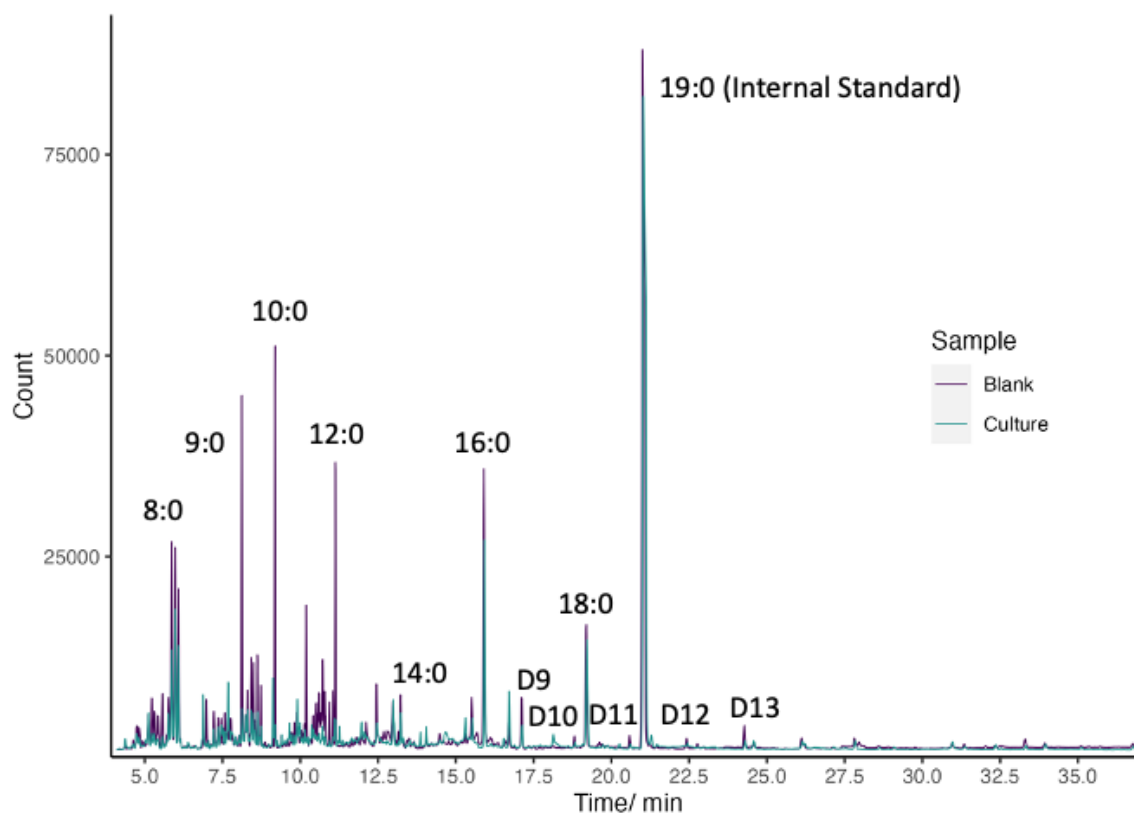
Figure 39 *– GC-MS chromatogram of the Skeletonema costatum 500 mL filtrate sample and 500 mL filtrate blank using the SIM MS method.*

Despite the potential contamination of the equipment, this work shows that with limited stressors, only negligible fatty acids were released by *S. costatum*. For this reason, in addition to the unusual growth curves of the cultures and instrument failures, phytoplankton work at University of York was halted to focus on the work presented in the previous chapter. Phytoplankton culturing was resumed at UIB, which is discussed next.

Impact of Stress Factors on Phytoplankton Cultures

Of the three species extracted, only the *Synechococcus* and *P. tricornutum* supernatant showed higher concentrations of fatty acids compared to the blank media following a blank subtraction. Note that all concentrations quoted hereafter are those where background concentrations measured in the blank media are subtracted from the culture concentrations. In both cases a more limited number of fatty acids was observed when compared to both the seawater samples described in the previous chapter and, in the case of *P. tricornutum*, to those found in the literature for these species (**Figure 40** and **Figure 41**).[94, 102, 103, 105, 107, 108, 111, 113] However, *P. tricornutum* did show high levels of C16 and C18 unsaturated fatty acids which were the dominant unsaturated fatty acids observed in the coastal seawater samples (Chapter 3). For *Synechococcus*, more fatty acids were observed than reported in the literature with regards to fatty acids within the cells, although this species is under-represented in the phytoplankton fatty acid dataset generated here. Bacteria are known to have fatty acid profiles dominated by C16 and C18 saturated and mono-unsaturated fatty acids, with the saturated fatty acids dominating.[23] C15 and its branched isomer were also observed here and are well known indicators for the presence of bacteria.[23, 100] The reduced range of fatty acids observed for the *P. tricornutum* supernatant may, in part, be due to the

77

SPE method used not being that well optimised for the extraction of fatty acids above C20 (see Chapter 2) which include many of the fatty acids observed in the literature. These long chain, polyunsaturated fatty acids are also very labile and, although they may be present in the cells, if released they may not last long due to biotic and abiotic decomposition, especially if the cultures are active and non-axenic.

The percentage contribution of each fatty acid to the total for the experimental cultures seen here was typically not comparable to the literature. As the literature data represents intracellular fatty acids and the data presented here is for the growth media, this is not entirely unexpected due to the difference in fates of the fatty acids inside and outside the cell with regards to decomposition. One key difference, in the case of *P. tricornutum*, is the marked increase in the relative proportions of 14:0, 16:2, 16:4 and 18:2 when exposed to heat stress, well above the proportions found in the literature. *Synechococus* did not display such a dramatic shift in relative proportions of fatty acids under stress, except for the increase in 18:0. **Figure 42** and **Figure 43** show the impact of different stressors on the concentrations of fatty acids found in the supernatant.
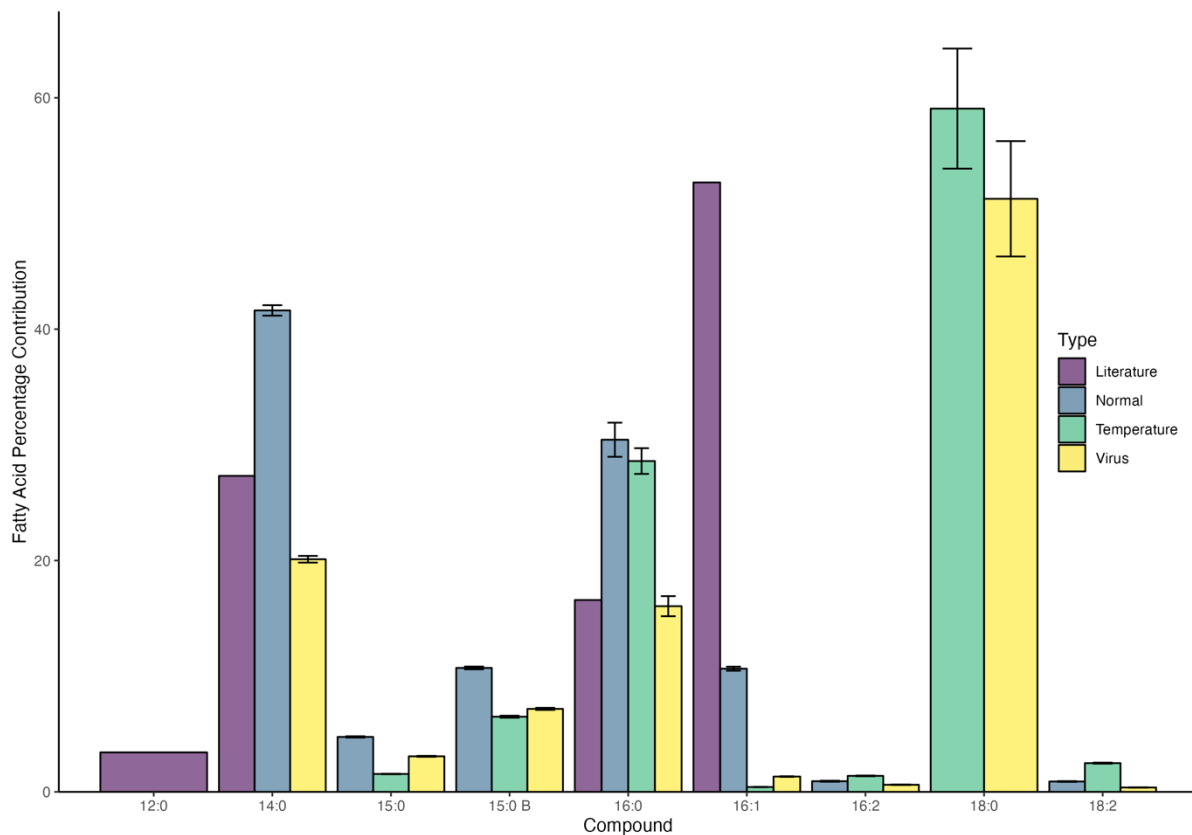
Figure 40 *– Comparison between the percentage composition of fatty acids extracted from the Synechococcus supernatant and intracellular fatty acids reported in the literature.[102] Normal represents the cultures grown under control conditions, and temperature and virus represent heat and viral stress respectively.*
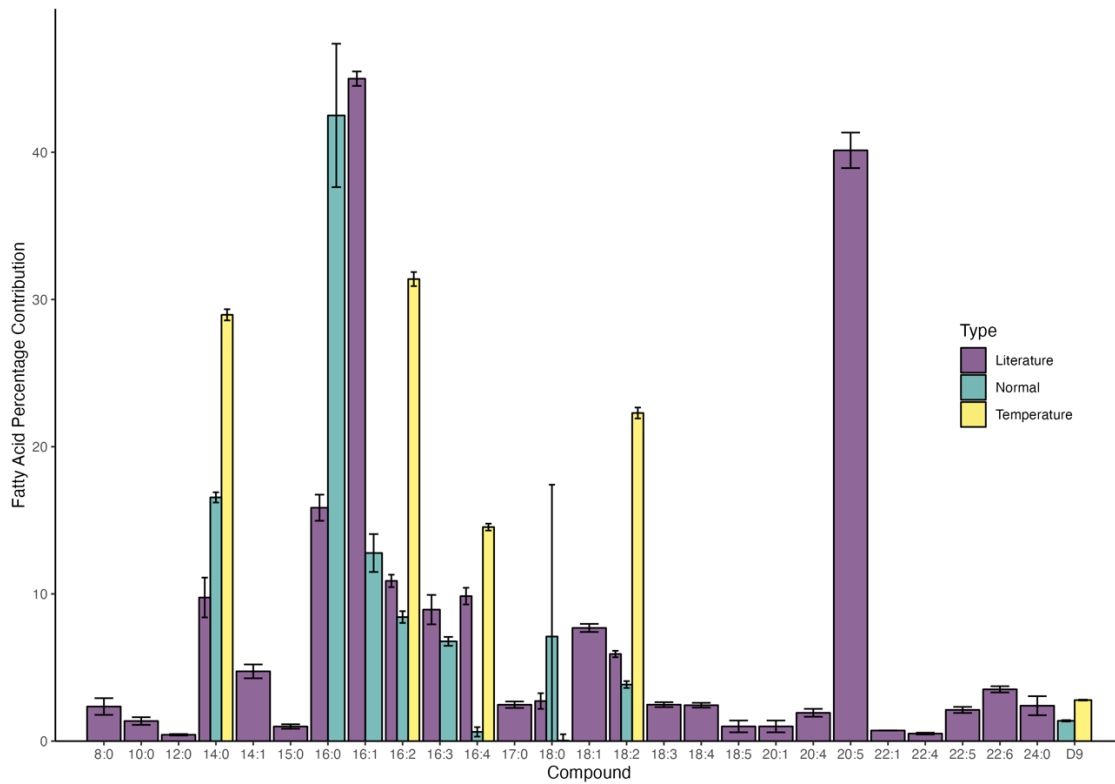
Figure 41 *– Comparison between the percentage composition of fatty acids extracted from the Phaeodactulum tricornutum supernatant and intracellular fatty acids reported in the literature across a range of studies.[94, 102, 103, 105, 107, 108, 111-113] Normal represents the cultures grown under control conditions and temperature represents cultures exposed to heat stress.*
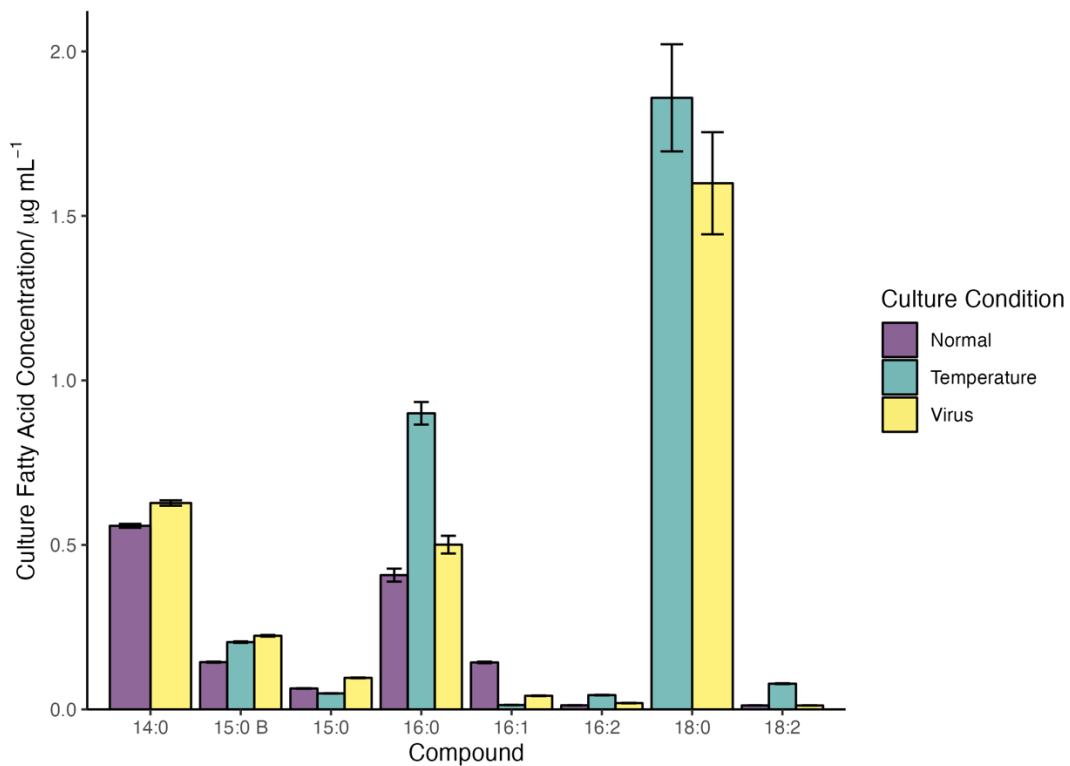
Figure 42 *– Impact of heat (temperature) and viral (virus) stress on Synechococcus supernatant fatty acid concentrations.*
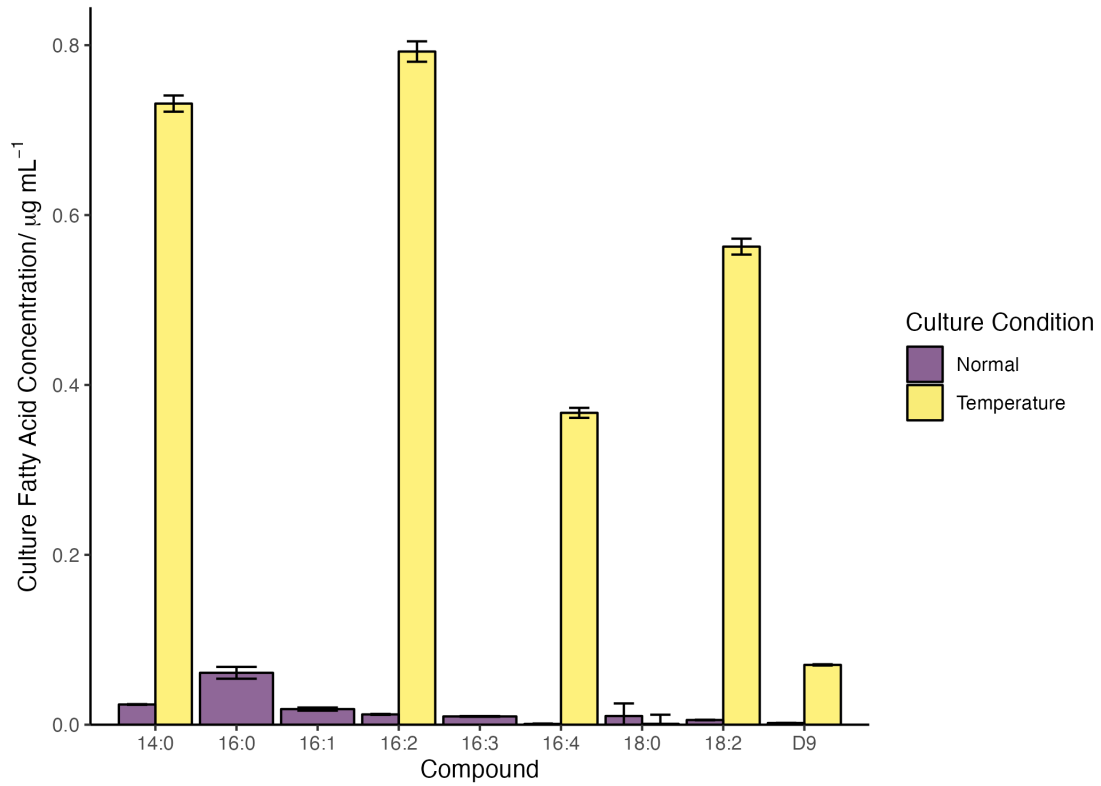
Figure 43 *– Impact of stress on Phaeodactulum tricornutum supernatant fatty acid concentrations. Normal represents the cultures grown under control conditions and temperature represents cultures exposed to heat stress.*
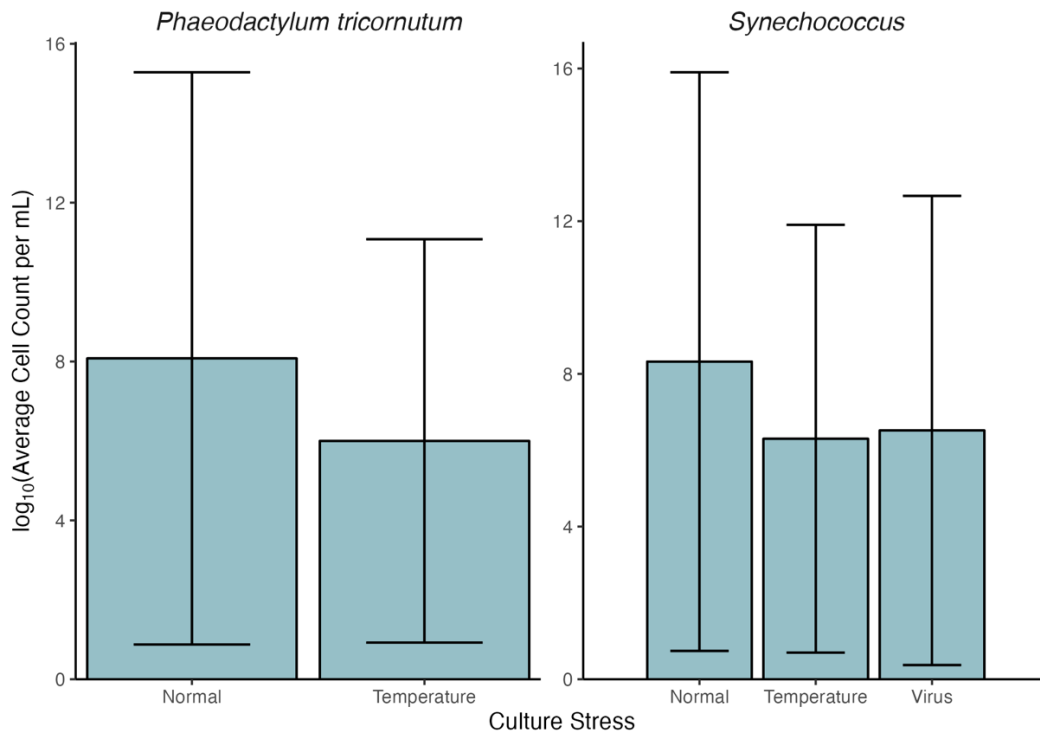
Figure 44 *– Average cell counts of the Phaeodactylum tricornutum and Synechococcus under both normal growth conditions and heat (temperature) and viral (virus) stressors with the error bars representing the standard deviation.*

Rousch et al.[105] studied the impacts of increased temperature on *P. tricornutum* and found the opposite result to this study. They observed that the levels of saturation of cellular fatty acids increased as temperatures increased, similar to what was seen for the *Synechococcus* cultures in this study. The reason why the opposite was seen in this study is unclear, especially as cell counts decreased following heat stress (**Figure 44**), indicating cell lysis and the release of cellular material into the growth media. The release of the lysate is also supported by the significant increase in fatty acid concentrations following temperature stress (**Figure 43**).

When comparing the impact of temperature stress and virus stress on *Synechococcus* fatty acids, the difference between the two appears to be insignificant. The decrease in cell numbers across the two stressors is broadly the same and the changes in fatty acid concentrations are comparable, except in the case of 16:0 where temperature stress increased the concentration of this compound significantly. 14:0 was not observed in the temperature stress cultures for this species, although the reason for this is uncertain. Overall, this result suggests that the stress response of *Synechococcus* is similar in both cases and that the virus altering the cell's metabolism towards its own reproduction does not impact fatty acid production.[127]

Overall, this test shows that although phytoplankton species do release fatty acids into the medium around them, this release appears to be limited under natural conditions, and the distribution of extracellular fatty acids may not directly compare to those found within the cells themselves. Stress-induced cell lysis does typically release more material into the media via cell lysis; this was most apparent in the case of *P. tricornutum*. However, this test represents only a few stress scenarios, and does not include zooplankton grazing which would directly release intracellular material from healthy cells and likely produce different fatty acid profiles to what is seen here.[127] This investigation also shows that the fatty acids released are broadly similar to those seen in the seawater samples analysed in Chapter 3, highlighting the link between marine biology and oceanic fatty acids.

Conclusions

A literature search of intracellular marine phytoplankton fatty acids reported from controlled culture studies yielded a general profile that, as expected, relates to the typical fatty acid markers for marine biota in seawater. These fatty acid profiles are also comparable to those measured in seawater samples described in the previous chapter as well as in the literature, confirming that phytoplankton are a key source of these compounds within the marine environment. The proportion of unsaturated fatty acids compared to the total intracellular fatty acid levels did not show statistically significant differences across different incubation conditions of temperature, culture growth stage, light duration, or nutrient availability. However, levels of unsaturation were negatively correlated with light intensity.

Although these results suggest limited environmental impacts on fatty acid unsaturation, this conclusion is not absolute and is likely influenced by sampling biases and the simplification of the data for analysis. For example, data was heavily biased towards replete nutrient conditions used for culturing. Also, most of the literature sampled studied individual phytoplankton cultures, which are not representative of the mixed stresses faced in an authentic marine environment.

Overall, no discernible trends were apparent in global distributions of proportion of unsaturated fatty acid derived from the combination of the literature fatty acid profiles and the locational data found within the OBIS database.[114] With regards to the global plotting of fatty acid unsaturation, averaging the data across all studied strains of a species means that differences between strains are not retained. This is particularly important for species that are found world-wide, such as *E. huxleyi*, whose different strains were isolated from different regions. As previously mentioned, the controlled culture conditions will not accurately mimic that of the marine environment and therefore applying measured fatty acid concentrations from such cultures to a global distribution will not produce a map that is representative of *in situ* phytoplankton and overall marine fatty acids. To improve on this, *in situ* measurements of both phytoplankton and seawater fatty acids are needed across the globe, with this data being analysed and plotted directly. This was at least partially achieved by the CONNECT cruise described in the previous chapter.

The culture experiments carried out in this study suggest that the intracellular and extracellular fatty acids typically have different profiles, at least when individual cultures are analysed. However, considering the small volume of the cultures (≤ 500 mL) it may be that the compounds not observed were below the detection limit. *S. costatum* and *Ostreococcus* showed no detectable fatty acid released into the media, whereas filtrate fatty acids were seen for both *P. tricornutum* and *Synechococcus* under both normal and stress conditions. The impact of stress was more marked on *P. tricornutum* than on *Synechococcus* when considering fatty acids, with fatty acid concentrations increasing significantly following thermal stress, with large increases in unsaturated fatty acid concentrations observed for *P. tricornutum*.

These experiments are a starting point in understanding the link between phytoplankton and oceanic fatty acids. However, technical difficulties limited the scope of this work. Difficulties achieving cultures that grew predictably meant that only one proof of concept species was investigated (*S. costatum*), and that species was only analysed at volumes of ≤ 500 mL at the end of the logarithmic growth phase. Further stress experiments were carried out on species that were not known to produce relatively high amounts of fatty acids due to the cultures available at UIB. The stressors were also limited to temperature and viral infection due to the loss of the grazers prior to culturing. If this work were repeated, more time should be dedicated to establishing large volume cultures of proof-of-concept species whose growth is well characterised and growth conditions are well optimised for such growth. By doing this, large culture volumes can be sampled at known growth stages, providing a more robust analysis of exuded phytoplankton fatty acids. Work can then move on to the influences of environmental stressors by altering the previously established growth conditions and the addition of other organisms including grazers.

Chapter Five – Summary and Conclusions

Overall, during this PhD three key objectives have been achieved: the development of a viable method for extracting and quantifying fatty acids in large volume aqueous samples; the successful application of this method to seawater and sea surface microlayer samples and phytoplankton cultures; and the identification and quantification of the fatty acids in coastal and open ocean waters and in phytoplankton extracts, in an attempt to elucidate whether biological activity has an influence on oceanic ozone deposition. Although there are many avenues for improvement, this work provides a good basis for further analysis of aquatic fatty acid analysis in the context of oceanic ozone deposition.

SPE and FAME Conversion Method

With regards to the extraction method, the overall process of extraction using PPL SPE cartridges followed by the conversion of the fatty acids to FAMEs proved successful and convenient in comparison to previously used extraction methods. Throughout this PhD it is estimated that approximately 500 L of seawater has been processed. In terms of sustainability, the value of this method for bulk seawater analysis is clear when considering the many litres of solvent that would have been needed if a classical liquid-liquid extraction was used instead. In the context of this work, it was useful to use the same type of SPE cartridge used for the parallel molecular DOM analysis by high resolution mass spectrometry so that the DOM and fatty acid datasets were directly comparable. However, it appears that this came at the detriment of extraction efficiencies for larger fatty acids, which were low (as low 2% for 9-octadecenoic acid). Extraction efficiencies may be improved by using SPE cartridges with different sorbents, such as a simple C18 sorbent. It is possible that to cover the full range of fatty acids present in seawater by using multiple cartridges of different types could be used in series to capture any compounds not retained by the previous cartridge. The elutes from each could then be pooled for the derivatisation step.

Another step which compromises the overall efficiency of the method is during derivatisation, as the acid-catalysed esterification typically does not go to completion. The best way to improve this is to heat the reaction mixture for longer, although with the equipment available in this work and the time constraints, this was not practical for this study. Losses during extraction were accounted for by the internal standard and recovery experiments, and measured concentrations were corrected for extraction efficiency.

The extract concentrations were often near the limits of detection of the GC-MS instrumentation. This was improved by switching to a SIM method for the mass spectrometer but due to the relatively large number of structurally different compounds targeted by the analysis, a selection of eight ions were monitored. This compromises the sensitivity when compared to a method only analysing a quantifier and qualifier ion. Pre-screening of samples with a full mass scan mode, ideally on a time-of-flight mass spectrometer rather than the quadrupole used, and creating a bespoke mass spectrometry method for the quadrupole would provide maximum sensitivity for both identification and quantification. However, this is not practical when used in a continuous campaign like this study, but may be viable for smaller, more discrete experiments.

Sampling Methods Improvements

Throughout this study there were contamination issues with regards to SML sampling. The Garrett screen used for SML sampling for both the PML campaign and CONNECT cruise both showed signs of contamination, specifically with diacids, despite use of screen cleaning protocols in both campaigns. This highlights the need for thorough blank characterisation when analysing organic compounds, especially fatty acids. These diacids are often used in manufacturing lubricants and were likely residues from when the screens were made. Even after significant use, contamination remained. Therefore, for future work involving the analysis of fatty acids, the construction of the screens should be kept separate from equipment that has been used alongside greases, and the individual components should be washed before assembly. Washing may include the use of detergents followed by the cleaning protocol introduced in the PML campaign. Other materials such as nylon, plastic or glass could also be used for the screens, but these would also need to be assessed for any leaching of organic compounds. Although steps were taken to reduce the possibility of ship-borne contamination, such as sampling as far as possible from the RV SONNE for the CONNECT samples, there may still have been some contamination from the smaller vessel used when sampling. This distance could be increased by using a remotely operated vessel carrying a rotating drum to collect SML samples, but this is beyond the scope of this study.[128]

Seawater Fatty Acid Concentrations

This work has contributed numerous seawater fatty acid profiles for both coastal waters and the open ocean, including a seasonal time series for said coastal waters. The fatty acids seen in the seawater samples collected from both the PML campaign and CONNECT cruise ranged from C8 to C18 with varying levels of unsaturation and concentrations between 0.0005 µg L^{-1} and 46 µg L^{-1}, contributing to between 0.002% and 8% of the total DOM pool. The compounds and concentrations were comparable to that in the literature, except for the absence of the larger fatty acids likely resulting from the extraction biases.

Overall, this study benefited from the ability to source large volumes of seawater for each sample. This was helpful due to the naturally low concentrations of SML fatty acids. However, compound identification and quantification may have been improved if sample volumes were comparable to *Dittmar et. al.*[41] of 10 L. Although this would have likely been impractical for a study like the PML campaign, it may be possible on a cruise like CONNECT where there was access to a continuously flowing underway system. This could be fed into an inline SPE cartridge which could be changed and eluted at regular intervals allowing for large volumes of seawater to be sampled. This, however, would not be possible for SML samples due to the nature of sampling.

No significant saturated fatty acid and diacid seasonality was seen in the coastal dataset and there were no spatial trends in the open ocean fatty acid data. There was, however, seasonality in the PML unsaturated fatty acid concentrations which could be linked to seasonal increases in biological activity. This variability is important when considering oceanic ozone uptake via its reaction with DOM, since the reactive fraction of DOM, including unsaturated fatty acids, may not exhibit the same temporal variation as total DOM. The latter has previously been used as a proxy for ozone reactivity at the sea surface. The estimated pseudo first order rate constant for the observed unsaturated fatty acids in the summer peak increased to above the estimated value for DOM as a whole. This is significant considering

the low contribution (up to 10%) fatty acids make to the DOM pool. This shows that using a single value for ozone reactivity towards SML DOM when estimating oceanic ozone dry deposition will not capture the seasonal variability in reactivity and will possibly underestimate deposition in productive waters, especially in biologically active seasons. This work highlights the need to comprehensively characterise the reactive portions of DOM when considering ozone dry deposition and more work needs to be done identifying these species in a variety of different marine environments if oceanic ozone fluxes are to be accurately quantified.

Phytoplankton Experiments
The phytoplankton experiments carried out in this study provide a starting point for understanding the links between biological activity and oceanic ozone dry deposition. The literature search generated a valuable dataset of phytoplankton fatty acid concentrations which could be used to identify species of interest in the context of this study. However, the conditions under which the species were grown were usually heavily biased towards optimised growth conditions and therefore the cellular fatty acid levels observed were unlikely to be representative of those produced in the natural environment. These biases were also a likely reason why it was difficult to robustly assess the impacts of changing environmental conditions on fatty acids.

The proof-of-concept experiments yielded limited results for multiple reasons. The first was the difficulty in establishing the cultures and getting them to grow in a predictable manner. In addition to cultures being lost due to facility failures, many attempts were made to culture an axenic strain of *T. pseudonana* but the culture failed when introduced to the LED lighting used for culturing. It is likely that these cultures needed a broader light spectrum to grow effectively. The cultures that were established repeatedly grew in an unpredictable manner and *S. costatum* was the only culture that grew reliably enough to be investigated. If this study was repeated, more time would be spent identifying the optimal growth conditions and set up which may have included different light types and regimes as well as intermittent or continuous culture agitation. Growth characterisation could also be assessed using a different metric such as cell count measured by flow cytometry.

The extraction of the *S. costatum* filtrate yielded no fatty acids above the background levels. This was surprising given the literature data suggesting this species produced an abundance of fatty acids. It was possible that these fatty acids remained in the cells and were not readily released at the end of their logarithmic growth phase. It was also possible that fatty acids were released but the culture volumes were too small, so the amount extracted was below the limit of detection of the instrument. If this line of work were to continue, filtrate extracts would be collected from higher volume cultures and at different stages of growth to investigate the fate of this species' fatty acids further.

The stress tests carried out on *P. tricornutum* and *Synechococcus* did however yield observable fatty acids in the growth medium. These fatty acids were present in both the control cultures and stressed cultures with *P. tricornutum* showing a large increase in fatty acid concentration when exposed to heat stress. This is more likely due to cell lysis releasing the intracellular fatty acids. The same response to stress was not observed for *Synechococcus* but this species is not known to produce high amounts of cellular fatty acids according to the

literature dataset. The fatty acids observed in this work were, in the case of *P. tricornutum*, much less varied than that in the literature data and more work is needed to understand why. It may be the case that, once again, the small culture volumes used meant that some fatty acids fell below the detection limit. It is also possible the labile fatty acids were released but were recycled and therefore removed from solution before extraction. If this work were to be progressed further, larger culture volumes should be used to hopefully boost the extracted fatty acid concentrations. Different environmental stressors should also be investigated, such as exposure to grazers, that are more representative of the stressors experienced in the marine environment. A study including grazers could involve introducing the grazers to the phytoplankton cultures during various stages of their growth to induce cell lysis when the cells are healthy during their growth phase and when they are dying off. The culture media could then be analysed at different time points following the addition of grazers to investigate how the organic matter released from cell lysis may change over time.

References

1. C. Hardacre, O. Wild and L. Emberson, *Atmospheric Chemistry and Physics*, 2015, **15**, 6419-6436.
2. L. Ganzeveld, D. Helmig, C. W. Fairall, J. Hare and A. Pozzer, *Global Biogeochemical Cycles*, 2009, **23**, 1-16.
3. D. Helmig, E. K. Lang, L. Bariteau, P. Boylan, C. W. Fairall, L. Ganzeveld, J. E. Hare, J. Hueber and M. Pallandt, *Journal of Geophysical Research Atmospheres*, 2012, **117**, 1-15.
4. J. H. Seinfeld, *Atmospheric chemistry and physics: from air pollution to climate change*, Wiley-Blackwell, 2nd e. edn., 2012.
5. M. Shrivastava, C. D. Cappa, J. Fan, A. H. Goldstein, A. B. Guenther, J. L. Jimenez, C. Kuang, A. Laskin, S. T. Martin, N. L. Ng, T. Petaja, J. R. Pierce, P. J. Rasch, P. Roldin, J. H. Seinfeld, J. Shilling, J. N. Smith, J. A. Thornton, R. Volkamer, J. Wang, D. R. Worsnop, R. A. Zaveri, A. Zelenyuk and Q. Zhang, *Reviews of Geophysics*, 2017, **55**, 509-559.
6. M. D. King, A. R. Rennie, K. C. Thompson, F. N. Fisher, C. C. Dong, R. K. Thomas, C. Pfrang and A. V. Hughes, *Physical Chemistry Chemical Physics*, 2009, **11**, 7699-7707.
7. P. J. Young, V. Naik, A. M. Fiore, A. Gaudel, J. Guo, M. Y. Lin, J. L. Neu, D. D. Parrish, H. E. Rieder, J. L. Schnell, S. Tilmes, O. Wild, L. Zhang, J. Ziemke, J. Brandt, A. Delcloo, R. M. Doherty, C. Geels, M. I. Hegglin, L. Hu, U. Im, R. Kumar, A. Luhar, L. Murray, D. Plummer, J. Rodriguez, A. Saiz-Lopez, M. G. Schultz, M. T. Woodhouse and G. Zeng, *Elementa-Science of the Anthropocene*, 2018, **6**.
8. R. Atkinson, *Journal*, 2000, **34**, 2063-2101.
9. M. Martino, B. Lézé, A. R. Baker and P. S. Liss, *Geophysical Research Letters*, 2012, **39**, 39-43.
10. M. D. Shaw and L. J. Carpenter, *Environmental Science and Technology*, 2013, **47**, 10947-10954.
11. D. Clifford, D. J. Donaldson, M. Brigante, B. D'Anna and C. George, *Environmental Science and Technology*, 2008, **42**, 1138-1143.
12. O. Wurl, L. Miller, R. Röttgers and S. Vagle, *Marine Chemistry*, 2009, **115**, 1-9.
13. O. Wurl, E. Wurl, L. Miller, K. Johnson and S. Vagle, *Biogeosciences*, 2011, **8**, 121-135.
14. M. Cunliffe, A. Engel, S. Frka, B. Ž. Gašparović, C. Guitart, J. C. Murrell, M. Salter, C. Stolle, R. Upstill-Goddard and O. Wurl, *Progress in Oceanography*, 2013, **109**, 104-116.
15. M. Van Pinxteren, C. Müller, Y. Iinuma, C. Stolle and H. Herrmann, *Environmental Science and Technology*, 2012, **46**, 10455-10462.
16. E. S. Van Vleet and P. M. Williams, *Limnology and Oceanography*, 1983, **28**, 401-414.
17. B. Gašparović, M. Plavšić, B. Ćosović and A. Saliot, *Marine Chemistry*, 2007, **105**, 1-14.
18. Z. Kozarac, D. Risović, S. Frka and D. Möbius, *Marine Chemistry*, 2005, **96**, 99-113.
19. B. Gašparović, Z. Kozarac, A. Saliot, B. Ćosović and D. Möbius, *Journal of Colloid and Interface Science*, 1998, **208**, 191-202.
20. U. Von Gunten, *Water Research*, 2003, **37**, 1443-1467.
21. L. Chuecas and J. P. Riley, *Journal of the Marine Biological Association of the United Kingdom*, 1969, **49**, 97-116.
22. M. Mochida, Y. Kitamori, K. Kawamura, Y. Nojiri and K. Suzuki, *Journal of Geophysical Research Atmospheres*, 2002, **107**, 4325-4325.
23. J. K. Volkman, S. W. Jeffrey, P. D. Nichols, G. I. Rogers and C. D. Garland, *Journal of Experimental Marine Biology and Ecology*, 1989, **128**, 219-240.

24.   A. Saliot, J. Tronczynski, P. Scribe and R. Letolle, *Estuarine, Coastal and Shelf Science*, 1988, **27**, 645-669.
25.   R. Pistocchi, G. Trigari, G. P. Serrazanetti, P. Taddei, G. Monti, S. Palamidesi, F. Guerrini, G. Bottura, P. Serratore, M. Fabbri, M. Pirini, V. Ventrella, A. Pagliarani, L. Boni and A. R. Borgatti, *Science of the Total Environment*, 2005, **353**, 287-299.
26.   S. Derieux, J. Fillaux and A. Saliot, *Organic Geochemistry*, 1998, **29**, 1609-1621.
27.   M. Tedetti, K. Kawamura, B. Charrièra, N. Chevalier and R. Sempéré, *Analytical Chemistry*, 2006, **78**, 6012-6018.
28.   S. M. Steinberg and J. L. Bada, *Journal of Marine Research*, 1984, **42**, 697-708.
29.   J. C. Marty, A. Saliot, P. Buat-Ménard, R. Chesselet and K. A. Hunter, *Journal of Geophysical Research*, 1979, **84**, 5707-5716.
30.   R. A. Daumas, T. L. Laborde, J. C. Marty and A. Saliot, *Limnology and Oceanography*, 1976, **21**, 319-326.
31.   J. F. Slowey, L. M. Jeffrey and D. W. Hood, *Geochimica et Cosmochimica Acta*, 1962, **26**, 607-616.
32.   R. E. Cochran, O. Laskina, T. Jayarathne, A. Laskin, J. Laskin, P. Lin, C. Sultana, C. Lee, K. A. Moore, C. D. Cappa, T. H. Bertram, K. A. Prather, V. H. Grassian and E. A. Stone, *Environ Sci Technol*, 2016, **50**, 2477-2486.
33.   L. A. Copeman and C. C. Parrish, *Marine Biology*, 2003, **143**, 1213-1227.
34.   J. D. Hearn, A. J. Lovett and G. D. Smith, *Phys Chem Chem Phys*, 2005, **7**, 501-511.
35.   Y. Dubowski, J. Vieceli, D. J. Tobias, A. Gomez, A. Lin, S. A. Nizkorodov, T. M. McIntire and B. J. Finlayson-Pitts, *Journal of Physical Chemistry A*, 2004, **108**, 10473-10485.
36.   O. Vesna, M. Sax, M. Kalberer, A. Gaschen and M. Ammann, *Atmospheric Environment*, 2009, **43**, 3662-3669.
37.   R. Criegee, *Angewandte Chemie International Edition in English*, 1975, **14**, 745-752.
38.   O. Welz, J. D. Savee, D. L. Osborn, S. S. Vasu, C. J. Percival, D. E. Shallcross and C. A. Taatjes, *Science*, 2012, **335**, 204-207.
39.   S. Zhou, L. Gonzalez, A. Leithead, Z. Finewax, R. Thalman, A. Vlasenko, S. Vagle, L. A. Miller, S. M. Li, S. Bureekul, H. Furutani, M. Uematsu, R. Volkamer and J. Abbatt, *Atmospheric Chemistry and Physics*, 2014, **14**, 1371-1384.
40.   I. Lisˇka, *Journal of Chromatography A*, 2000, **885**, 3-16.
41.   T. Dittmar, B. Koch, N. Hertkorn and G. Kattner, *Limnology and Oceanography: Methods*, 2008, **6**, 230-235.
42.   S. Abdulkadir and M. Tsuchiya, *Journal of Experimental Marine Biology and Ecology*, 2008, **354**, 1-8.
43.   K. Eder, *Journal of Chromatography B: Biomedical Sciences and Applications*, 1995, **671**, 113-131.
44.   S. H. Jónasdóttir, *Marine Drugs*, 2019, **17**, 151-151.
45.   W. D. Garrett, *Limnology and Oceanography*, 1965, **10**, 602-605.
46.   D. W. Tarasick and R. Slater, *Atmosphere - Ocean*, 2008, **46**, 93-115.
47.   J. Lelieveld and F. J. Dentener, *Journal of Geophysical Research: Atmospheres*, 2000, **105**, 3531-3551.
48.   D. A. Hansell and C. A. Carlson, *Oceanography*, 2001, **14**, 41-49.
49.   D. A. Hansell, C. A. Carlson, D. J. Repeta and R. Schlitzer, *Oceanography*, 2009, **22**, 202-211.
50.   A. Momzikoff, A. Brinis, S. Dallot, G. Gondry, A. Saliot and P. Lebaron, *Limnology and Oceanography: Methods*, 2004, **2**, 374-386.

51.   N. M. Frew, J. C. Goldman, M. R. Dennett and A. Sherwood Johnson, *JGR Oceans*, 1990, **95**, 3337-3352.

52.   S. P. McKenna and W. R. McGillis, *International Journal of Heat and Mass Transfer*, 2004, **47**, 539-553.

53.   R. Pereira, K. Schneider-Zapp and R. C. Upstill-Goddard, *Biogeosciences*, 2016, **13**, 3981-3989.

54.   H.-C. Tsai, *Marine Geology*, 1996, **134**, 95-112.

55.   W.-t. Tsai, *Journal of Geophysical Research: Oceans*, 1998, **103**, 27919-27930.

56.   L. J. Carpenter and P. D. Nightingale, *Chemical Reviews*, 2015, **115**, 4015-4034.

57.   V. F. McNeill, G. M. Wolfe and J. A. Thornton, *Journal of Physical Chemistry A*, 2007, **111**, 1073-1083.

58.   K. Kawamura, H. Kasukabe and L. A. Barrie, *Journal of Geophysical Research*, 2010, **115**.

59.   D. J. Steele, G. A. Tarran, C. E. Widdicombe, E. M. S. Woodward, S. A. Kimmance, D. J. Franklin and R. L. Airs, *Progress in Oceanography*, 2015, **137**, 434-445.

60.   A. J. Southward, O. Langmead, N. J. Hardman-Mountford, J. Aiken, G. T. Boalch, P. R. Dando, M. J. Genner, I. Joint, M. A. Kendall, N. C. Halliday, R. P. Harris, R. Leaper, N. Mieszkowska, R. D. Pingree, A. J. Richardson, D. W. Sims, T. Smith, A. W. Walne and S. J. Hawkins, *Advances in Marine Biology*, 2005, **47**, 1-105.

61.   D. C. Loades, M. Yang, T. G. Bell, A. R. Vaughan, R. J. Pound, S. Metzger, J. D. Lee and L. J. Carpenter, *Atmospheric Measurement Techniques*, 2020, **13**, 6915-6931.

62.   M. K. Barnes, G. H. Tilstone, D. J. Suggett, C. E. Widdicombe, J. Bruun, V. Martinez-Vicente and T. J. Smyth, *Progress in Oceanography*, 2015, **137**, 470-483.

63.   R. J. Kieber, L. H. Hydro and P. J. Seaton, *Limnology and Oceanography*, 1997, **42**, 1454-1462.

64.   G. Sarwar, D. Kang, K. Foley, D. Schwede, B. Gantt and R. Mathur, *Atmospheric Environment*, 2016, **141**, 255-262.

65.   C. A. Carlson, H. W. Ducklow and A. F. Michaels, *Nature*, 1994, **371**, 405-408.

66.   N. B. Nelson, D. A. Siegel and J. A. Yoder, *Deep Sea Research Part II: Topical Studies in Oceanography*, 2004, **51**, 987-1000.

67.   E. Lovecchio, N. Gruber, M. Münnich and Z. Lachkar, *Biogeosciences*, 2017, **14**, 3337-3369.

68.   P. A. Thompson, M. x. Guo and P. J. Harrison, *Aquaculture*, 1996, **143**, 379-391.

69.   Y. C. Chen, *Food Chemistry*, 2012, **131**, 211-219.

70.   M. J. Pullin, S. Bertilsson, J. V. Goldstone and B. M. Voelker, *Limnology and Oceanography*, 2004, **49**, 2011-2022.

71.   A. S. Kester and J. W. Foster, *Journal of bacteriology*, 1963, **85**, 859-869.

72.   K. Kawamura, R. Sempéré, Y. Imai, Y. Fujii and M. Hayashi, *Journal of Geophysical Research: Atmospheres*, 1996, **101**, 18721-18728.

73.   E. González-Labrada, R. Schmidt and C. E. DeWolf, *Physical Chemistry Chemical Physics*, 2007, **9**, 5814-5821.

74.   J. Kleber, K. Lass and G. Friedrichs, *J Phys Chem A*, 2013, **117**, 7863-7875.

75.   M. D. King, C. E. Canosa-MAS and R. P. Wayne, *Physical Chemistry Chemical Physics*, 1999, **1**, 2239-2246.

76.   G. W. Harvey and L. A. Burzell, *Limnology and Oceanography*, 1972, **17**, 156-157.

77.   N. Simon, A. L. Cras, E. Foulon and R. Lemee, *C R Biol*, 2009, **332**, 159-170.

78. P. Falkowski, M. E. Katz, A. H. Knoll, A. Quigg, J. A. Raven, O. Schofield and F. J. R. Taylor, *Science*, 2004, **305**.

79. A. Z. Worden, J. K. Nolan and B. Palenik, *Limnology and Oceanography*, 2004, **49**, 168-179.

80. P. Heydarizadeh, I. Poirier, D. Loizeau, L. Ulmann, V. Mimouni, B. Schoefs and M. Bertrand, *Marine Drugs*, 2013, **11**, 3425-3471.

81. A. Muhlroth, K. Li, G. Rokke, P. Winge, Y. Olsen, M. F. Hohmann-Marriott, O. Vadstein and A. M. Bones, *Mar Drugs*, 2013, **11**, 4662-4697.

82. A. W. E. Galloway and M. Winder, *PLOS ONE*, 2015, **10**, e0130053-e0130053.

83. M. R. Brown, G. A. Dunstan, S. J. Torrcd and K. A. Mzller, *Journal of Phycology*, 1996, **73**, 64-73.

84. X. Chen, S. G. Wakeham and N. S. Fishera, *Limnology and Oceanography*, 2011, **56**, 716-724.

85. M. Chen, H. Liu and B. Chen, *Marine Ecology Progress Series*, 2012, **455**, 95-110.

86. P. D. Nichols, J. K. Volkman, G. M. Hallegraeff and S. I. Blackburn, *Phytochemistry*, 1987, **26**, 2537-2541.

87. G. A. Dunstan, J. K. Volkman, S. W. Jeffrey and S. M. Barrett, *Journal of Experimental Marine Biology and Ecology*, 1992, **161**, 115-134.

88. G. A. Dunstan, J. K. Volkman, S. M. Barrett, J. M. Leroi and S. W. Jeffrey, *Phytochemistry*, 1993, **35**, 155-161.

89. G. A. Dunstan, M. R. Brown and J. K. Volkman, *Phytochemistry*, 2005, **66**, 2557-2570.

90. J. Fábregas, A. Maseda, A. Domínguez and A. Otero, *World Journal of Microbiology and Biotechnology*, 2004, **20**, 31-35.

91. S. B. George, C. Fox and S. Wakeham, *Aquaculture*, 2008, **285**, 167-173.

92. M. Graeve, G. Kattner and W. Hagen, *Journal of Experimental Marine Biology and Ecology*, 1994, **182**, 97-110.

93. S. H. Jónasdóttir, A. W. Visser and C. Jespersen, *Marine Ecology Progress Series*, 2009, **382**, 139-150.

94. S. O. Lourenço, E. Barbarino, J. Mancini-Filho, K. P. Schinke and E. Aidar, *Phycologia*, 2002, **41**, 158-168.

95. M. P. Mansour, J. K. Volkman, A. E. Jackson and S. I. Blackburn, *Journal of Phycology*, 1999, **35**, 710-720.

96. J. A. Marshall, P. D. Nichols and G. M. Hallegraeff, *Journal of Applied Phycology*, 2002, **14**, 255-265.

97. B. D. Mooney, P. D. Nichols, M. F. De Salas and G. M. Hallegraeff, *Journal of Phycology*, 2007, **43**, 101-111.

98. G. Mourente, L. M. Lubián and J. M. Odriozola, *Hydrobiologia*, 1990, **203**, 147-154.

99. P. D. Nichols, G. J. Jones, J. W. De Leeuw and R. B. Johns, *Phytochemistry*, 1984, **23**, 1043-1047.

100. P. D. Nichols, J. H. Skerratt, A. Davidson, H. Burton and T. A. McMeekin, *Phytochemistry*, 1991, **30**, 3209-3214.

101. C. C. Parrish, V. M. French and M. J. Whiticar, *Journal of Plankton Research*, 2012, **34**, 356-375.

102. V. Patil, T. Källqvist, E. Olsen, G. Vogt and H. R. Gislerød, *Aquaculture International*, 2007, **15**, 1-9.

103. K. I. Reitan, J. R. Rainuzzo and Y. Olsen, *Journal of Phycology*, 1994, **30**, 972-979.

104. U. Riebesell, A. T. Revill, D. G. Holdsworth and J. K. Volkman, *Geochimica et Cosmochimica Acta*, 2000, **64**, 4179-4192.
105. J. M. Rousch, S. E. Bingham and M. R. Sommerfeld, *Journal of Experimental Marine Biology and Ecology*, 2003, **295**, 145-156.
106. K. W. Tang, H. H. Jakobsen and A. W. Visser, *Limnology and Oceanography*, 2001, **46**, 1860-1870.
107. P. A. Thompson, P. J. Harrison and J. N. C. Whyte, *Journal of Phycology*, 1990, **26**, 278-288.
108. P. A. Thompson, M. x. x. Guo, P. J. Harrison and J. N. C. Whyte, *Journal of Phycology*, 1992, **28**, 488-497.
109. A. Torstensson, C. Jiménez, A. K. Nilsson and A. Wulff, *Polar Biology*, 2019, **42**, 2149-2164.
110. R. Tremblay, S. Cartier, P. Miner, F. Pernet, C. Quéré, J. Moal, M. L. Muzellec, M. Mazuret and J. F. Samain, *Aquaculture*, 2007, **262**, 410-418.
111. A.-C. Viso and J.-C. Marty, *Phytochemistry*, 1993, **34**, 1521-1533.
112. N. V. Zhukova and N. A. Aizdaicher, *Phytochemistry*, 1995, **39**, 351-356.
113. F. Alonzo, P. Virtue, S. Nicol and P. D. Nichols, *Marine Ecology Progress Series*, 2005, **296**, 89-91.
114. OBIS (2020) Ocean Biodiversity Information System. Intergovernmental Oceanographic Commission of UNESCO. www.iobis.org).
115. D. Righetti, M. Vogt, N. Gruber, A. Psomas and N. E. Zimmermann, *Science Advances*, 2019, **5**, 1-11.
116. P. J. Harrison, R. E. Waters and F. J. R. Taylor, *Journal of Phycology*, 1980, **16**, 28-35.
117. M. D. Keller, R. C. Selvin, W. Claus and R. R. L. Guillard, *Journal of Phycology*, 1987, **23**, 633-638.
118. J. C. Goldman and M. R. Dennett, *Journal of Experimental Marine Biology and Ecology*, 1985, **86**, 47-58.
119. R. R. L. Guillard and J. H. Ryther, *Canadian Journal of Microbiology*, 1962, **8**, 229-239.
120. R. B. Gagosian, E. T. Peltzer and O. C. Zafiriou, *Nature*, 1981, **291**, 312-314.
121. J. Fang, K. Kawamura, Y. Ishimura and K. Matsumoto, *Environmental Science and Technology*, 2002, **36**, 2598-2604.
122. W. H. Kruskal and W. A. Wallis, *Journal of the American Statistical Association*, 1952, **47**, 583-621.
123. O. J. Dunn, *Technometrics*, 1964, **6**, 241-252.
124. F. Guihéneuf, V. Mimouni, G. Tremblin and L. Ulmann, *Journal of Agricultural and Food Chemistry*, 2015, **63**, 1261-1267.
125. V. Ẑutić, B. Ćosović, E. Marčenko, N. Bihari and F. Kršinić, *Marine Chemistry*, 1981, **10**, 505-520.
126. J. A. Hellebust, *Limnology and Oceanography*, 1965, **10**, 192-206.
127. X. Ma, M. L. Coleman and J. R. Waldbauer, *Environ Microbiol*, 2018, **20**, 3001-3011.
128. G. W. Harvey, *Limnology and Oceanography*, 1996, **11**, 608-613.